

Modular invariant flavor model of A_4 and hierarchical structures at nearby fixed points

Hiroshi Okada ^{a,b*} and Morimitsu Tanimoto ^{c†}

^a*Asia Pacific Center for Theoretical Physics, Pohang 37673, Republic of Korea*

^b*Department of Physics, Pohang University of Science and Technology, Pohang 37673, Republic of Korea*

^c*Department of Physics, Niigata University, Niigata 950-2181, Japan*

Abstract

In the modular invariant flavor model of A_4 , we study the hierarchical structure of lepton/quark flavors at nearby fixed points of $\tau = i$ and $\tau = \omega$ of the modulus, which are in the fundamental domain of $\text{PSL}(2, \mathbb{Z})$. These fixed points correspond to the residual symmetries $\mathbb{Z}_2^S = \{I, S\}$ and $\mathbb{Z}_3^{ST} = \{I, ST, (ST)^2\}$ of A_4 , where S and T are generators of the A_4 group. The infinite $\tau = i\infty$ also preserves the residual symmetry of the subgroup $\mathbb{Z}_3^T = \{I, T, T^2\}$ of A_4 . We study typical two-type mass matrices for charged leptons and quarks in terms of modular forms of weights 2, 4 and 6 while the neutrino mass matrix with the modular forms of weight 4 through the Weinberg operator. Linear modular forms are obtained approximately by performing Taylor expansion of modular forms around fixed points. By using them, the flavor structure of the lepton and quark mass matrices are examined at nearby fixed points. The hierarchical structure of these mass matrices is clearly shown in the diagonal base of S , T and ST . The observed PMNS and CKM mixing matrices can be reproduced at nearby fixed points in some cases of mass matrices. By scanning model parameters numerically at nearby fixed points, our discussion are confirmed for both the normal hierarchy and inverted one of neutrino masses. Predictions are given for the sum of neutrino masses and the CP violating Dirac phase of leptons at each nearby fixed point.

*E-mail address: hiroshi.okada@apctp.org

†E-mail address: tanimoto@muse.sc.niigata-u.ac.jp

1 Introduction

In spite of the remarkable success of the standard model (SM), the origin of the flavor of quarks and leptons is still a challenging issue. Indeed, a lot of works have been presented by using the discrete groups for flavors to understand the flavor structures of quarks and leptons. In the early models of quark masses and mixing angles, the S_3 symmetry was used [1, 2]. It was also discussed to understand the large mixing angle [3] in the oscillation of atmospheric neutrinos [4]. For the last twenty years, the discrete symmetries of flavors have been developed, that is motivated by the precise observation of flavor mixing angles of leptons [5–14].

Many models have been proposed by using the non-Abelian discrete groups S_3 , A_4 , S_4 , A_5 and other groups with larger orders to explain the large neutrino mixing angles. Among them, the A_4 flavor model is attractive one because the A_4 group is the minimal one including a triplet irreducible representation, which allows for a natural explanation of the existence of three families of leptons [15–21]. However, variety of models is so wide that it is difficult to show clear evidences of the A_4 flavor symmetry.

Recently, a new approach to the lepton flavor problem appeared based on the invariance of the modular group [22], where the model of the finite modular group $\Gamma_3 \simeq A_4$ has been presented. This work inspired further studies of the modular invariance to the lepton flavor problem. The finite groups S_3 , A_4 , S_4 and A_5 are formed as the quotient groups of the modular group and its principal congruence subgroups [23]. Therefore, an interesting framework for the construction of flavor models has been put forward based on the $\Gamma_3 \simeq A_4$ modular group [22], and further, based on $\Gamma_2 \simeq S_3$ [24]. The flavor models have been proposed by using modular symmetries $\Gamma_4 \simeq S_4$ [25] and $\Gamma_5 \simeq A_5$ [26]. Phenomenological discussions of the neutrino flavor mixing have been done based on A_4 [27–29], S_4 [30–32] and A_5 [33]. A clear prediction of the neutrino mixing angles and the CP violating phase was presented in the simple lepton mass matrices with A_4 modular symmetry [28]. The Double Covering groups T' [34, 35] and S'_4 [36, 37] have also obtained from the modular symmetry.

The A_4 modular symmetry has been also applied to the leptogenesis [38–40], on the other hand, it is discussed in the $SU(5)$ grand unified theory (GUT) of quarks and leptons [41, 42]. The residual symmetry of the A_4 modular symmetry has presented the interesting phenomenology [43]. Furthermore, modular forms for $\Delta(96)$ and $\Delta(384)$ were constructed [44], and the extension of the traditional flavor group is discussed with modular symmetries [45]. The level 7 finite modular group $\Gamma_7 \simeq \text{PSL}(2, Z_7)$ is also presented for the lepton mixing [46]. Moreover, multiple modular symmetries are proposed as the origin of flavor [47]. The modular invariance has been also studied combining with the CP symmetries for theories of flavors [48, 49]. The quark mass matrix has been discussed in the S_3 and A_4 modular symmetries as well [50–52]. Besides mass matrices of quarks and leptons, related topics have been discussed in the baryon number violation [50], the dark matter [53, 54] and the modular symmetry anomaly [55]. Further phenomenology has been developed in many works [56–74] while theoretical investigations are also proceeded [75–79].

As well known, in non-Abelian discrete symmetries of flavors, residual symmetries provide interesting phenomenology of flavors. They arise whenever the modulus τ breaks the modular group only partially. In this work, we study the hierarchical flavor structure of leptons and quarks in context with the residual symmetry, in which the modulus τ is at fixed points. We examine the flavor structure of mass matrices of leptons and quarks at nearby fixed points of the modulus τ in the framework of the modular invariant flavor model of A_4 . It is challenging to reproduce the Pontecorvo-Maki-Nakagawa-Sakata (PMNS) mixing angles [83, 84] and the CP violating Dirac phase of leptons which is expected to be observed at T2K and $\text{NO}\nu A$ experiments [85, 86], as well as observed Cabibbo-Kobayashi-Maskawa (CKM) matrix

elements at nearby fixed points.

We have already discussed numerically both mass matrices of leptons and quarks in the A_4 modular symmetry [52, 82], where modular forms of weights 2, 4 and 6 are used. In the same framework, we discuss the flavor structure of the lepton and quark mass matrices focusing on nearby fixed points. For this purpose, we give linear forms of $Y_1(\tau)$, $Y_2(\tau)$ and $Y_3(\tau)$ approximately by performing Taylor expansion of modular forms around fixed points of the modulus τ in the A_4 modular symmetry.

The paper is organized as follows. In section 2, we give a brief review on the modular symmetry and modular forms of weights 2, 4 and 6. In section 3, we discuss the residual symmetry of A_4 and modular forms at fixed points. In section 4, we present modular forms at nearby fixed points. In section 5 and 6, we discuss flavor mixing angles at nearby fixed points in lepton mass matrices and quark mass matrices, respectively. In section 7, the numerical results and predictions are presented. Section 8 is devoted to a summary. In Appendix A, the tensor product of the A_4 group is presented. In Appendix B, the transformation of mass matrices are discussed in the arbitrary bases of S and T . In Appendix C, the modular forms are given at nearby fixed points. In Appendix D, we present how to obtain Dirac CP phase, Majorana phases and the effective mass of the $0\nu\beta\beta$ decay.

2 Modular group and modular forms of weights 2, 4, 6

The modular group $\bar{\Gamma}$ is the group of linear fractional transformation γ acting on the modulus τ , belonging to the upper-half complex plane as:

$$\tau \longrightarrow \gamma\tau = \frac{a\tau + b}{c\tau + d}, \quad \text{where } a, b, c, d \in \mathbb{Z} \text{ and } ad - bc = 1, \quad \text{Im}[\tau] > 0, \quad (1)$$

which is isomorphic to $\text{PSL}(2, \mathbb{Z}) = \text{SL}(2, \mathbb{Z})/\{\mathbb{I}, -\mathbb{I}\}$ transformation. This modular transformation is generated by S and T ,

$$S : \tau \longrightarrow -\frac{1}{\tau}, \quad T : \tau \longrightarrow \tau + 1, \quad (2)$$

which satisfy the following algebraic relations,

$$S^2 = \mathbb{I}, \quad (ST)^3 = \mathbb{I}. \quad (3)$$

We introduce the series of groups $\Gamma(N)$ ($N = 1, 2, 3, \dots$), called principal congruence subgroups of $\text{SL}(2, \mathbb{Z})$, defined by

$$\Gamma(N) = \left\{ \begin{pmatrix} a & b \\ c & d \end{pmatrix} \in \text{SL}(2, \mathbb{Z}), \quad \begin{pmatrix} a & b \\ c & d \end{pmatrix} = \begin{pmatrix} 1 & 0 \\ 0 & 1 \end{pmatrix} \pmod{N} \right\}. \quad (4)$$

For $N = 2$, we define $\bar{\Gamma}(2) \equiv \Gamma(2)/\{\mathbb{I}, -\mathbb{I}\}$. Since the element $-\mathbb{I}$ does not belong to $\Gamma(N)$ for $N > 2$, we have $\bar{\Gamma}(N) = \Gamma(N)$. The quotient groups defined as $\Gamma_N \equiv \bar{\Gamma}/\bar{\Gamma}(N)$ are finite modular groups. In these finite groups Γ_N , $T^N = \mathbb{I}$ is imposed. The groups Γ_N with $N = 2, 3, 4, 5$ are isomorphic to S_3 , A_4 , S_4 and A_5 , respectively [23].

Modular forms of level N are holomorphic functions $f(\tau)$ transforming under the action of $\Gamma(N)$ as:

$$f(\gamma\tau) = (c\tau + d)^k f(\tau), \quad \gamma \in \Gamma(N), \quad (5)$$

where k is the so-called as the modular weight.

Superstring theory on the torus T^2 or orbifold T^2/Z_N has the modular symmetry [87–92]. Its low energy effective field theory is described in terms of supergravity theory, and string-derived supergravity theory has also the modular symmetry. Under the modular transformation of Eq. (1), chiral superfields $\phi^{(I)}$ transform as [93],

$$\phi^{(I)} \rightarrow (c\tau + d)^{-k_I} \rho^{(I)}(\gamma) \phi^{(I)}, \quad (6)$$

where $-k_I$ is the modular weight and $\rho^{(I)}(\gamma)$ denotes an unitary representation matrix of $\gamma \in \Gamma_N$.

In this paper, we study global supersymmetric models, e.g., minimal supersymmetric extensions of the Standard Model (MSSM). The superpotential which is built from matter fields and modular forms is assumed to be modular invariant, i.e., to have a vanishing modular weight. For given modular forms this can be achieved by assigning appropriate weights to the matter superfields.

The kinetic terms are derived from a Kähler potential. The Kähler potential of chiral matter fields $\phi^{(I)}$ with the modular weight $-k_I$ is given simply by

$$K^{\text{matter}} = \frac{1}{[i(\bar{\tau} - \tau)]^{k_I}} |\phi^{(I)}|^2, \quad (7)$$

where the superfield and its scalar component are denoted by the same letter, and $\bar{\tau} = \tau^*$ after taking the vacuum expectation value (VEV). Therefore, the canonical form of the kinetic terms is obtained by changing the normalization of parameters [28]. The general Kähler potential consistent with the modular symmetry possibly contains additional terms [94]. However, we consider only the simplest form of the Kähler potential.

For $\Gamma_3 \simeq A_4$, the dimension of the linear space $\mathcal{M}_k(\Gamma_3)$ of modular forms of weight k is $k+1$ [95–97], i.e., there are three linearly independent modular forms of the lowest non-trivial weight 2. These forms have been explicitly obtained [22] in terms of the Dedekind eta-function $\eta(\tau)$:

$$\eta(\tau) = q^{1/24} \prod_{n=1}^{\infty} (1 - q^n), \quad q = \exp(i2\pi\tau), \quad (8)$$

where $\eta(\tau)$ is a so called modular form of weight 1/2. In what follows we will use the following base of the A_4 generators S and T in the triplet representation:

$$S = \frac{1}{3} \begin{pmatrix} -1 & 2 & 2 \\ 2 & -1 & 2 \\ 2 & 2 & -1 \end{pmatrix}, \quad T = \begin{pmatrix} 1 & 0 & 0 \\ 0 & \omega & 0 \\ 0 & 0 & \omega^2 \end{pmatrix}, \quad (9)$$

where $\omega = \exp(i\frac{2}{3}\pi)$. The modular forms of weight 2, $\mathbf{Y}_3^{(2)} = (Y_1(\tau), Y_2(\tau), Y_3(\tau))^T$ transforming as a triplet of A_4 can be written in terms of $\eta(\tau)$ and its derivative [22]:

$$\begin{aligned} Y_1(\tau) &= \frac{i}{2\pi} \left(\frac{\eta'(\tau/3)}{\eta(\tau/3)} + \frac{\eta'((\tau+1)/3)}{\eta((\tau+1)/3)} + \frac{\eta'((\tau+2)/3)}{\eta((\tau+2)/3)} - \frac{27\eta'(3\tau)}{\eta(3\tau)} \right), \\ Y_2(\tau) &= \frac{-i}{\pi} \left(\frac{\eta'(\tau/3)}{\eta(\tau/3)} + \omega^2 \frac{\eta'((\tau+1)/3)}{\eta((\tau+1)/3)} + \omega \frac{\eta'((\tau+2)/3)}{\eta((\tau+2)/3)} \right), \\ Y_3(\tau) &= \frac{-i}{\pi} \left(\frac{\eta'(\tau/3)}{\eta(\tau/3)} + \omega \frac{\eta'((\tau+1)/3)}{\eta((\tau+1)/3)} + \omega^2 \frac{\eta'((\tau+2)/3)}{\eta((\tau+2)/3)} \right). \end{aligned} \quad (10)$$

The triplet modular forms of weight 2 have the following q -expansions:

$$\mathbf{Y}_3^{(2)} = \begin{pmatrix} Y_1(\tau) \\ Y_2(\tau) \\ Y_3(\tau) \end{pmatrix} = \begin{pmatrix} 1 + 12q + 36q^2 + 12q^3 + \dots \\ -6q^{1/3}(1 + 7q + 8q^2 + \dots) \\ -18q^{2/3}(1 + 2q + 5q^2 + \dots) \end{pmatrix}. \quad (11)$$

They satisfy also the constraint [22]:

$$(Y_2(\tau))^2 + 2Y_1(\tau)Y_3(\tau) = 0. \quad (12)$$

The modular forms of the higher weight, k , can be obtained by the A_4 tensor products of the modular forms with weight 2, $\mathbf{Y}_3^{(2)}$, as given in Appendix A. For $k = 4$, there are five modular forms by the tensor product of $\mathbf{3} \otimes \mathbf{3}$ as:

$$\begin{aligned} \mathbf{Y}_1^{(4)} = Y_1^2 + 2Y_2Y_3, \quad \mathbf{Y}_{1'}^{(4)} = Y_3^2 + 2Y_1Y_2, \quad \mathbf{Y}_{1''}^{(4)} = Y_2^2 + 2Y_1Y_3 = 0, \\ \mathbf{Y}_3^{(4)} = \begin{pmatrix} Y_1^{(4)} \\ Y_2^{(4)} \\ Y_3^{(4)} \end{pmatrix} = \begin{pmatrix} Y_1^2 - Y_2Y_3 \\ Y_3^2 - Y_1Y_2 \\ Y_2^2 - Y_1Y_3 \end{pmatrix}, \end{aligned} \quad (13)$$

where $\mathbf{Y}_{1''}^{(4)}$ vanishes due to the constraint of Eq. (12). For $k = 6$, there are seven modular forms by the tensor products of A_4 as:

$$\begin{aligned} \mathbf{Y}_1^{(6)} = Y_1^3 + Y_2^3 + Y_3^3 - 3Y_1Y_2Y_3, \\ \mathbf{Y}_3^{(6)} \equiv \begin{pmatrix} Y_1^{(6)} \\ Y_2^{(6)} \\ Y_3^{(6)} \end{pmatrix} = \begin{pmatrix} Y_1^3 + 2Y_1Y_2Y_3 \\ Y_1^2Y_2 + 2Y_2^2Y_3 \\ Y_1^2Y_3 + 2Y_3^2Y_2 \end{pmatrix}, \quad \mathbf{Y}_{3'}^{(6)} \equiv \begin{pmatrix} Y_1'^{(6)} \\ Y_2'^{(6)} \\ Y_3'^{(6)} \end{pmatrix} = \begin{pmatrix} Y_3^3 + 2Y_1Y_2Y_3 \\ Y_3^2Y_1 + 2Y_1^2Y_2 \\ Y_3^2Y_2 + 2Y_2^2Y_1 \end{pmatrix}. \end{aligned} \quad (14)$$

By using these modular forms of weights 2, 4, 6, we discuss lepton and quark mass matrices.

3 Residual symmetry of A_4 at fixed points

3.1 Modular forms at fixed points

Residual symmetries arise whenever the VEV of the modulus τ breaks the modular group $\bar{\Gamma}$ only partially. Fixed points of modulus are the case. There are only 2 inequivalent finite points in the fundamental domain of $\bar{\Gamma}$, namely, $\tau = i$ and $\tau = \omega = -1/2 + i\sqrt{3}/2$. The first point is invariant under the S transformation $\tau = -1/\tau$. In the case of A_4 symmetry, the subgroup $\mathbb{Z}_2^S = \{I, S\}$ is preserved at $\tau = i$. The second point is the left cusp in the fundamental domain of the modular group, which is invariant under the ST transformation $\tau = -1/(\tau + 1)$. Indeed, $\mathbb{Z}_3^{ST} = \{I, ST, (ST)^2\}$ is one of subgroups of A_4 group. The right cusp at $\tau = -\omega^2 = 1/2 + i\sqrt{3}/2$ is related to $\tau = \omega$ by the T transformation. There is also infinite point $\tau = i\infty$, in which the subgroup $\mathbb{Z}_3^T = \{I, T, T^2\}$ of A_4 is preserved.

k	\mathbf{r}	$\tau = i$	$\tau = \omega$	$\tau = i\infty$
2	$\mathbf{3}$	$Y_0(1, 1 - \sqrt{3}, -2 + \sqrt{3})$	$Y_0(1, \omega, -\frac{1}{2}\omega^2)$	$Y_0(1, 0, 0)$
4	$\mathbf{3}$ $\{\mathbf{1}, \mathbf{1}'\}$	$(6 - 3\sqrt{3})Y_0^2(1, 1, 1)$ $Y_0^2\{6\sqrt{3} - 9, 9 - 6\sqrt{3}\}$	$\frac{3}{2}Y_0^2(1, -\frac{1}{2}\omega, \omega^2)$ $\{0, \frac{9}{4}Y_0^2\omega\}$	$Y_0^2(1, 0, 0)$ $\{Y_0^2, 0\}$
6	$\mathbf{3}$ $\mathbf{3}'$ $\mathbf{1}$	$3Y_0^3(-3 + 2\sqrt{3}, -9 + 5\sqrt{3}, 12 - 7\sqrt{3})$ $3Y_0^3(-12 + 7\sqrt{3}, 3 - 2\sqrt{3}, 9 - 5\sqrt{3})$ 0	0 $\frac{9}{8}Y_0^3(-1, 2\omega, 2\omega^2)$ $\frac{27}{8}Y_0^3$	$Y_0^3(1, 0, 0)$ 0 Y_0^3
	Y_0	$Y_1(i) = 1.0225\dots$	$Y_1(\omega) = 0.9486\dots$	$Y_1(i\infty) = 1$

Table 1: Modular forms of weight $k = 2$, $k = 4$ and $k = 6$ at fixed points of τ .

It is possible to calculate the values of the A_4 triplet modular forms of weight 2, 4 and 6 at $\tau = i$, $\tau = \omega$ and $\tau = i\infty$. The results are summarized in Table 1.

If a residual symmetry of A_4 is preserved in mass matrices of leptons and quarks, we have commutation relations between the mass matrices and the generator $G \equiv S, T, ST$ as:

$$[M_{RL}^\dagger M_{RL}, G] = 0, \quad [M_{LL}, G] = 0, \quad (15)$$

where M_{RL} denotes the mass matrix of charged leptons and quarks, M_E and M_q , on the other hand, M_{LL} denotes the left-handed Majorana neutrino mass matrix M_ν .

Therefore, the mass matrices $M_E^\dagger M_E$, $M_q^\dagger M_q$ and M_ν could be diagonal in the diagonal base of G at the fixed points. The hierarchical structures of flavor mixing are easily realized near those fixed points. However, we should be careful with the generator S , in which two eigenvalues are degenerate. At $\tau = i$, one (2×2) submatrix of the mass matrix respecting S are not diagonal in general since two eigenvalues of S are degenerate such as $(-1, 1, -1)$. Therefore, the S symmetry provides us an advantage to reproduce the large mixing angle of neutrinos as discussed in section 5.

3.2 Diagonal base of S and ST

3.2.1 Diagonal base of S

The modular forms of Eq. (10) is obtained in the base of Eq. (9) for S and T . In order to present the mass matrices in the diagonal base of S , we move to the diagonal base of S as follows:

$$V_{S1} S V_{S1}^\dagger = \begin{pmatrix} -1 & 0 & 0 \\ 0 & 1 & 0 \\ 0 & 0 & -1 \end{pmatrix}, \quad V_{S2} S V_{S2}^\dagger = \begin{pmatrix} 1 & 0 & 0 \\ 0 & -1 & 0 \\ 0 & 0 & -1 \end{pmatrix}, \quad V_{S3} S V_{S3}^\dagger = \begin{pmatrix} -1 & 0 & 0 \\ 0 & -1 & 0 \\ 0 & 0 & 1 \end{pmatrix}, \quad (16)$$

where

$$V_{Si} \equiv P_i \begin{pmatrix} \frac{2}{\sqrt{6}} & -\frac{1}{\sqrt{6}} & -\frac{1}{\sqrt{6}} \\ \frac{1}{\sqrt{3}} & \frac{1}{\sqrt{3}} & \frac{1}{\sqrt{3}} \\ 0 & -\frac{1}{\sqrt{2}} & \frac{1}{\sqrt{2}} \end{pmatrix}, \quad P_1 = \begin{pmatrix} 1 & 0 & 0 \\ 0 & 1 & 0 \\ 0 & 0 & 1 \end{pmatrix}, \quad P_2 = \begin{pmatrix} 0 & 1 & 0 \\ 1 & 0 & 0 \\ 0 & 0 & 1 \end{pmatrix}, \quad P_3 = \begin{pmatrix} 1 & 0 & 0 \\ 0 & 0 & 1 \\ 0 & 1 & 0 \end{pmatrix}. \quad (17)$$

Then, the generator T is not anymore diagonal.

If there is a residual symmetry of A_4 in the Dirac mass matrix M_{RL} , for example, $\mathbb{Z}_2^S = \{I, S\}$, the generator S commutes with $M_{RL}^\dagger M_{RL}$,

$$\left[M_{RL}^\dagger M_{RL}, S \right] = 0. \quad (18)$$

Therefore, the mass matrix is expected to be diagonal in the diagonal base of S . However, the eigenvalue -1 of S is degenerated, and so one pair among off diagonal terms of $M_{RL}^\dagger M_{RL}$ is not necessarily to vanish depending on V_i of Eq. (17). For diagonal matrices $S = (-1, 1, -1)$, $(1, -1, -1)$ and $(-1, -1, 1)$, those are:

$$M_{RL}^\dagger M_{RL} = \begin{pmatrix} \times & 0 & \times \\ 0 & \times & 0 \\ \times & 0 & \times \end{pmatrix}, \quad \begin{pmatrix} \times & 0 & 0 \\ 0 & \times & \times \\ 0 & \times & \times \end{pmatrix}, \quad \begin{pmatrix} \times & \times & 0 \\ \times & \times & 0 \\ 0 & 0 & \times \end{pmatrix}, \quad (19)$$

respectively, where " \times " denotes non-vanishing entry. Thus, one flavor mixing angle appears even if there exists the $\mathbb{Z}_2^S = \{I, S\}$ symmetry..

3.2.2 Diagonal base of ST and T

If there exists the residual symmetries of the A_4 group $\mathbb{Z}_3^{ST} = \{I, ST, (ST)^2\}$ or $\mathbb{Z}_3^T = \{I, T, T^2\}$, we have

$$\left[M_{RL}^\dagger M_{RL}, ST \right] = 0, \quad \left[M_{RL}^\dagger M_{RL}, T \right] = 0, \quad (20)$$

respectively, which lead to the diagonal $M_{RL}^\dagger M_{RL}$ because ST and T have three different eigenvalues.

The generator T is already diagonal in the original base of Eq. (9). On the other hand, we can move to the diagonal base of ST by the unitary transformation V_{ST} as follows:

$$V_{STi} ST V_{STi}^\dagger = P_i \begin{pmatrix} \omega^2 & 0 & 0 \\ 0 & \omega & 0 \\ 0 & 0 & 1 \end{pmatrix} P_i^T, \quad (21)$$

where

$$V_{STi} = \frac{1}{3} P_i \begin{pmatrix} -2\omega^2 & -2\omega & 1 \\ -\omega^2 & 2\omega & 2 \\ 2\omega^2 & -\omega & 2 \end{pmatrix}, \quad P_4 = \begin{pmatrix} 0 & 0 & 1 \\ 0 & 1 & 0 \\ 1 & 0 & 0 \end{pmatrix}, \quad P_5 = \begin{pmatrix} 0 & 0 & 1 \\ 1 & 0 & 0 \\ 0 & 1 & 0 \end{pmatrix}, \quad (22)$$

and $P_i (i = 1, 2, 3)$ are given in Eq. (17). The order of eigenvalues of ST depends on P_i . We have eigenvalues $(\omega, \omega^2, 1)$ for P_2 , $(\omega^2, 1, \omega)$ for P_3 , $(1, \omega, \omega^2)$ for P_4 and $(1, \omega^2, \omega)$ for P_5 , respectively.

In the diagonal bases of S and ST , the Dirac mass matrix \hat{M}_{RL} is given by the unitary transformation as (See Appendix B):

$$\hat{M}_{RL} = M_{RL} V_{Si}^\dagger, \quad \hat{M}_{RL} = M_{RL} V_{STi}^\dagger, \quad (23)$$

respectively. On the other hand, the Majorana mass matrix M_{LL} is given as:

$$\hat{M}_{LL} = V_{Si} M_{LL} V_{Si}^\dagger, \quad \hat{M}_{LL} = V_{STi} M_{LL} V_{STi}^\dagger, \quad (24)$$

respectively. We will discuss the lepton and quark mass matrices in the diagonal bases of the generators by using these transformations.

4 Modular forms at nearby fixed points

The mass matrices of leptons and quarks have simple flavor structures due to simple modular forms at fixed points. At $\tau = i$, those mass matrices have one flavor mixing angle because the representation of S for the A_4 triplet has two degenerate eigenvalues. On the other hand, at $\tau = \omega$ and $\tau = i\infty$, the square of the mass matrix is diagonal one because ST and T of the A_4 triplet have three different eigenvalues. Therefore, the modulus τ should deviate from the fixed point to reproduce the observed PMNS and CKM matrix elements. We present the explicit modular forms by performing Taylor expansion around fixed points.

4.1 Modular forms at nearby $\tau = i$

Let us discuss the behavior of modular forms at nearby $\tau = i$. We consider linear approximation of the modular forms $Y_1(\tau)$, $Y_2(\tau)$ and $Y_3(\tau)$ by performing Taylor expansion around $\tau = i$. We parametrize τ as:

$$\tau = i + \epsilon, \quad (25)$$

where $|\epsilon|$ is supposed as $|\epsilon| \ll 1$. We obtain the ratios of the modular forms approximately as:

$$\frac{Y_2(\tau)}{Y_1(\tau)} \simeq (1 + \epsilon_1)(1 - \sqrt{3}), \quad \frac{Y_3(\tau)}{Y_1(\tau)} \simeq (1 + \epsilon_2)(-2 + \sqrt{3}), \quad \epsilon_1 = \frac{1}{2}\epsilon_2 = 2.05 i \epsilon. \quad (26)$$

These approximate forms are agreement with exact numerical values within 0.1% for $|\epsilon| \leq 0.05$. Details are given in Appendix C.1. The higher weight modular forms $Y_i^{(k)}$ in Eqs. (13) and (14) are also given in terms of ϵ_1 and ϵ_2 in Appendix C.1.

4.2 Modular forms at nearby $\tau = \omega$

We perform linear approximation of the modular forms $Y_1(\tau)$, $Y_2(\tau)$ and $Y_3(\tau)$ by performing Taylor expansion around $\tau = \omega$. We parametrize τ as:

$$\tau = \omega + \epsilon = -\frac{1}{2} + \frac{\sqrt{3}}{2}i + \epsilon, \quad (27)$$

where we suppose $|\epsilon| \ll 1$. We obtain the ratios of modular forms approximately as:

$$\frac{Y_2(\tau)}{Y_1(\tau)} \simeq \omega(1 + \epsilon_1), \quad \frac{Y_3(\tau)}{Y_1(\tau)} \simeq -\frac{1}{2}\omega^2(1 + \epsilon_2), \quad \epsilon_1 = \frac{1}{2}\epsilon_2 = 2.1 i \epsilon. \quad (28)$$

These approximate forms are agreement with exact numerical values within 1% for $|\epsilon| \leq 0.05$. Details are given in Appendix C.2.

The higher weight modular forms $Y_i^{(k)}$ in Eqs. (13) and (14) are also given in terms of ϵ_1 and ϵ_2 in Appendix C.2.

4.3 Modular forms towards $\tau = i\infty$

We show the behavior of modular forms at large $\text{Im}\tau$, where the magnitude of $q = \exp(2\pi i\tau)$ is suppressed. Taking leading terms of Eq. (11), we can express modular forms approximately as:

$$Y_1(\tau) \simeq 1 + 12p\epsilon, \quad Y_2(\tau) \simeq -6p^{\frac{1}{3}}\epsilon^{\frac{1}{3}}, \quad Y_3(\tau) \simeq -18p^{\frac{2}{3}}\epsilon^{\frac{2}{3}}, \quad p = e^{2\pi i \text{Re}\tau}, \quad \epsilon = e^{-2\pi \text{Im}\tau}. \quad (29)$$

Indeed, we obtain $\epsilon = 3.487 \times 10^{-6}$ for $\text{Im}\tau = 2$. The leading correction is $\epsilon^{\frac{1}{3}} = 0.0152$ in $Y_2(\tau)$ while other corrections of $\epsilon^{\frac{2}{3}}$ and ϵ is negligibly small. Then,

$$|Y_1(2i)| \simeq 1.00004, \quad |Y_2(2i)| \simeq 0.09098, \quad |Y_3(2i)| \simeq 0.00413, \quad (30)$$

which agree with exact values within 0.1%. Higher weight modular forms $Y_i^{(k)}$ in Eqs. (13) and (14) are also given in terms of p and ϵ approximately in Appendix C.3.

5 Lepton mass matrices in the A_4 modular invariance

5.1 Model of lepton mass matrices

Let us discuss models of the lepton mass matrices. There are freedoms for the assignments of irreducible representations of A_4 and modular weights to charged leptons and Higgs doublets. The simplest assignment has been given in the conventional A_4 model [17, 18], in which three left-handed leptons are components of the triplet of the A_4 group, but three right-handed charged leptons, (e^c, μ^c, τ^c) are three different singlets $(\mathbf{1}, \mathbf{1}'', \mathbf{1}')$ of A_4 , respectively.

Supposing neutrinos to be Majorana particles, we present the neutrino mass matrix through the Weinberg operator. The simple one is given by assigning the A_4 triplet and weight -2 to the lepton doublets ¹, where the Higgs fields are supposed to be A_4 singlets with weight 0. On the other hand, the charged lepton mass matrix depends on the assignment of weight for the right-handed charged leptons. If those weights are 0 for all right-handed charged leptons, the charged lepton mass matrix are given in terms of only the weight 2 modular forms of Eq. (10). That is the simplest one.

Alternatively, we also consider weight 4 and 6 modular forms of Eqs. (13) and (14) in addition to weight 2 modular forms by taking non-vanishing weights. The assignment is summarized in Table 2.

	L	(e^c, μ^c, τ^c)	H_u	H_d	$\mathbf{Y}_3^{(6)}, \mathbf{Y}_{3'}^{(6)}$	$\mathbf{Y}_3^{(4)}, \mathbf{Y}_1^{(4)}, \mathbf{Y}_{1'}^{(4)}$	$\mathbf{Y}_3^{(2)}$
$SU(2)$	$\mathbf{2}$	$\mathbf{1}$	$\mathbf{2}$	$\mathbf{2}$	$\mathbf{1}$	$\mathbf{1}$	$\mathbf{1}$
A_4	$\mathbf{3}$	$(\mathbf{1}, \mathbf{1}'', \mathbf{1}')$	$\mathbf{1}$	$\mathbf{1}$	$\mathbf{3}$	$\mathbf{3}, \mathbf{1}, \mathbf{1}'$	$\mathbf{3}$
$-k_I$	-2	I: $(0, 0, 0)$ II: $(-4, -2, 0)$	0	0	$k = 6$	$k = 4$	$k = 2$

Table 2: Assignments of representations and weights $-k_I$ for MSSM fields and modular forms.

¹There is a possible assignment of weight -1 to the lepton doublets of the A_4 triplet. The neutrino mass matrix is given in terms of weight 2 modular forms through the Weinberg operator. However, this case is too simple to reproduce the lepton mixing angles as discussed in Ref. [28].

5.1.1 Neutrino mass matrix

Let us begin with discussing the neutrino mass matrix. The superpotential of the neutrino mass term, w_ν is given as:

$$w_\nu = -\frac{1}{\Lambda}(H_u H_u L L \mathbf{Y}_r^{(k)})_1, \quad (31)$$

where L is the left-handed A_4 triplet leptons, H_u is the Higgs doublet, and Λ is a relevant cut off scale. Since the left-handed lepton doublet has weight -2 , the superpotential is given in terms of modular forms of weight 4, $\mathbf{Y}_3^{(4)}$, $\mathbf{Y}_1^{(4)}$ and $\mathbf{Y}_{1'}^{(4)}$. By putting the VEV of the neutral component of H_u , v_u and taking $(\nu_e, \nu_\mu, \nu_\tau)$ for left-handed neutrinos of L , we have

$$\begin{aligned} w_\nu &= \frac{v_u^2}{\Lambda} \left[\begin{pmatrix} 2\nu_e \nu_e - \nu_\mu \nu_\tau - \nu_\tau \nu_\mu \\ 2\nu_\tau \nu_\tau - \nu_e \nu_\mu - \nu_\mu \nu_e \\ 2\nu_\mu \nu_\mu - \nu_\tau \nu_e - \nu_e \nu_\tau \end{pmatrix} \otimes \mathbf{Y}_3^{(4)} \right. \\ &\quad \left. + (\nu_e \nu_e + \nu_\mu \nu_\tau + \nu_\tau \nu_\mu) \otimes g_{\nu 1} \mathbf{Y}_1^{(4)} + (\nu_e \nu_\tau + \nu_\mu \nu_\mu + \nu_\tau \nu_e) \otimes g_{\nu 2} \mathbf{Y}_{1'}^{(4)} \right] \\ &= \frac{v_u^2}{\Lambda} \left[(2\nu_e \nu_e - \nu_\mu \nu_\tau - \nu_\tau \nu_\mu) Y_1^{(4)} + (2\nu_\tau \nu_\tau - \nu_e \nu_\mu - \nu_\mu \nu_e) Y_3^{(4)} + (2\nu_\mu \nu_\mu - \nu_\tau \nu_e - \nu_e \nu_\tau) Y_2^{(4)} \right. \\ &\quad \left. + (\nu_e \nu_e + \nu_\mu \nu_\tau + \nu_\tau \nu_\mu) g_{\nu 1} \mathbf{Y}_1^{(4)} + (\nu_e \nu_\tau + \nu_\mu \nu_\mu + \nu_\tau \nu_e) g_{\nu 2} \mathbf{Y}_{1'}^{(4)} \right], \quad (32) \end{aligned}$$

where $\mathbf{Y}_3^{(4)}$, $\mathbf{Y}_1^{(4)}$ and $\mathbf{Y}_{1'}^{(4)}$ are given in Eq. (13), and $g_{\nu 1}$, $g_{\nu 2}$ are complex parameters. The neutrino mass matrix is written as follows:

$$M_\nu = \frac{v_u^2}{\Lambda} \left[\begin{pmatrix} 2Y_1^{(4)} & -Y_3^{(4)} & -Y_2^{(4)} \\ -Y_3^{(4)} & 2Y_2^{(4)} & -Y_1^{(4)} \\ -Y_2^{(4)} & -Y_1^{(4)} & 2Y_3^{(4)} \end{pmatrix} + g_{\nu 1} \mathbf{Y}_1^{(4)} \begin{pmatrix} 1 & 0 & 0 \\ 0 & 0 & 1 \\ 0 & 1 & 0 \end{pmatrix} + g_{\nu 2} \mathbf{Y}_{1'}^{(4)} \begin{pmatrix} 0 & 0 & 1 \\ 0 & 1 & 0 \\ 1 & 0 & 0 \end{pmatrix} \right]_{LL}. \quad (33)$$

5.1.2 Charged lepton mass matrix

The relevant superpotentials of the charged lepton masses are given for two cases as follows:

$$\text{I : } w_E = \alpha_e e^c H_d \mathbf{Y}_3^{(2)} L + \beta_e \mu^c H_d \mathbf{Y}_3^{(2)} L + \gamma_e \tau^c H_d \mathbf{Y}_3^{(2)} L, \quad (34)$$

$$\text{II : } w_E = \alpha_e e^c H_d \mathbf{Y}_3^{(6)} L + \alpha'_e e^c H_d \mathbf{Y}_3^{(6)} L + \beta_e \mu^c H_d \mathbf{Y}_3^{(4)} L + \gamma_e \tau^c H_d \mathbf{Y}_3^{(2)} L, \quad (35)$$

where L is the left-handed A_4 triplet leptons, H_d is the Higgs doublet.

The charged lepton mass matrices M_E are given as:

$$\text{I : } M_E = v_d \begin{pmatrix} \alpha_e & 0 & 0 \\ 0 & \beta_e & 0 \\ 0 & 0 & \gamma_e \end{pmatrix} \left[\begin{pmatrix} Y_1^{(2)} & Y_3^{(2)} & Y_2^{(2)} \\ Y_2^{(2)} & Y_1^{(2)} & Y_3^{(2)} \\ Y_3^{(2)} & Y_2^{(2)} & Y_1^{(2)} \end{pmatrix} \right]_{RL}, \quad (36)$$

$$(37)$$

$$\text{II : } M_E = v_d \begin{pmatrix} \alpha_e & 0 & 0 \\ 0 & \beta_e & 0 \\ 0 & 0 & \gamma_e \end{pmatrix} \left[\begin{pmatrix} Y_1^{(6)} + g_e Y_1'^{(6)} & Y_3^{(6)} + g_e Y_3'^{(6)} & Y_2^{(6)} + g_e Y_2'^{(6)} \\ Y_2^{(4)} & Y_1^{(4)} & Y_3^{(4)} \\ Y_3^{(2)} & Y_2^{(2)} & Y_1^{(2)} \end{pmatrix} \right]_{RL}, \quad (38)$$

respectively, where coefficients α_e , β_e and γ_e are real parameters while g_e is complex one, and v_d is VEV of the neutral component of H_d .

Model parameters of leptons are α_e , β_e , γ_e , (g_e) , $g_{\nu 1}$ and $g_{\nu 2}$ in addition to the modulus τ . We examine these mass matrices around the fixed points.

5.2 Lepton mass matrix at $\tau = i$

5.2.1 Neutrino mass matrix at $\tau = i$

We get the neutrino mass matrix at $\tau = i$ by putting modular forms in Table 1 into Eq. (33) as:

$$M_\nu = \frac{v_u^2}{\Lambda} (6 - 3\sqrt{3}) Y_0^2 \left[\begin{pmatrix} 2 & -1 & 1 \\ -1 & 2 & -1 \\ -1 & -1 & 2 \end{pmatrix} + g_1 \begin{pmatrix} 1 & 0 & 0 \\ 0 & 0 & 1 \\ 0 & 1 & 0 \end{pmatrix} + g_2 \begin{pmatrix} 0 & 0 & 1 \\ 0 & 1 & 0 \\ 1 & 0 & 0 \end{pmatrix} \right], \quad (39)$$

where

$$g_1 = \frac{6\sqrt{3} - 9}{6 - 3\sqrt{3}} g_{\nu 1} = \sqrt{3} g_{\nu 1}, \quad g_2 = \frac{9 - 6\sqrt{3}}{6 - 3\sqrt{3}} g_{\nu 2} = -\sqrt{3} g_{\nu 2}. \quad (40)$$

We move to the diagonal basis of S . By using the unitary transformation of Eq. (22), V_{S2} , the mass matrix is transformed as:

$$\hat{M}_\nu \equiv V_{S2}^* M_\nu V_{S2}^\dagger = \frac{v_u^2}{\Lambda} Y_0^2 \begin{pmatrix} g_1 + g_2 & 0 & 0 \\ 0 & 3 + g_1 - \frac{1}{2}g_2 & \frac{\sqrt{3}}{2}g_2 \\ 0 & \frac{\sqrt{3}}{2}g_2 & 3 - g_1 + \frac{1}{2}g_2 \end{pmatrix}. \quad (41)$$

Off diagonal entries of (2,3) and (3,2) are non-zero as discussed in Eq. (19). At the limit of vanishing g_1 and g_2 , the lightest neutrino mass is zero and other ones are degenerated.

In order to discuss the flavor mixing angle, we show $\hat{M}_\nu^\dagger \hat{M}_\nu$ as

$$\mathcal{M}_\nu^{2(0)} \equiv \hat{M}_\nu^\dagger \hat{M}_\nu = \left(\frac{v_u^2}{\Lambda} Y_0^2 \right)^2 \begin{pmatrix} |g_1 + g_2|^2 & 0 & 0 \\ 0 & G_\nu + 6\text{Re}[g_1] - 3\text{Re}[g_2] & \frac{\sqrt{3}}{2} (6\text{Re}[g_2] + 2i\text{Im}[g_1^* g_2]) \\ 0 & \frac{\sqrt{3}}{2} (6\text{Re}[g_2] - 2i\text{Im}[g_1^* g_2]) & G_\nu - 6\text{Re}[g_1] + 3\text{Re}[g_2] \end{pmatrix}, \quad (42)$$

where

$$G_\nu = 9 + |g_1|^2 + |g_2|^2 - \text{Re}[g_1^* g_2]. \quad (43)$$

The imaginary part of this matrix is factored out by using a phase matrix P_ν as:

$$\left(\frac{v_u^2}{\Lambda} Y_0^2 \right)^2 P_\nu \begin{pmatrix} |g_1 + g_2|^2 & 0 & 0 \\ 0 & G_\nu + 6\text{Re}[g_1] - 3\text{Re}[g_2] & \sqrt{3} \sqrt{9(\text{Re}[g_2])^2 + (\text{Im}[g_1^* g_2])^2} \\ 0 & \sqrt{3} \sqrt{9(\text{Re}[g_2])^2 + (\text{Im}[g_1^* g_2])^2} & G_\nu - 6\text{Re}[g_1] + 3\text{Re}[g_2] \end{pmatrix} P_\nu^*, \quad (44)$$

where

$$P_\nu = \begin{pmatrix} 1 & 0 & 0 \\ 0 & 1 & 0 \\ 0 & 0 & e^{-i\phi_\nu} \end{pmatrix}, \quad (45)$$

with

$$\tan \phi^\nu = \frac{\text{Im}[g_1^* g_2]}{3 \text{Re}[g_2]}. \quad (46)$$

On the other hand, mass eigenvalues m_{01}^2 , m_{02}^2 and m_{03}^2 of $\mathcal{M}_\nu^{2(0)}$ satisfy:

$$m_{01}^2 = |g_1 + g_2|^2, \quad m_{02}^2 + m_{03}^2 = 18 + 2(|g_1|^2 + |g_2|^2) - 2\text{Re}(g_1^* g_2), \quad m_{02}^2 m_{03}^2 = |9 - g_1^2 - g_2^2 + g_1 g_2|^2, \quad (47)$$

in the unit of $(v_u^2/\Lambda)^2 Y_0^4$. The mixing angle between the 2nd- and 3rd-family, θ_{23}^ν is given as:

$$\tan 2\theta_{23}^\nu = \frac{1}{\sqrt{3}} \frac{\sqrt{9(\text{Re}[g_2])^2 + (\text{Im}[g_1^* g_2])^2}}{\text{Re}[g_2] - 2\text{Re}[g_1]}. \quad (48)$$

If we put $\text{Re}[g_2] = 2\text{Re}[g_1]$, we obtain the maximal mixing angle $\theta_{23}^\nu = 45^\circ$. Thus, the large mixing angle is easily obtained by choosing relevant parameters g_1 and g_2 . It is also noticed that θ_{23}^ν vanishes for $g_2 = 0$. Thus, θ_{23}^ν could be 0–45° depending on g_1 and g_2 .

5.2.2 Neutrino mass matrix at nearby $\tau = i$

As discussed in the previous subsection, the large θ_{23}^ν is easily reproduced at $\tau = i$. The large flavor mixing angle between the 1st- and 2nd-family, θ_{12}^ν is also realized at nearby $\tau = i$. Mass matrix of neutrinos in Eq. (33), M_ν are corrected due to the deviation from the fixed point of $\tau = i$. Putting modular forms of Eq. (26) (see also Appendix C.1) into M_ν , the corrections to Eq. (42) are given by only a small variable ϵ in Eq. (26) in the diagonal base of S . In the 1st order approximation of ϵ , the correction $\mathcal{M}_\nu^{2(1)}$ is given as:

$$\mathcal{M}_\nu^{2(1)} = \left(\frac{v_u^2}{\Lambda} Y_0^2 \right)^2 \begin{pmatrix} 0 & \delta_{\nu 2} & \delta_{\nu 3} \\ \delta_{\nu 2}^* & \delta_{\nu 4} & \delta_{\nu 5} \\ \delta_{\nu 3}^* & \delta_{\nu 5}^* & \delta_{\nu 6} \end{pmatrix}, \quad (49)$$

where $\delta_{\nu i}$ ($i = 2-6$) are given in terms of ϵ , g_1 and g_2 . Due to the 1st order perturbation of ϵ , we can obtain the mixing angle θ_{12}^ν , which vanishes in the 0th order of perturbation. In order to estimate the flavor mixing angles, we present relevant $\delta_{\nu i}$ explicitly as:

$$\begin{aligned} \delta_{\nu 2} &= \frac{-1}{\sqrt{2}} \{ (g_1^* + g_2^*) [(1 + \sqrt{3})\epsilon_1 + \epsilon_2] + \epsilon_1^* [(3 + g_1)(1 + \sqrt{3}) - 2g_2] + \epsilon_2^* [(3 + g_1) + (1 - \sqrt{3})g_2] \} \\ &\simeq -3.34(g_1^* + g_2^*)\epsilon_1 - (10.04 + 3.35g_1 - 2.45g_2)\epsilon_1^*, \\ \delta_{\nu 3} &= \frac{1}{\sqrt{6}} \{ (g_1^* + g_2^*) [(3 - \sqrt{3})\epsilon_1 + (2\sqrt{3} - 3)\epsilon_2] + \epsilon_1^* [(3 - \sqrt{3})(3 - g_1) - 2\sqrt{3}g_2] \\ &\quad + \epsilon_2^* [(2\sqrt{3} - 3)(3 - g_1) - (3 - \sqrt{3})g_2] \} \simeq 0.90(g_1^* + g_2^*)\epsilon_1 + (2.69 - 0.90g_1 - 2.45g_2)\epsilon_1^*, \end{aligned} \quad (50)$$

where $\epsilon_1 = 2.05i\epsilon$, and $\epsilon_2 = 2\epsilon_1$ in Eq. (26) is used in last approximate equalities.

Let us estimate the mixing angles, θ_{12}^ν and θ_{13}^ν in terms of $\delta_{\nu 2}$ and $\delta_{\nu 3}$. The eigenvectors of the lowest order in $\mathcal{M}_\nu^{2(0)}$ is given,

$$u_{\nu 1}^{(0)} = \begin{pmatrix} 1 \\ 0 \\ 0 \end{pmatrix}, \quad u_{\nu 2}^{(0)} = \begin{pmatrix} 0 \\ \cos \theta_{23}^\nu \\ -\sin \theta_{23}^\nu e^{-i\phi^\nu} \end{pmatrix}, \quad u_{\nu 3}^{(0)} = \begin{pmatrix} 0 \\ \sin \theta_{23}^\nu \\ \cos \theta_{23}^\nu e^{-i\phi^\nu} \end{pmatrix}, \quad (51)$$

for eigenvalues m_{01}^2 , m_{02}^2 and m_{03}^2 of Eq. (47), respectively.

We can calculate corrections of eigenvectors in the 1st order of ϵ . In order to estimate the non-vanishing mixing angle between the 1st- and 2nd-family, we calculate the eigenvector of 1st order, $u_{\nu 2}^{(1)}$, which is given

$$u_{\nu 2}^{(1)} = C_{21}^\nu u_{\nu 1}^{(0)} + C_{23}^\nu u_{\nu 3}^{(0)}, \quad (52)$$

where

$$C_{ji}^\nu = \frac{\langle u_{\nu j}^{(0)} | \mathcal{M}_\nu^{2(1)} | u_{\nu i}^{(0)} \rangle}{m_{0j}^2 - m_{0i}^2}. \quad (53)$$

Therefore, the non-vanishing (1-2) mixing appears at the first component of $u_{\nu 2}^{(1)}$ as:

$$u_{\nu 2}^{(1)}[1, 1] = C_{21}^\nu = \frac{\delta_{\nu 2}^* \cos \theta_{23}^\nu - \delta_{\nu 3}^* \sin \theta_{23}^\nu e^{i\phi^\nu}}{m_{02}^2 - m_{01}^2}. \quad (54)$$

Here, we take $2g_1 = g_2$, which leads to the maximal mixing $\theta_{23}^\nu = 45^\circ$ as seen in Eq. (48). Then, the mass squares are given from Eq. (47) as:

$$m_{01}^2 = 9|g_1^2|, \quad m_{02}^2 = 3 \left(3 + |g_1^2| - 2\sqrt{3}|\text{Re}g_1| \right), \quad m_{03}^2 = 3 \left(3 + |g_1^2| + 2\sqrt{3}|\text{Re}g_1| \right), \quad (55)$$

in the unit of $(v_u^2/\Lambda)^2 Y_0^4$. Supposing NH of neutrino masses, we take the observed ratio of $\Delta m_{\text{atm}}^2/\Delta m_{\text{sol}}^2 = 34.2$, which leads to $g_1 = 0.61$ by neglecting the imaginary part of g_1 . Then, $\delta_{\nu 2}^*$ and $\delta_{\nu 3}^*$ are given in terms of ϵ by using $\epsilon_1 = 2.05 i \epsilon$ in Eq. (26) as follows:

$$\delta_{\nu 2}^* = -18.6 i \epsilon - 12.6 i \epsilon^*, \quad \delta_{\nu 3}^* = -1.76 i \epsilon - 0.52 i \epsilon^*. \quad (56)$$

Neglecting $\delta_{\nu 3}$ because of $|\delta_{\nu 2}^*| \gg |\delta_{\nu 3}^*|$, we have

$$u_{\nu 2}^{(1)}[1, 1] \simeq \frac{\delta_{\nu 2}^* \cos \theta_{23}^\nu}{m_{02}^2 - m_{01}^2} = -i \frac{18.6 \epsilon + 12.6 \epsilon^*}{0.383\sqrt{2}}, \quad (57)$$

where $\theta_{23}^\nu = 45^\circ$ is put. We obtain $u_{\nu 2}^{(1)}[1, 1] \simeq 0.55$ ($\theta_{12}^\nu \simeq 35^\circ$) by putting $\epsilon = 0.05 i$. Thus, the large (1-2) mixing angle could be reproduced by the correction terms in the neutrino mass matrix due to the small deviation from $\tau = i$. It is remarked that the sum of three neutrino masses is around 110 meV taking $2g_1 = g_2 = 1.22$.

On the other hand, the non-vanishing (1-3) mixing is derived as:

$$u_{\nu 3}^{(1)}[1, 1] = C_{31}^\nu = \frac{\delta_{\nu 2}^* \sin \theta_{23}^\nu + \delta_{\nu 3}^* \cos \theta_{23}^\nu e^{i\phi^\nu}}{m_{03}^2 - m_{01}^2}. \quad (58)$$

Since $(m_{03}^2 - m_{01}^2)$ is 30 times larger than $(m_{02}^2 - m_{01}^2)$, $u_{\nu 3}^{(1)}[1, 1]$ is suppressed compared with $u_{\nu 2}^{(1)}[1, 1]$. Indeed, the (1-3) mixing angle is $\mathcal{O}(0.01)$. Therefore, the observed $\theta_{13} \sim 0.15$ of the PMNS matrix should be derived from the charged lepton sector. It is noted that the correction to the (2-3) mixing is also $\mathcal{O}(0.01)$ because $u_{\nu 3}^{(1)}[2, 1]$ is suppressed due to the large $(m_{03}^2 - m_{01}^2)$.

We can also discuss the case of IH of the neutrino masses by taking $\Delta m_{\text{atm}}^2/\Delta m_{\text{sol}}^2 = -34.2$. The large mixing angles θ_{23}^ν and θ_{12}^ν are obtained if we take $g_1 = g_2/2 = -2.45$. The sum of three neutrino masses is around 90 meV.

Thus, our neutrino mass matrix is attractive one at nearby $\tau = i$. Therefore, we should examine the contribution from the charged lepton sector carefully for both NH and IH of neutrinos.

5.2.3 Charged lepton mass matrix I at $\tau = i$

The charged lepton mass matrix I is the simplest one, which is given by using only weight 2 modular forms. It is given at fixed points of $\tau = i$ in the base of S of Eq. (9) as follows:

$$M_E = v_d \begin{pmatrix} \alpha_e & 0 & 0 \\ 0 & \beta_e & 0 \\ 0 & 0 & \gamma_e \end{pmatrix} \begin{pmatrix} Y_1 & Y_3 & Y_2 \\ Y_2 & Y_1 & Y_3 \\ Y_3 & Y_2 & Y_1 \end{pmatrix} = \begin{pmatrix} \tilde{\alpha}_e & 0 & 0 \\ 0 & \tilde{\beta}_e & 0 \\ 0 & 0 & \tilde{\gamma}_e \end{pmatrix} \begin{pmatrix} 1 & -2 + \sqrt{3} & 1 - \sqrt{3} \\ 1 - \sqrt{3} & 1 & -2 + \sqrt{3} \\ -2 + \sqrt{3} & 1 - \sqrt{3} & 1 \end{pmatrix}, \quad (59)$$

where $\tilde{\alpha}_e = v_d Y_0 \alpha_e$, $\tilde{\beta}_e = v_d Y_0 \beta_e$ and $\tilde{\gamma}_e = v_d Y_0 \gamma_e$. We move to the diagonal base of S . By using the unitary transformation of Eq. (17), the mass matrix is transformed as presented in Eq. (23). Then, we have:

$$\mathcal{M}_E^{2(0)} \equiv V_{S2} M_E^\dagger M_E V_{S2}^\dagger = \frac{3}{2} \begin{pmatrix} 0 & 0 & 0 \\ 0 & \tilde{\alpha}_e^2 + 2(2 - \sqrt{3})\tilde{\beta}_e^2 + (7 - 4\sqrt{3})\tilde{\gamma}_e^2 & -(2 - \sqrt{3})(\tilde{\alpha}_e^2 - 2\tilde{\beta}_e^2 + \tilde{\gamma}_e^2) \\ 0 & -(2 - \sqrt{3})(\tilde{\alpha}_e^2 - 2\tilde{\beta}_e^2 + \tilde{\gamma}_e^2) & (7 - 4\sqrt{3})\tilde{\alpha}_e^2 + 2(2 - \sqrt{3})\tilde{\beta}_e^2 + \tilde{\gamma}_e^2 \end{pmatrix}, \quad (60)$$

which is a real matrix with rank 2.

Since the lightest charged lepton is massless at $\tau = i$, the small deviation from $\tau = i$ is required to obtain the electron mass. It is remarked that the flavor mixing between 2nd- and 3rd-family appears at the fixed point $\tau = i$ as seen in Eq. (60). It is given as:

$$\tan 2\theta_{23}^e = -2 \frac{(2 - \sqrt{3})(\tilde{\alpha}_e^2 - 2\tilde{\beta}_e^2 + \tilde{\gamma}_e^2)}{2(2\sqrt{3} - 3)(\tilde{\gamma}_e^2 - \tilde{\alpha}_e^2)} = -\frac{1}{\sqrt{3}} \frac{\tilde{\alpha}_e^2 - 2\tilde{\beta}_e^2 + \tilde{\gamma}_e^2}{\tilde{\gamma}_e^2 - \tilde{\alpha}_e^2}, \quad (61)$$

which leads to $\theta_{23}^e \simeq 15^\circ$ for $\tilde{\alpha}_e \gg \tilde{\beta}_e, \tilde{\gamma}_e$, $\theta_{23}^e \simeq -15^\circ$ for $\tilde{\gamma}_e \gg \tilde{\beta}_e, \tilde{\alpha}_e$, $\theta_{23}^e \simeq 45^\circ$ for $\tilde{\beta}_e \gg \tilde{\alpha}_e \gg \tilde{\gamma}_e$ and $\theta_{23}^e \simeq -45^\circ$ for $\tilde{\beta}_e \gg \tilde{\gamma}_e \gg \tilde{\alpha}_e$, respectively. This mixing angle leads to θ_{23} of the PMNS matrix by cooperating with the neutrino mixing angle θ_{23}^ν in Eq. (48).

5.2.4 Charged lepton mass matrix I at nearby $\tau = i$

In order to obtain the electron mass, τ should be deviated a little bit from the fixed point $\tau = i$. By using modular forms at nearby $\tau = i$ in Eq. (26), we obtain the additional contribution $\mathcal{M}_E^{2(1)}$ to $\mathcal{M}_E^{2(0)}$ in Eq. (60) of order ϵ as:

$$\mathcal{M}_E^{2(1)} \simeq \begin{pmatrix} 0 & \delta_{e2} & \delta_{e3} \\ \delta_{e2}^* & \delta_{e4} & \delta_{e5} \\ \delta_{e3}^* & \delta_{e5}^* & \delta_{e6} \end{pmatrix}, \quad (62)$$

where δ_{ei} are given in terms of ϵ , $\tilde{\alpha}_e^2$, $\tilde{\beta}_e^2$ and $\tilde{\gamma}_e^2$. In order to estimate the flavor mixing angles, we present relevant δ_{ei} as:

$$\begin{aligned} \delta_{e2} &= \frac{1}{\sqrt{2}} \{[(\sqrt{3} - 1)\epsilon_1^* + (\sqrt{3} - 2)\epsilon_2^*]\tilde{\alpha}_e^2 + [(4 - 2\sqrt{3})\epsilon_1^* + (3\sqrt{3} - 5)\epsilon_2^*]\tilde{\beta}_e^2 \\ &+ [(3\sqrt{3} - 5)\epsilon_1^* + (7 - 4\sqrt{3})\epsilon_2^*]\tilde{\gamma}_e^2\} \simeq \frac{1}{\sqrt{2}} \epsilon_1^* [(3\sqrt{3} - 5)\tilde{\alpha}_e^2 + 2(2\sqrt{3} - 3)\tilde{\beta}_e^2 + (9 - 5\sqrt{3})\tilde{\gamma}_e^2], \end{aligned} \quad (63)$$

$$\begin{aligned} \delta_{e3} &= \frac{1}{\sqrt{6}} \{[(9 - 5\sqrt{3})\epsilon_1^* + (7\sqrt{3} - 12)\epsilon_2^*]\tilde{\alpha}_e^2 + [(4\sqrt{3} - 6)\epsilon_1^* + (9 - 5\sqrt{3})\epsilon_2^*]\tilde{\beta}_e^2 \\ &+ [(\sqrt{3} - 3)\epsilon_1^* + (3 - 2\sqrt{3})\epsilon_2^*]\tilde{\gamma}_e^2\} \simeq \frac{\sqrt{6}}{2} \epsilon_1^* [(3\sqrt{3} - 5)\tilde{\alpha}_e^2 + 2(2 - \sqrt{3})\tilde{\beta}_e^2 + (1 - \sqrt{3})\tilde{\gamma}_e^2], \end{aligned} \quad (64)$$

where $\epsilon_2 = 2\epsilon_1$ in Eq. (26) is used in the last approximate equalities. The mixing angle of 1st- and 2nd-family as:

$$\tan 2\theta_{12}^e = \frac{2|\delta_{e2}|}{\frac{3}{2}[\tilde{\alpha}_e^2 + 2(2 - \sqrt{3})\tilde{\beta}_e^2 + (7 - 4\sqrt{3})\tilde{\gamma}_e^2]} \simeq \frac{4}{3\sqrt{2}} \frac{9 - 5\sqrt{3}}{7 - 4\sqrt{3}} |\epsilon_1^*| \simeq \frac{4}{3\sqrt{2}} (3 + \sqrt{3}) |\epsilon_1^*| \simeq 4.46 |\epsilon_1^*|, \quad (65)$$

where the denominator comes from the (2, 2) element of Eq. (60). In the last approximate equality, we take $\tilde{\gamma}_e \gg \tilde{\alpha}_e, \tilde{\beta}_e$, which is the case in the numerical fits of section 7. We estimate θ_{12}^e to be 0.22 at $|\epsilon_1| = |2.05 i \epsilon| = 0.1$. This magnitude of θ_{12}^e leads to $\theta_{13} \simeq 0.15$ of the PMNS matrix by cooperating with the neutrino mixing angle θ_{23}^ν in Eq. (48). The mixing angle between 1st- and 3rd-family θ_{13}^e is found to be much smaller than θ_{12}^e in the similar calculation.

In conclusion, the charged lepton mass matrix I combined with the neutrino mass matrix of Eq. (33) is expected to be consistent with the observed three PMNS mixing angles at nearby $\tau = i$. Indeed, this case works well for both NH and IH as seen in numerical results of section 7. The output of the Dirac CP violating phase and the sum of neutrino masses will be tested in the future experiments.

5.2.5 Charged lepton mass matrix II at $\tau = i$

We discuss another charged lepton mass matrix II at $\tau = i$, which is:

$$M_E = v_d \begin{pmatrix} \alpha_e & 0 & 0 \\ 0 & \beta_e & 0 \\ 0 & 0 & \gamma_e \end{pmatrix} \begin{pmatrix} Y_1^{(6)} + g_e Y_1'^{(6)} & Y_3^{(6)} + g_e Y_3'^{(6)} & Y_2^{(6)} + g_e Y_2'^{(6)} \\ Y_2^{(4)} & Y_1^{(4)} & Y_3^{(4)} \\ Y_3^{(2)} & Y_2^{(2)} & Y_1^{(2)} \end{pmatrix} \\ = v_q \begin{pmatrix} \tilde{\alpha}_e & 0 & 0 \\ 0 & \tilde{\beta}_e & 0 \\ 0 & 0 & \tilde{\gamma}_e \end{pmatrix} \begin{pmatrix} 2\sqrt{3} - 3 + g_e(7\sqrt{3} - 12) & 12 - 7\sqrt{3} + g_e(9 - 5\sqrt{3}) & 5\sqrt{3} - 9 + g_e(3 - 2\sqrt{3}) \\ 1 & 1 & 1 \\ -2 + \sqrt{3} & 1 - \sqrt{3} & 1 \end{pmatrix}, \quad (66)$$

where $\tilde{\alpha}_e = 3v_d^2 Y_0^3 \alpha_e$, $\tilde{\beta}_e = (6 - 3\sqrt{3})v_d^2 Y_0^2 \beta_e$ and $\tilde{\gamma}_e = v_d^2 Y_0 \gamma_e$.

We move to the diagonal base of S . The mass matrix $M_E^\dagger M_E$ is transformed by the unitary transformation V_{S2} as:

$$\mathcal{M}_E^{2(0)} \equiv V_{S2} M_E^\dagger M_E V_{S2}^\dagger = \frac{3}{2} \begin{pmatrix} 2\tilde{\beta}_e^2 & 0 & 0 \\ 0 & A\tilde{\gamma}_e^2 + 3(A + B_{1e} + |g_e|^2 C)\tilde{\alpha}_e^2 & -D\tilde{\gamma}_e^2 - 3(B_{2e} + Ag_e + Cg_e^*)\tilde{\alpha}_e^2 \\ 0 & -D\tilde{\gamma}_e^2 - 3(B_{2e} + Ag_e^* + Cg_e)\tilde{\alpha}_e^2 & \tilde{\gamma}_e^2 + 3(C + B_{1e} + |g_e|^2 A)\tilde{\alpha}_e^2 \end{pmatrix}, \quad (67)$$

where

$$A = 7 - 4\sqrt{3}, \quad B = 26 - 15\sqrt{3}, \quad C = 97 - 56\sqrt{3}, \quad D = 2 - \sqrt{3}, \\ B_{1e} = B(g_e + g_e^*) = 2B \operatorname{Re}[g_e], \quad B_{2e} = B(1 + |g_e|^2), \quad A^2 = C, \quad D^2 = A, \quad A + C = 4B. \quad (68)$$

The flavor mixing between the 2nd- and 3rd-family appears at the $\tau = i$ as well as the charged lepton mass matrix I.

The mass eigenvalues satisfy

$$\begin{aligned} m_{e1}^2 &= 3\tilde{\beta}_e^2, & m_{e2}^2 m_{e3}^2 &= 81(97 - 56\sqrt{3})\tilde{\alpha}_e^2 \tilde{\gamma}_e^2, \\ m_{e2}^2 + m_{e3}^2 &= 6(2 - \sqrt{3})\tilde{\gamma}_e^2 + 3(78 - 45\sqrt{3})(2 + 2\text{Re}[g_e] + |g_e|^2)\tilde{\alpha}_e^2. \end{aligned} \quad (69)$$

The imaginary part of the matrix in Eq. (67) is factored out by using a phase matrix P_e as:

$$\frac{3}{2} P_e \begin{pmatrix} 2\tilde{\beta}_e^2 & 0 & 0 \\ 0 & A\tilde{\gamma}_e^2 + 3(A + B_{1e} + |g_e|^2 C)\tilde{\alpha}_e^2 & -\sqrt{[D\tilde{\gamma}_e^2 + 3(B_{2e} + E_e)\tilde{\alpha}_e^2]^2 + F_e^2 \tilde{\alpha}_e^4} \\ 0 & -\sqrt{[D\tilde{\gamma}_e^2 + 3(B_{2e} + E_e)\tilde{\alpha}_e^2]^2 + F_e^2 \tilde{\alpha}_e^4} & \tilde{\gamma}_e^2 + 3(C + B_{1e} + |g_e|^2 A)\tilde{\alpha}_e^2 \end{pmatrix} P_e^*, \quad (70)$$

where

$$E_e = (A + C)\text{Re}[g_e], \quad F_e = (A - C)\text{Im}[g_e], \quad (71)$$

and

$$P_e = \begin{pmatrix} 1 & 0 & 0 \\ 0 & 1 & 0 \\ 0 & 0 & e^{-i\phi^e} \end{pmatrix}, \quad (72)$$

with

$$\tan \phi^e = \frac{F_e \tilde{\alpha}_e^2}{D\tilde{\gamma}_e^2 + 3(B_{2e} + E_e)\tilde{\alpha}_e^2}. \quad (73)$$

The mixing angle θ_{23}^e is given as:

$$\tan 2\theta_{23}^e = \frac{-\sqrt{[D\tilde{\gamma}_e^2 + 3(B_{2e} + E_e)\tilde{\alpha}_e^2]^2 + F_e^2 \tilde{\alpha}_e^4}}{(2\sqrt{3} - 3)\tilde{\gamma}_e^2 + 3(45 - 26\sqrt{3})(1 - |g_e|^2)\tilde{\alpha}_e^2}. \quad (74)$$

Neglecting the imaginary part of g_e ($g_e = \text{Re}[g_e]$), it is given simply as:

$$\tan 2\theta_{23}^e = -\frac{1}{\sqrt{3}} \frac{\tilde{\gamma}_e^2 + 3(7 - 4\sqrt{3})(1 + 4g_e + g_e^2)\tilde{\alpha}_e^2}{\tilde{\gamma}_e^2 - 3(7 - 4\sqrt{3})(1 - g_e^2)\tilde{\alpha}_e^2}. \quad (75)$$

We take $\tilde{\beta}_e^2 \ll \tilde{\alpha}_e^2, \tilde{\gamma}_e^2$ due to the mass hierarchy of the charged lepton masses. There are two possible choices of $\tilde{\alpha}_e^2 \ll \tilde{\gamma}_e^2$ and $\tilde{\gamma}_e^2 \ll \tilde{\alpha}_e^2$.

In the case of $\tilde{\alpha}_e^2 \ll \tilde{\gamma}_e^2$,

$$\tan 2\theta_{23}^e \simeq -\frac{1}{\sqrt{3}} [1 + 6(7 - 4\sqrt{3})(1 + 2g_e) \frac{\tilde{\alpha}_e^2}{\tilde{\gamma}_e^2}]. \quad (76)$$

At the limit of $\tilde{\alpha}_e^2/\tilde{\gamma}_e^2 = 0$, we obtain $\theta_{23}^e = -15^\circ$.

On the other hand, in the case of $\tilde{\alpha}_e^2 \gg \tilde{\gamma}_e^2$, Eq. (75) turns to

$$\tan 2\theta_{23}^e \simeq \frac{1}{\sqrt{3}} \frac{1 + 4g_e + g_e^2}{1 - g_e^2}, \quad (77)$$

which gives $|\theta_{23}^e| = 0-45^\circ$ by choosing relevant g_e . Thus, the large θ_{23}^e is obtained easily.

5.2.6 Charged lepton mass matrix \mathbf{II} at nearby $\tau = i$

The mass matrix of the charged lepton in Eq. (66), M_E is corrected due to the deviation from the fixed point of $\tau = i$. In the 1st order approximation of ϵ , the correction $\mathcal{M}_E^{2(1)}$ to $\mathcal{M}_E^{2(0)}$ of Eq. (67) is given by the following matrix:

$$\mathcal{M}_E^{2(1)} = \begin{pmatrix} \delta_{e1} & \delta_{e2} & \delta_{e3} \\ \delta_{e2}^* & \delta_{e4} & \delta_{e5} \\ \delta_{e3}^* & \delta_{e5}^* & \delta_{e6} \end{pmatrix}, \quad (78)$$

where δ_{ei} are given in terms of ϵ , g_e , $\tilde{\alpha}_e^2$, $\tilde{\beta}_e^2$ and $\tilde{\gamma}_e^2$. By the 1st order perturbation of ϵ , we can obtain the mixing angle θ_{12}^e , which vanishes in the 0th order of perturbation. In order to estimate the flavor mixing angles, we present relevant δ_{ei} as:

$$\begin{aligned} \delta_{e2} &= \frac{3}{\sqrt{2}}\tilde{\alpha}_e^2(g_e^* - 1)\{[(11\sqrt{3} - 19) + (41\sqrt{3} - 71)g_e]\epsilon_1^* - [(15\sqrt{3} - 26) + (56\sqrt{3} - 97)g_e]\epsilon_2^*\} \\ &\quad + \frac{1}{\sqrt{2}}\tilde{\gamma}_e^2[(3\sqrt{3} - 5)\epsilon_1^* + (7 - 4\sqrt{3})\epsilon_2^*] \simeq (0.193 + 0.052g_e)\tilde{\alpha}_e^2(g_e^* - 1)\epsilon_1^* + 0.240\tilde{\gamma}_e^2\epsilon_1^*, \\ \delta_{e3} &= \frac{1}{\sqrt{6}}\tilde{\alpha}_e^2(g_e^* - 1)\{[3(71\sqrt{3} - 123) + 3(19\sqrt{3} - 33)g_e]\epsilon_1^* - [3(97\sqrt{3} - 168) + (26\sqrt{3} - 45)g_e]\epsilon_2^*\} \\ &\quad + \frac{1}{\sqrt{2}}\tilde{\gamma}_e^2[(1 - \sqrt{3})\epsilon_1^* + (\sqrt{3} - 2)\epsilon_2^*] \simeq -(0.052 + 0.138g_e)\tilde{\alpha}_e^2(g_e^* - 1)\epsilon_1^* - 0.897\tilde{\gamma}_e^2\epsilon_1^*, \end{aligned} \quad (79)$$

where $\mathcal{O}(\tilde{\beta}_e^2)$ is neglected and $\epsilon_2 = 2\epsilon_1$ of Eq. (26) is taken in last approximate equalities.

Let us discuss the mixing angles of θ_{12}^e and θ_{13}^e of the charged lepton flavors, which vanish in the leading terms of the mass matrix. As seen in Eq. (79), both δ_{e2} and δ_{e3} are of $\mathcal{O}(\tilde{\alpha}_e^2, \tilde{\gamma}_e^2) \times \epsilon_1$ for $g_e = \mathcal{O}(1)$. Suppose $\tilde{\gamma}_e^2 \ll \tilde{\alpha}_e^2$ to realize the hierarchy of charged lepton masses in Eq. (69)². Then, we have mass eigenvalues from Eq. (69) as:

$$m_{e1}^2 = 3\tilde{\beta}_e^2, \quad m_{e2}^2 \simeq \frac{9(2 - \sqrt{3})}{2 + 2\text{Re}[g_e] + |g_e|^2}\tilde{\gamma}_e^2, \quad m_{e3}^2 \simeq 3(78 - 45\sqrt{3})(2 + 2\text{Re}[g_e] + |g_e|^2)\tilde{\alpha}_e^2, \quad (80)$$

which lead to

$$\frac{m_{e2}^2}{m_{e3}^2} \simeq \frac{7 + 4\sqrt{3}}{(2 + 2\text{Re}[g_e] + |g_e|^2)^2}\frac{\tilde{\gamma}_e^2}{\tilde{\alpha}_e^2}. \quad (81)$$

The mixing angles between 1st- and 2nd-family θ_{12}^e and between 1st- and 3rd-family θ_{13}^e are given approximately as:

$$\theta_{12}^e \simeq \left| \frac{\delta_{e2}}{m_{e2}^2} \right|, \quad \theta_{13}^e \simeq \left| \frac{\delta_{e3}}{m_{e3}^2} \right|, \quad (82)$$

where

$$\delta_{e2} \simeq (0.193 + 0.052g_e)\tilde{\alpha}_e^2(g_e^* - 1)\epsilon_1^*, \quad \delta_{e3} \simeq -(0.052 + 0.138g_e)\tilde{\alpha}_e^2(g_e^* - 1)\epsilon_1^*, \quad (83)$$

²Indeed, a successful numerical result is obtained for $\tilde{\gamma}_e^2 \ll \tilde{\alpha}_e^2$ in section 7.

respectively. Substituting mass eigenvalues of Eq. (80) into mixing angles in Eq. (82), we can estimate magnitudes of θ_{12}^e and θ_{13}^e . The mixing angle of θ_{12}^e is given as:

$$\begin{aligned}\theta_{12}^e &\simeq \left| \frac{(0.193 + 0.052g_e)(g_e^* - 1)}{9(2 - \sqrt{3})} (2 + 2\text{Re}[g_e] + |g_e|^2) \frac{\tilde{\alpha}_e^2}{\tilde{\gamma}_e^2} \epsilon_1^* \right| \\ &= \left| \frac{(0.193 + 0.052g_e)(g_e^* - 1)(26 + 15\sqrt{3})}{9(2 + 2\text{Re}[g_e] + |g_e|^2)} \frac{m_{e3}^2}{m_{e2}^2} \epsilon_1^* \right| \simeq 1.7 \frac{|(0.193 + 0.052g_e)(g_e^* - 1)|}{2 + 2\text{Re}[g_e] + |g_e|^2} |\epsilon_1^*| \times 10^3, \quad (84)\end{aligned}$$

where the mass ratio of Eq. (81) is used to remove the ratio $\tilde{\gamma}_e^2/\tilde{\alpha}_e^2$. In the last equality, observed masses of the tauon and the muon are input. Suppose the magnitude of $|\epsilon_1^*|$ to be 0.02 as a typical value. As seen in Eq. (84), θ_{12}^e depends on g_e . Indeed, θ_{12}^e vanishes at $g_e = 1$ or -3.62 while it is of order one if $|g_e| \ll 1$ or $|g_e| \gg 1$. On the other hand, θ_{13}^e is suppressed due to the factor of $1/m_{e3}^2$ as seen Eq. (82).

In conclusion, the charged lepton mass matrix II combined with the neutrino mass matrix of Eq. (33) is expected to be consistent with the observed three PMNS mixing angles at nearby $\tau = i$ as well as charged lepton mass matrix I. Indeed, this case works well for NH, but it leads to the sum of neutrino masses larger than 120 meV for IH as seen in numerical results of section 7.

5.3 Lepton mass matrix at $\tau = \omega$

5.3.1 Neutrino mass matrix at $\tau = \omega$

Let us consider the neutrino mass matrix at $\tau = \omega$, where there exists the residual symmetry of the A_4 group $\mathbb{Z}_3^{ST} = \{I, ST, (ST)^2\}$. By putting the modular forms in Table 1 into Eq. (33), the neutrino mass matrix is written as:

$$M_\nu = \frac{v_u^2}{\Lambda} Y_0^2 \left[\frac{3}{2} \begin{pmatrix} 2 & -\omega^2 & \frac{1}{2}\omega \\ -\omega^2 & -\omega & -1 \\ \frac{1}{2}\omega & -1 & 2\omega^2 \end{pmatrix} + \frac{9}{4} \omega g_{\nu 2} \begin{pmatrix} 0 & 0 & 1 \\ 0 & 1 & 0 \\ 1 & 0 & 0 \end{pmatrix} \right], \quad (85)$$

where the $g_{\nu 1}$ term of Eq. (33) disappears because of $\mathbf{Y}_1^{(4)} = 0$ at $\tau = \omega$. We move to the diagonal base of ST . By using the unitary transformation of Eq. (22), V_{ST4} or V_{ST5} , the neutrino mass matrix is transformed as:

$$\mathcal{M}_\nu^{2(0)} \equiv V_{ST4(5)} \hat{M}_\nu^\dagger \hat{M}_\nu V_{ST4(5)}^\dagger = \left(\frac{9}{4} \frac{v_u^2}{\Lambda} Y_0^2 \right)^2 \begin{pmatrix} |2 + g_{\nu 2}|^2 & 0 & 0 \\ 0 & |1 - g_{\nu 2}|^2 & 0 \\ 0 & 0 & |1 - g_{\nu 2}|^2 \end{pmatrix}. \quad (86)$$

The neutrino mass matrix is diagonal and two neutrinos are degenerated at $\tau = \omega$. Three neutrino masses are degenerate if $g_{\nu 2} = -0.5$. Then, large flavor mixing angles are possibly reproduced if small off diagonal elements are generated by the deviation from $\tau = \omega$.

5.3.2 Neutrino mass matrix at nearby $\tau = \omega$

Neutrino mass matrix in Eq. (33), M_ν is corrected due to the deviation from the fixed point of $\tau = \omega$. After putting modular forms of Eq. (28) and moving to the diagonal base of ST by V_{ST4} , the corrections

to Eq. (86) are given by only a small variable ϵ of in Eq. (28). In the 1st order approximation of ϵ , the correction $\mathcal{M}_\nu^{2(1)}$ to $\mathcal{M}_\nu^{2(0)}$ of Eq. (86) is given by the following matrix:

$$\mathcal{M}_\nu^{2(1)} = \left(\frac{9 v_u^2}{4 \Lambda} Y_0^2 \right)^2 \begin{pmatrix} \delta_{\nu 1} & \delta_{\nu 2} & \delta_{\nu 3} \\ \delta_{\nu 2}^* & \delta_{\nu 4} & \delta_{\nu 5} \\ \delta_{\nu 3}^* & \delta_{\nu 5}^* & \delta_{\nu 6} \end{pmatrix}, \quad (87)$$

where $\delta_{\nu i}$ are given in terms of ϵ , $g_{\nu 1}$ and $g_{\nu 2}$. By the 1st order perturbation of ϵ , we can obtain the mixing angle θ_{12}^ν , which vanishes in the 0th order of perturbation. In order to estimate the flavor mixing angles, we present off diagonal elements, $\delta_{\nu 2}$, $\delta_{\nu 3}$ and $\delta_{\nu 5}$ as:

$$\begin{aligned} \delta_{\nu 2} &= \frac{3}{4}(2 + g_{\nu 2}^*)\epsilon_1 + \frac{3}{8}(1 + 6g_{\nu 1}^*)(1 - g_{\nu 2})\epsilon_1^* - \frac{21}{8}(2 + g_{\nu 2}^*)\epsilon_2 - \frac{3}{4}(4 - 3g_{\nu 1}^*)(1 - g_{\nu 2})\epsilon_2^* \\ &\simeq -\frac{9}{2}(2 + g_{\nu 2}^*)\epsilon_1 - \frac{9}{8}(5 - 6g_{\nu 1}^*)(1 - g_{\nu 2})\epsilon_1^*, \\ \delta_{\nu 3} &= \frac{3}{8}(1 + 6g_{\nu 1})(2 + g_{\nu 2}^*)\epsilon_1 + \frac{3}{4}(1 - g_{\nu 2})\epsilon_1^* - \frac{3}{4}(4 - 3g_{\nu 1})(2 + g_{\nu 2}^*)\epsilon_2 - \frac{21}{8}(1 - g_{\nu 2})\epsilon_2^* \\ &\simeq -\frac{9}{8}(5 - 6g_{\nu 1})(2 + g_{\nu 2}^*)\epsilon_1 - \frac{9}{2}(1 - g_{\nu 2})\epsilon_1^*, \\ \delta_{\nu 5} &= \frac{3}{4}(1 - 3g_{\nu 1}^*)(1 - g_{\nu 2})\epsilon_1^* - \frac{3}{2}(1 - g_{\nu 2}^*)\epsilon_1 - \frac{3}{4}(8 + 3g_{\nu 1}^*)(1 - g_{\nu 2})\epsilon_2^* + \frac{21}{4}(1 - g_{\nu 2}^*)\epsilon_2 \\ &\simeq -\frac{9}{4}(5 + 3g_{\nu 1}^*)(1 - g_{\nu 2})\epsilon_1^* + 9(1 - g_{\nu 2}^*)\epsilon_1, \end{aligned} \quad (88)$$

where $\epsilon_1 = 2.1i\epsilon$, and $\epsilon_2 = 2\epsilon_1$ of Eq. (28) is used for last approximate equalities. If we move to the diagonal base of ST by using V_{ST5} instead of V_{ST4} , we obtain the corrections by exchanging the above results as:

$$\delta_{\nu 2} \leftrightarrow \delta_{\nu 3}, \quad \delta_{\nu 5} \leftrightarrow \delta_{\nu 5}^*. \quad (89)$$

Indeed, we move to the diagonal base of ST by using V_{ST5} for the charged lepton mass matrix II in section 5.3.5.

It is noticed that the off-diagonal elements are enhanced by large coefficients in front of ϵ_1 and ϵ_1^* . For example, $|\delta_{\nu 5}|$ could be comparable to diagonal element if $|\epsilon_1| = 0.1$ is taken. Since the 2nd and 3rd eigenvalues are degenerated as seen in Eq. (86), the large (2–3) mixing angle is easily obtained due to those corrections. The large (1–2) mixing angle is also possible by choosing relevant $g_{\nu 1}$ and $g_{\nu 2}$. The (1–3) mixing angle is relatively small due to the fixed mass square difference Δm_{31}^2 . On the other hand, the sum of neutrino masses may increase if mass eigenvalues become quasi-degenerate. Then, its cosmological upper-bound provides a crucial test for the lepton mass matrices. Therefore, we should examine the contribution from the charged lepton sector carefully for both NH and IH of neutrinos to judge it working well or not. Indeed, we will see in section 7 that the model of the charged lepton mass matrix I is excluded by the sum of neutrino masses while the model with the charged lepton mass matrix II is consistent with it for both NH and IH of neutrino masses.

5.3.3 Charged lepton mass matrix \mathbf{I} at $\tau = \omega$

We discuss the charged lepton mass matrix \mathbf{I} at the fixed point $\tau = \omega$ by using modular forms in Table 1. In the base of S and T of Eq. (9), the charged lepton mass matrix \mathbf{I} in Eq. (36) is given as:

$$M_E = \begin{pmatrix} \tilde{\alpha}_e & 0 & 0 \\ 0 & \tilde{\beta}_e & 0 \\ 0 & 0 & \tilde{\gamma}_e \end{pmatrix} \begin{pmatrix} 1 & -\frac{1}{2}\omega^2 & \omega \\ \omega & 1 & -\frac{1}{2}\omega^2 \\ -\frac{1}{2}\omega^2 & \omega & 1 \end{pmatrix}, \quad (90)$$

where $\tilde{\alpha}_e = v_d Y_0 \alpha_e$, $\tilde{\beta}_e = v_d Y_0 \beta_e$ and $\tilde{\gamma}_e = v_d Y_0 \gamma_e$. By using the unitary transformation of Eq. (22), V_{ST4} , like the case of the neutrino mass matrix, $M_E^\dagger M_E$ is transformed as:

$$\mathcal{M}_E^{2(0)} \equiv V_{ST4} M_E^\dagger M_E V_{ST4}^\dagger = \frac{9}{4} \begin{pmatrix} \tilde{\alpha}_e^2 & 0 & 0 \\ 0 & \tilde{\gamma}_e^2 & 0 \\ 0 & 0 & \tilde{\beta}_e^2 \end{pmatrix}. \quad (91)$$

It is remarked that it is diagonal one as well as the neutrino mass matrix in Eq. (86).

5.3.4 Charged lepton mass matrix \mathbf{I} at nearby $\tau = \omega$

The charged lepton mass matrix in Eq. (90), M_E is corrected due to the deviation from the fixed point of $\tau = \omega$. After putting modular forms of Eq. (28) and moving to the diagonal base of ST by V_{ST4} , the correction $\mathcal{M}_E^{2(1)}$ to $\mathcal{M}_E^{2(0)}$ of Eq. (91) is given in the 1st order approximation of ϵ as:

$$\mathcal{M}_E^{2(1)} = \begin{pmatrix} \delta_{e1} & \delta_{e2} & \delta_{e3} \\ \delta_{e2}^* & \delta_{e4} & \delta_{e5} \\ \delta_{e3}^* & \delta_{e5}^* & \delta_{e6} \end{pmatrix}, \quad (92)$$

where

$$\delta_{e2} = i \tilde{\alpha}_e^2 (\epsilon_1 - \frac{1}{2} \epsilon_2) + \frac{1}{2} i \tilde{\gamma}_e^2 (\epsilon_1^* + \epsilon_2^*) = \frac{3}{2} i \tilde{\gamma}_e^2 \epsilon_1^*, \quad (93)$$

$$\delta_{e3} = \frac{1}{2} i \tilde{\alpha}_e^2 (\epsilon_1 + \epsilon_2) + i \tilde{\beta}_e^2 (\epsilon_1^* - \frac{1}{2} \epsilon_2^*) = \frac{3}{2} i \tilde{\alpha}_e^2 \epsilon_1, \quad (94)$$

$$\delta_{e5} = -i \tilde{\gamma}_e^2 (\epsilon_1 - \frac{1}{2} \epsilon_2) - \frac{1}{2} i \tilde{\beta}_e^2 (\epsilon_1^* + \epsilon_2^*) = -\frac{3}{2} i \tilde{\beta}_e^2 \epsilon_1^*, \quad (95)$$

where $\epsilon_2 = 2\epsilon_1$ of Eq. (28) is used for last equalities. Due to $\tilde{\beta}_e^2 \gg \tilde{\gamma}_e^2 \gg \tilde{\alpha}_e^2$, mixing angles θ_{ij}^e are easily obtained by using $\epsilon_1 = 2.1i\epsilon$ as follows:

$$\theta_{12}^e \simeq \theta_{23}^e \simeq \frac{2}{3} |\epsilon_1| \simeq \frac{4.2}{3} |\epsilon|, \quad (96)$$

which are smaller than 0.1, moreover, θ_{13}^e is highly suppressed due to the factor $\tilde{\alpha}_e^2/\tilde{\beta}_e^2$. Thus, the flavor mixing angles of the charged lepton are very small at nearby the fixed point $\tau = \omega$. The PMNS mixing angles come from mainly the neutrino sector in this case. Therefore, the increase of the sum of neutrino masses is unavoidable since mass eigenvalues become quasi-degenerate in order to reproduce large mixing angles.

5.3.5 Charged lepton mass matrix II at $\tau = \omega$

We discuss the charged lepton mass matrix II at the fixed point $\tau = \omega$ by using modular forms in Table 1. The charged lepton mass matrix II in Eq. (38) is given as:

$$M_E = \begin{pmatrix} \tilde{\alpha}_e & 0 & 0 \\ 0 & \tilde{\beta}_e & 0 \\ 0 & 0 & \tilde{\gamma}_e \end{pmatrix} \begin{pmatrix} g_e & -2\omega^2 g_e & -2\omega g_e \\ -\frac{1}{2}\omega & 1 & \omega^2 \\ -\frac{1}{2}\omega^2 & \omega & 1 \end{pmatrix}, \quad (97)$$

where $\tilde{\alpha}_e = (9/8)v_d Y_0^3 \alpha_d$, $\tilde{\beta}_e = (3/2)v_d Y_0^2 \beta_q$ and $\tilde{\gamma}_e = v_d Y_0 \gamma_e$. By using the unitary transformation of Eq. (22), V_{ST5} , which is different from the case of the charged lepton mass matrix I, $M_E^\dagger M_E$ is transformed as:

$$\mathcal{M}_E^{2(0)} \equiv V_{ST5} M_E^\dagger M_E V_{ST5}^\dagger = \frac{9}{4} \begin{pmatrix} 0 & 0 & 0 \\ 0 & 0 & 0 \\ 0 & 0 & 4\tilde{\alpha}_e^2 |g_e|^2 + \tilde{\beta}_e^2 + \tilde{\gamma}_e^2 \end{pmatrix}, \quad (98)$$

which gives two massless charged leptons.

5.3.6 Charged lepton mass matrix II at nearby $\tau = \omega$

The charged lepton mass matrix in Eq. (97), M_E is corrected due to the deviation from the fixed point of $\tau = \omega$. After putting modular forms of Eq. (28) and moving to the diagonal base of ST by V_{ST5} , the correction $\mathcal{M}_E^{2(1)}$ to $\mathcal{M}_E^{2(0)}$ of Eq. (98) is given as:

$$\mathcal{M}_E^{2(1)} = \begin{pmatrix} 0 & 0 & \delta_{e3} \\ 0 & 0 & \delta_{e5} \\ \delta_{e3}^* & \delta_{e5}^* & \delta_{e6} \end{pmatrix} \quad (99)$$

where δ_{ei} are given in terms of ϵ , g_e , $\tilde{\alpha}_e^2$, $\tilde{\beta}_e^2$ and $\tilde{\gamma}_e^2$. By the 1st order perturbation of ϵ , we can obtain the mixing angles θ_{23}^e and θ_{13}^e , which vanish in the 0th order of perturbation. In order to estimate the flavor mixing angles, we present δ_{e3} and δ_{e5} as:

$$\begin{aligned} \delta_{e3} &= -2\tilde{\alpha}_e^2 g_e (2 + g_e^*) (\epsilon_1^* + \epsilon_2^*) + \frac{1}{6} \tilde{\beta}_e^2 (\epsilon_1^* - 8\epsilon_2^*) + \frac{1}{2} i \tilde{\gamma}_e^2 (\epsilon_1^* + \epsilon_2^*) \\ &\simeq [-6\tilde{\alpha}_e^2 g_e (2 + g_e^*) - \frac{5}{2} \tilde{\beta}_e^2 + \frac{3}{2} i \tilde{\gamma}_e^2] \epsilon_1^*, \\ \delta_{e5} &= \tilde{\alpha}_e^2 |g_e|^2 (-4\epsilon_1^* + 2\epsilon_2^*) + \tilde{\beta}_e^2 (\frac{1}{3}\epsilon_1^* - \frac{7}{6}\epsilon_2^*) + i \tilde{\gamma}_e^2 (\epsilon_1^* - \frac{1}{2}\epsilon_2^*) \simeq -2\tilde{\beta}_e^2 \epsilon_1^*, \end{aligned} \quad (100)$$

where $\epsilon_2 = 2\epsilon_1$ of Eq. (28) is used in last approximate equalities. If $\tilde{\beta}_e^2 \gg \tilde{\alpha}_e^2 |g_e|^2, \tilde{\gamma}_e^2$, mixing angles θ_{23}^e and θ_{13}^e are given :

$$\theta_{23}^e \simeq \frac{8}{9} |\epsilon_1| \simeq \frac{17}{9} |\epsilon|, \quad \theta_{13}^e \simeq \frac{10}{9} |\epsilon_1| \simeq \frac{21}{9} |\epsilon|, \quad (101)$$

where $\epsilon_1 = 2.1i\epsilon$ in Eq. (28) is taken. Therefore, these mixing angles are at most 0.1. It is noticed that θ_{12}^e vanishes.

On the other hand, if $\tilde{\alpha}_e^2 |g_e^2| \gg \tilde{\beta}_e^2, \tilde{\gamma}_e^2$, the mixing angle θ_{13}^e is given :

$$\theta_{13}^e \simeq \frac{2}{3} \left| \frac{2 + g_e^*}{g_e} \epsilon_1 \right| \simeq \frac{8.4}{3} \left| \frac{1}{g_e} \epsilon \right|, \quad (102)$$

where $|g_e|$ is supposed to be much smaller than 1 in the last equality. Therefore, θ_{13}^e is enhanced by taking $|g_e| \simeq 0.1$. It could be of order 1 if $|\epsilon| = 0.05$. Thus, the flavor mixing angle θ_{13}^e contributes significantly to the PMNS mixing angle θ_{13} .

Indeed, we obtain the allowed region of $|\epsilon| \simeq 0.1$ with $|g_e| \simeq 0.2$ for NH of neutrinos by performing numerical scan in section 7. However, for IH of neutrinos, $|\epsilon| \simeq 0.15$ is obtained with large $|g_e| = 5-10$.

5.4 Lepton mass matrix at $\tau = i\infty$

5.4.1 Neutrino mass matrix at $\tau = i\infty$

Let us consider the neutrino mass matrix at $\tau = i\infty$, where there exists the residual symmetries of the A_4 group $\mathbb{Z}_3^T = \{I, T, T^2\}$. By putting the modular forms in Table 1 into Eq. (33), the neutrino mass matrix is written as:

$$M_\nu = \frac{v_u^2 Y_0^2}{\Lambda} \left[\begin{pmatrix} 2 & 0 & 0 \\ 0 & 0 & -1 \\ 0 & -1 & 0 \end{pmatrix} + g_{\nu 1} \begin{pmatrix} 1 & 0 & 0 \\ 0 & 0 & 1 \\ 0 & 1 & 0 \end{pmatrix} \right], \quad (103)$$

where the $g_{\nu 2}$ term of Eq. (33) disappears because of $\mathbf{Y}_{\mathbf{1}'}^{(4)} = 0$ at $\tau = i\infty$. Since T is already in the diagonal base as seen in Eq. (9), we can write down $M_\nu^\dagger M_\nu$ straightforward as follows:

$$\mathcal{M}_\nu^{2(0)} \equiv M_\nu^\dagger M_\nu = \left(\frac{v_u^2 Y_0^2}{\Lambda} \right)^2 \begin{pmatrix} |2 + g_{\nu 1}|^2 & 0 & 0 \\ 0 & |1 - g_{\nu 1}|^2 & 0 \\ 0 & 0 & |1 - g_{\nu 1}|^2 \end{pmatrix}, \quad (104)$$

which is a diagonal matrix as well as the neutrino mass matrix at $\tau = \omega$ in Eq. (86). Three neutrino masses are degenerate if $g_{\nu 1} = -0.5$. Then, large flavor mixing angles are possibly reproduced if small off diagonal elements are generated due to finite effect of τ .

5.4.2 Neutrino mass matrix towards $\tau = i\infty$

Neutrino mass matrix in Eq. (33), M_ν is given from the finite correction of $\tau = i\infty$. Taking account of modular forms of Eq. (29), the corrections to Eq. (104) are given by only a small variable ϵ of in Eq. (29). In the 1st order approximation of ϵ , the correction $\mathcal{M}_\nu^{2(1)}$ to $\mathcal{M}_\nu^{2(0)}$ of Eq. (104) is given in terms of

$$\delta = -6 e^{\frac{2}{3}\pi i \text{Re} \tau} e^{-\frac{2}{3}\pi \text{Im} \tau}. \quad (105)$$

It is given by the following matrix:

$$\mathcal{M}_\nu^{2(1)} \simeq \left(\frac{v_u^2 Y_0^2}{\Lambda} \right)^2 \begin{pmatrix} 0 & -\delta^* (1 - g_{\nu 1})(1 + 2g_{\nu 2}^*) & \delta (2 + g_{\nu 1}^*)(1 + 2g_{\nu 2}) \\ -\delta (1 - g_{\nu 1}^*)(1 + 2g_{\nu 2}) & 0 & 2\delta^* (1 - g_{\nu 1})(1 - g_{\nu 2}^*) \\ \delta^* (2 + g_{\nu 1})(1 + 2g_{\nu 2}^*) & 2\delta (1 - g_{\nu 1}^*)(1 - g_{\nu 2}) & 0 \end{pmatrix}. \quad (106)$$

If we take $\text{Im}\tau = 1.6$, we get $|\delta| \simeq 0.21$, which is derived in Eq. (105). Thus, the large (2–3) mixing angle is easily obtained since 2nd and 3rd eigenvalues are degenerated as seen in Eq. (104). The large (1–2) mixing angle is also possible by choosing relevant $g_{\nu 1}$ and $g_{\nu 2}$. The (1–3) mixing angle is expected relatively small due to the fixed mass square difference Δm_{31}^2 . Then, the cosmological upper-bound of the sum of neutrino masses is a crucial criterion to test neutrino mass matrices. In section 7, we will see that both charged lepton mass matrix I and II satisfy the sum of neutrino masses less than the cosmological upper-bound 120 meV for NH of neutrinos, but they do not satisfy it for IH.

5.4.3 Charged lepton mass matrix I and II at $\tau = i\infty$

The charged lepton mass matrices of I and II in Eqs. (36) and (38) are simple at $\tau = i\infty$ since the modular forms of weight 2, 4 and 6 are given in the T diagonal base. Putting them of Table 1 into the charged lepton mass matrices in Eqs. (36) and (38), we obtain

$$M_E = \begin{pmatrix} \tilde{\alpha}_e & 0 & 0 \\ 0 & \tilde{\beta}_e & 0 \\ 0 & 0 & \tilde{\gamma}_e \end{pmatrix}, \quad (107)$$

where $\tilde{\alpha}_e = v_d Y_0 \alpha_e$, $\tilde{\beta}_e = v_d Y_0 \beta_e$ and $\tilde{\gamma}_e = v_d Y_0 \gamma_e$ for the case I and $\tilde{\alpha}_e = v_d Y_0^3 \alpha_e$, $\tilde{\beta}_e = v_d Y_0^2 \beta_e$ and $\tilde{\gamma}_e = v_d Y_0 \gamma_e$ for the case II. The mass matrix $M_E^\dagger M_E$ is given as:

$$\mathcal{M}_E^{2(0)} \equiv M_E^\dagger M_E = \begin{pmatrix} \tilde{\alpha}_e^2 & 0 & 0 \\ 0 & \tilde{\beta}_e^2 & 0 \\ 0 & 0 & \tilde{\gamma}_e^2 \end{pmatrix}. \quad (108)$$

The flavor mixing appears through the finite effect of $\text{Im}[\tau]$.

5.4.4 Charged lepton mass matrix I and II towards $\tau = i\infty$

The charged lepton mass matrices of I and II in Eqs. (36) and (38) are given from the finite correction of $\tau = i\infty$. By using modular forms of Eq. (29), the corrections to Eq. (108) are given by only a small variable ϵ of Eq. (29). In the 1st order approximation of ϵ , the correction $\mathcal{M}_E^{2(1)}$ to $\mathcal{M}_E^{2(0)}$ of Eq. (108) is given in terms of δ of Eq. (105) as:

$$\mathcal{M}_E^{2(1)} \simeq \begin{pmatrix} 0 & \delta^* \tilde{\beta}_e^2 & \delta \tilde{\alpha}_e^2 \\ \delta \tilde{\beta}_e^2 & 0 & \delta^* \tilde{\gamma}_e^2 \\ \delta^* \tilde{\alpha}_e^2 & \delta \tilde{\gamma}_e^2 & 0 \end{pmatrix}, \quad (109)$$

for the charged lepton mass matrix I. On the other hand, for the charged lepton mass matrix II, it is:

$$\mathcal{M}_E^{2(1)} \simeq \begin{pmatrix} 0 & -\delta^* \tilde{\beta}_e^2 & (1 + 2g_e) \delta \tilde{\alpha}_e^2 \\ -\delta \tilde{\beta}_e^2 & 0 & \delta^* \tilde{\gamma}_e^2 \\ (1 + 2g_e^*) \delta \tilde{\alpha}_e^2 & \delta \tilde{\gamma}_e^2 & 0 \end{pmatrix}. \quad (110)$$

In both charged lepton mass matrices I and II, (1–2) and (2–3) families mixing angles θ_{23}^e , θ_{12}^e , are given as:

$$\theta_{12}^e \simeq \frac{|\delta^*| \tilde{\beta}_e^2}{\tilde{\beta}_e^2} \simeq |\delta|, \quad \theta_{23}^e \simeq \frac{|\delta^*| \tilde{\gamma}_e^2}{\tilde{\gamma}_e^2} = |\delta|, \quad (111)$$

respectively, where $\tilde{\gamma}_e^2 \gg \tilde{\beta}_e^2 \gg \tilde{\alpha}_e^2$. If we take $\text{Im}\tau = 1.6$, the magnitude of $\theta_{12}^e \simeq |\delta| \simeq 0.21$. This magnitude of θ_{12}^e contributes significantly to the PMNS mixing angle θ_{13} . On the other hand, the mixing angle θ_{13}^e between 1st- and 3rd-family is highly suppressed due to the factor $\tilde{\alpha}_e^2/\tilde{\gamma}_e^2$.

It is remarked that the mass matrix of Eq. (110) is agreement with Eq.(109) in the case of $|g_e| \ll 1$ apart from the minus sign in front of (1,2) and (2,1) entries. However, this minus sign of the charged lepton mass matrix II spoils to reproduce large mixing angles of the PMNS matrix, θ_{12} and θ_{23} together although the charged lepton mass matrix I is successful to reproduce the observed PMNS mixing angles.

Alternatively, the observed PMNS mixing angles can be reproduced in the charged lepton mass matrix II if a large mixing angle for θ_{13}^e is obtained by taking $|g_e| \gg 1$ with $\tilde{\alpha}_e^2 \gg \tilde{\beta}_e^2, \tilde{\gamma}_e^2$. This case is shown numerically in section 7.

6 Quark mass matrices in the A_4 modular invariance

If flavors of quarks and leptons are originated from a same two-dimensional compact space, the leptons and quarks have same flavor symmetry and the same value of the modulus τ . Therefore, the modular symmetry provides a new approach towards the unification of quark and lepton flavors. In order to investigate the possibility of the quark/lepton unification, we discuss a A_4 modular invariant flavor model for quarks together with the lepton sector.

6.1 Model of quark mass matrices

We take the assignments of A_4 irreducible representations and modular weights for quarks like the charged leptons. That is, three left-handed quarks are components of the triplet of the A_4 group, but three right-handed quarks, (u^c, c^c, t^c) and (d^c, s^c, b^c) are three different singlets $(\mathbf{1}, \mathbf{1}'', \mathbf{1}')$ of A_4 , respectively. Quark mass matrices depend on modular weights of the left-handed and the right-handed quarks since the sum of their weight including modular forms should vanish. Let us fix the weights of left-handed quarks to be -2 like the left-handed charged leptons. If the weight is 0 for all right-handed quarks like right-handed charged leptons, both up-type and down-type mass matrices are given in terms of only the weight 2 modular forms of Eq. (10). However, this case is inconsistent with the observed CKM matrix as well known [52]. In order to overcome this failure, we introduce weight 4 and 6 modular forms of Eqs. (13) and (14) in addition to weight 2 modular forms [52]. We consider one simple model in the case I, where the up-type right-handed quarks have different weights from the weight 0 of the right-handed down-type quarks. The assignment is presented in Table 3, in which the weight of right-handed up-type quarks is -4 . Therefore, the up-type quark mass matrix is given in terms of the weight 6 modular forms, in which two different triplet modular forms are available. This model has already discussed in Ref. [52] numerically. We reexamine the flavor structure of these quark mass matrices at nearby fixed point explicitly, and then we can understand why this model works well.

Alternatively, another quark mass matrix is also considered as the case II. In this case, weights of the right-handed up-type quarks and the down-type ones are same ones, which are also discussed numerically in Ref. [82]. The modular forms of weight 6 join only in the 1st-family.

	Q	$(u^c, c^c, t^c), (d^c, s^c, b^c)$	H_q	$\mathbf{Y}_3^{(6)}, \mathbf{Y}_{3'}^{(6)}$	$\mathbf{Y}_3^{(4)}$	$\mathbf{Y}_3^{(2)}$
$SU(2)$	2	1	2	1	1	1
A_4	3	(1, 1'', 1')	1	3	3	3
$-k_I$	-2	I: $(-4, -4, -4), (0, 0, 0)$ II: $(-4, -2, 0), (-4, -2, 0)$	0	$k = 6$	$k = 4$	$k = 2$

Table 3: Assignments of representations and weights $-k_I$ for MSSM fields and modular forms.

The relevant superpotentials of the quark sector are given for two cases as follows:

$$\begin{aligned}
\text{I : } \quad w_u &= \alpha_u u^c H_u \mathbf{Y}_3^{(6)} Q + \alpha'_u u^c H_u \mathbf{Y}_{3'}^{(6)} Q + \beta_u c^c H_u \mathbf{Y}_3^{(6)} Q + \beta'_u c^c H_u \mathbf{Y}_{3'}^{(6)} Q \\
&\quad + \gamma_u t^c H_u \mathbf{Y}_3^{(6)} Q + \gamma'_u t^c H_u \mathbf{Y}_{3'}^{(6)} Q, \\
w_d &= \alpha_d d^c H_d \mathbf{Y}_3^{(2)} Q + \beta_d s^c H_d \mathbf{Y}_3^{(2)} Q + \gamma_d b^c H_d \mathbf{Y}_3^{(2)} Q, \tag{112}
\end{aligned}$$

$$\text{II : } \quad w_q = \alpha_q q_1^c H_q \mathbf{Y}_3^{(6)} Q + \alpha'_q q_1^c H_q \mathbf{Y}_{3'}^{(6)} Q + \beta_q q_2^c H_q \mathbf{Y}_3^{(4)} Q + \gamma_q q_3^c H_q \mathbf{Y}_3^{(2)} Q, \tag{113}$$

where $q = u, d$, and the argument τ in the modular forms $Y_i(\tau)$ is omitted. Couplings $\alpha_q, \alpha'_q, \beta_q, \beta'_q, \gamma_q$ and γ'_q can be adjusted to the observed quark masses.

The quark mass matrices are written as:

$$\begin{aligned}
\text{I : } \quad M_u &= v_u \begin{pmatrix} \alpha_u & 0 & 0 \\ 0 & \beta_u & 0 \\ 0 & 0 & \gamma_u \end{pmatrix} \left[\begin{pmatrix} Y_1^{(6)} & Y_3^{(6)} & Y_2^{(6)} \\ Y_2^{(6)} & Y_1^{(6)} & Y_3^{(6)} \\ Y_3^{(6)} & Y_2^{(6)} & Y_1^{(6)} \end{pmatrix} + \begin{pmatrix} g_{u1} & 0 & 0 \\ 0 & g_{u2} & 0 \\ 0 & 0 & g_{u3} \end{pmatrix} \begin{pmatrix} Y_1'^{(6)} & Y_3'^{(6)} & Y_2'^{(6)} \\ Y_2'^{(6)} & Y_1'^{(6)} & Y_3'^{(6)} \\ Y_3'^{(6)} & Y_2'^{(6)} & Y_1'^{(6)} \end{pmatrix} \right]_{RL}, \\
M_d &= v_d \begin{pmatrix} \alpha_d & 0 & 0 \\ 0 & \beta_d & 0 \\ 0 & 0 & \gamma_d \end{pmatrix} \begin{pmatrix} Y_1 & Y_3 & Y_2 \\ Y_2 & Y_1 & Y_3 \\ Y_3 & Y_2 & Y_1 \end{pmatrix}_{RL}, \tag{114}
\end{aligned}$$

$$\text{II : } \quad M_q = v_q \begin{pmatrix} \alpha_q & 0 & 0 \\ 0 & \beta_q & 0 \\ 0 & 0 & \gamma_q \end{pmatrix} \begin{pmatrix} Y_1^{(6)} + g_q Y_1'^{(6)} & Y_3^{(6)} + g_q Y_3'^{(6)} & Y_2^{(6)} + g_q Y_2'^{(6)} \\ Y_2^{(4)} & Y_1^{(4)} & Y_3^{(4)} \\ Y_3^{(2)} & Y_2^{(2)} & Y_1^{(2)} \end{pmatrix}_{RL}, \tag{115}$$

where $g_{u1} = \alpha'_u/\alpha_u, g_{u2} = \beta'_u/\beta_u, g_{u3} = \gamma'_u/\gamma_u$ and $g_q \equiv \alpha'_q/\alpha_q$. The VEV of the Higgs field H_q is denoted by v_q . Parameters $\alpha_q, \beta_q, \gamma_q$ can be taken to be real, on the other hand, $g_{u1}, g_{u2}, g_{u3}, g_u$ and g_d are complex parameters.

These mass matrices turn to the simple ones at the fixed points, $\tau = i, \tau = \omega$ and $\tau = i\infty$. We discuss them in the diagonal bases of S, ST and T , respectively.

6.2 Quark mass matrix at the fixed point of $\tau = i$

6.2.1 Quark mass matrix I at $\tau = i$

The quark matrix I is given by using modular forms in Table 1 at fixed point $\tau = i$ in the base of S of Eq. (9) as follows:

$$M_u = \begin{pmatrix} \tilde{\alpha}_u & 0 & 0 \\ 0 & \tilde{\beta}_u & 0 \\ 0 & 0 & \tilde{\gamma}_u \end{pmatrix} \times \begin{pmatrix} 2\sqrt{3} - 3 + g_{u1}(7\sqrt{3} - 12) & 12 - 7\sqrt{3} + g_{u1}(9 - 5\sqrt{3}) & 5\sqrt{3} - 9 + g_{u1}(3 - 2\sqrt{3}) \\ 5\sqrt{3} - 9 + g_{u2}(3 - 2\sqrt{3}) & 2\sqrt{3} - 3 + g_{u2}(7\sqrt{3} - 12) & 12 - 7\sqrt{3} + g_{u2}(9 - 5\sqrt{3}) \\ 12 - 7\sqrt{3} + g_{u3}(9 - 5\sqrt{3}) & 5\sqrt{3} - 9 + g_{u3}(3 - 2\sqrt{3}) & 2\sqrt{3} - 3 + g_{u3}(7\sqrt{3} - 12) \end{pmatrix}, \quad (116)$$

$$M_d = \begin{pmatrix} \tilde{\alpha}_d & 0 & 0 \\ 0 & \tilde{\beta}_d & 0 \\ 0 & 0 & \tilde{\gamma}_d \end{pmatrix} \begin{pmatrix} 1 & -2 + \sqrt{3} & 1 - \sqrt{3} \\ 1 - \sqrt{3} & 1 & -2 + \sqrt{3} \\ -2 + \sqrt{3} & 1 - \sqrt{3} & 1 \end{pmatrix},$$

where $\tilde{\alpha}_u = 3v_u Y_0^3 \alpha_u$, $\tilde{\beta}_u = 3v_u Y_0^3 \beta_u$, $\tilde{\gamma}_u = 3v_u Y_0^3 \gamma_u$, $\tilde{\alpha}_d = (6 - 3\sqrt{3})v_d Y_0^2 \alpha_d$, $\tilde{\beta}_d = (6 - 3\sqrt{3})v_d Y_0^2 \beta_d$ and $\tilde{\gamma}_d = (6 - 3\sqrt{3})v_d Y_0^2 \gamma_d$.

We move the quark mass matrix to the diagonal base of S . By using the unitary transformation of Eq. (17), V_{S2} , the mass matrix $M_u^\dagger M_u$ is transformed as:

$$\mathcal{M}_u^{2(0)} \equiv V_{S2} M_u^\dagger M_u V_{S2}^\dagger = \frac{9}{2} \begin{pmatrix} 0 & 0 & 0 \\ 0 & a_{22}\tilde{\alpha}_u^2 + b_{22}\tilde{\beta}_u^2 + c_{22}\tilde{\gamma}_u^2 & a_{23}\tilde{\alpha}_u^2 + b_{23}\tilde{\beta}_u^2 + c_{23}\tilde{\gamma}_u^2 \\ 0 & a_{23}^*\tilde{\alpha}_u^2 + b_{23}^*\tilde{\beta}_u^2 + c_{23}^*\tilde{\gamma}_u^2 & a_{33}\tilde{\alpha}_u^2 + b_{33}\tilde{\beta}_u^2 + c_{33}\tilde{\gamma}_u^2 \end{pmatrix}. \quad (117)$$

Each coefficient is given as:

$$\begin{aligned} a_{22} &= A + 2B\text{Re}[g_{u1}] + C|g_{u1}|^2, & b_{22} &= 2B + 2(A - B)\text{Re}[g_{u2}] + A|g_{u2}|^2, \\ c_{22} &= C + 2(C - B)\text{Re}[g_{u3}] + 2B|g_{u3}|^2, & a_{23} &= -B - Ag_{u1} - Cg_{u1}^* - B|g_{u1}|^2, \\ b_{23} &= 2B + (C - B)g_{u2} + (A - B)g_{u2}^* - B|g_{u2}|^2, & c_{23} &= -B + (C - B)g_{u3} + (A - B)g_{u3}^* + 2B|g_{u3}|^2, \\ a_{33} &= C + 2B\text{Re}[g_{u1}] + A|g_{u1}|^2, & b_{33} &= 2B + 2(C - B)\text{Re}[g_{u2}] + C|g_{u2}|^2, \\ c_{33} &= A + 2(A - B)\text{Re}[g_{u3}] + 2B|g_{u3}|^2, \end{aligned} \quad (118)$$

where A , B and C are given in Eq. (68). On the other hand, the mass matrix $M_d^\dagger M_d$ is transformed as:

$$\mathcal{M}_d^{2(0)} \equiv V_{S2} M_d^\dagger M_d V_{S2}^\dagger = \frac{3}{2} \begin{pmatrix} 0 & 0 & 0 \\ 0 & \tilde{\alpha}_d^2 + 2D\tilde{\beta}_d^2 + A\tilde{\gamma}_d^2 & -D(\tilde{\alpha}_d^2 - 2\tilde{\beta}_d^2 + \tilde{\gamma}_d^2) \\ 0 & -D(\tilde{\alpha}_d^2 - 2\tilde{\beta}_d^2 + \tilde{\gamma}_d^2) & A\tilde{\alpha}_d^2 + 2D\tilde{\beta}_d^2 + \tilde{\gamma}_d^2 \end{pmatrix}. \quad (119)$$

It is remarked that the lightest quarks are massless for both up-type and down-type quarks at $\tau = i$. Therefore, the small deviation from $\tau = i$ is required to avoid the massless quark. There exists a non-vanishing flavor mixing angle θ_{23}^u at $\tau = i$ as discussed in Eq. (19). Supposing $\tilde{\gamma}_q \gg \tilde{\beta}_q, \tilde{\alpha}_q$, the mixing angle θ_{23}^u is given from Eq. (117) as:

$$\begin{aligned} \tan 2\theta_{23}^u &\simeq 2 \frac{|-B + (C - B)g_{u3} + (A - B)g_{u3}^* + 2B|g_{u3}|^2|}{(A - C)(1 + 2\text{Re}[g_{u3}])} \\ &= 2 \frac{\sqrt{[-B + 2B\text{Re}[g_{u3}] + 2B|g_{u3}|^2]^2 + [(C - A)\text{Im}g_{u3}]^2}}{2\sqrt{3}B(1 + 2\text{Re}[g_{u3}])} \simeq \frac{1}{\sqrt{3}} \left| \frac{2g_{u3}^2 + 2g_{u3} - 1}{1 + 2g_{u3}} \right|, \end{aligned} \quad (120)$$

where $A + C = 4B$ is used and the imaginary part of g_q is neglected in the last equation ($g_{u3} = \text{Re}[g_{u3}]$). In this case, $\tan 2\theta_{23}^u$ vanishes at $g_{u3} = (-1 \pm \sqrt{3})/2$, while $\theta_{23}^u = 15^\circ$ at $g_{u3} = 0$.

On the other hand, the mixing angle θ_{23}^d is simply given from Eq. (119) as:

$$\tan 2\theta_{23}^d \simeq 2 \frac{D}{1-A} = \frac{1}{\sqrt{3}}, \quad (121)$$

which leads to $\theta_{23}^d = 15^\circ$. Since the observed small CKM mixing angle θ_{23}^{CKM} (around 2°) is given by the difference ($\theta_{23}^d - \theta_{23}^u$), the magnitude of g_{u3} should be small in order to realize the enough cancellation between θ_{23}^d and θ_{23}^u . Indeed, $|g_{u3}|$ is in $[0, 0.2, 0.07]$ in our numerical result of section 7.

6.2.2 Quark mass matrix I at nearby $\tau = i$

By using the approximate modular forms of weight 2 and 6 in Eqs. (183) and (185) of Appendix C.1, we present the deviations from $\mathcal{M}_u^{2(0)}$ and $\mathcal{M}_d^{2(0)}$ in Eqs. (117) and (119). Then, the additional contribution $\mathcal{M}_u^{2(1)}$ to $\mathcal{M}_u^{2(0)}$ of Eq. (117) of order ϵ is given in terms of A , B and C in Eq. (68) as follows:

$$\mathcal{M}_u^{2(1)} \simeq \begin{pmatrix} 0 & \delta_{u2} & \delta_{u3} \\ \delta_{u2}^* & \delta_{u4} & \delta_{u5} \\ \delta_{u3}^* & \delta_{u5}^* & \delta_{u6} \end{pmatrix}, \quad (122)$$

where

$$\begin{aligned} \delta_{u2} &= \frac{3}{\sqrt{2}} \{ [(A - B + (B - C)g_{u1})\epsilon_1^* + (B + Cg_{u1})\epsilon_2^*](g_{u1}^* - 1)\tilde{\alpha}_u^2 \\ &\quad + (-2B + (B - A)g_{u2})\epsilon_1^* + (C - B - Bg_{u2})\epsilon_2^*](g_{u2}^* - 1)\tilde{\beta}_u^2 \\ &\quad + (C - B + 2Bg_{u3})\epsilon_1^* + (-C + (B - C)g_{u3})\epsilon_2^*](g_{u3}^* - 1)\tilde{\gamma}_u^2 \} \\ &\simeq \frac{3}{\sqrt{2}} \epsilon_1^* \{ [(A + B) + (B + C)g_{u1}](g_{u1}^* - 1)\tilde{\alpha}_u^2 + [2(C - 2B) - (A + B)g_{u2}](g_{u2}^* - 1)\tilde{\beta}_u^2 \\ &\quad + [-(B + C) + 2(2B - C)g_{u3}](g_{u3}^* - 1)\tilde{\gamma}_u^2 \}, \\ \delta_{u3} &= \frac{3}{\sqrt{2}} \{ [(C - B - (A - B)g_{u1})\epsilon_1^* - (C + Bg_{u1})\epsilon_2^*](g_{u1}^* - 1)\tilde{\alpha}_u^2 \\ &\quad + (-2B + (B - C)g_{u2})\epsilon_1^* + (C - B - Cg_{u2})\epsilon_2^*](g_{u2}^* - 1)\tilde{\beta}_u^2 \\ &\quad + (A - B + 2Bg_{u3})\epsilon_1^* + (B + (B - C)g_{u3})\epsilon_2^*](g_{u3}^* - 1)\tilde{\gamma}_u^2 \} \\ &\simeq \frac{3}{\sqrt{2}} \epsilon_1^* \{ -[(C + B) + (A + B)g_{u1}](g_{u1}^* - 1)\tilde{\alpha}_u^2 + [2(C - 2B) + (B + C)g_{u2}](g_{u2}^* - 1)\tilde{\beta}_u^2 \\ &\quad + [A + B + 2(2B - C)g_{u3}](g_{u3}^* - 1)\tilde{\gamma}_u^2 \}. \end{aligned} \quad (123)$$

In the approximate equalities, $\epsilon_2 = 2\epsilon_1$ in Eq. (26) is put. In order to estimate the Cabibbo angle, we calculate the mixing angle of the 1st- and 2nd-family as:

$$\tan 2\theta_{12}^u = \frac{2|\delta_{u2}|}{\frac{9}{2}(a_{22}\tilde{\alpha}_u^2 + b_{22}\tilde{\beta}_u^2 + c_{22}\tilde{\gamma}_u^2)} \simeq \frac{4}{3\sqrt{2}} \frac{B+C}{C} |\epsilon_1^*| \simeq \frac{4}{3\sqrt{2}} (3 + \sqrt{3}) |\epsilon_1^*| \simeq 4.46 |\epsilon_1^*|, \quad (125)$$

where the denominator comes from the (2, 2) element of Eq. (117). In the second approximate equality, $\tilde{\gamma}_u \gg \tilde{\alpha}_u, \tilde{\beta}_u$ and $|g_{u3}| \ll 1$ are put, while c_{22} is given in Eq. (118).

The additional contribution $\mathcal{M}_d^{2(1)}$ to $\mathcal{M}_d^{2(0)}$ of Eq. (119) of order ϵ is:

$$\mathcal{M}_d^{2(1)} \simeq \begin{pmatrix} 0 & \delta_{d2} & \delta_{d3} \\ \delta_{d2}^* & \delta_{d4} & \delta_{d5} \\ \delta_{d3}^* & \delta_{d5}^* & \delta_{d6} \end{pmatrix}, \quad (126)$$

where

$$\begin{aligned} \delta_{d2} &= \frac{1}{\sqrt{2}} \{[(\sqrt{3}-1)\epsilon_1^* + (\sqrt{3}-2)\epsilon_2^*]\tilde{\alpha}_d^2 + [(4-2\sqrt{3})\epsilon_1^* + (3\sqrt{3}-5)\epsilon_2^*]\tilde{\beta}_d^2 \\ &+ [(3\sqrt{3}-5)\epsilon_1^* + (7-4\sqrt{3})\epsilon_2^*]\tilde{\gamma}_d^2\} \simeq \frac{1}{\sqrt{2}} \epsilon_1^* [(3\sqrt{3}-5)\tilde{\alpha}_d^2 + 2(2\sqrt{3}-3)\tilde{\beta}_d^2 + (9-5\sqrt{3})\tilde{\gamma}_d^2], \end{aligned} \quad (127)$$

$$\begin{aligned} \delta_{d3} &= \frac{1}{\sqrt{6}} \{[(9-5\sqrt{3})\epsilon_1^* + (7\sqrt{3}-12)\epsilon_2^*]\tilde{\alpha}_d^2 + [(4\sqrt{3}-6)\epsilon_1^* + (9-5\sqrt{3})\epsilon_2^*]\tilde{\beta}_d^2 \\ &+ [(\sqrt{3}-3)\epsilon_1^* + (3-2\sqrt{3})\epsilon_2^*]\tilde{\gamma}_d^2\} \simeq \frac{\sqrt{6}}{2} \epsilon_1^* [(3\sqrt{3}-5)\tilde{\alpha}_d^2 + 2(2-\sqrt{3})\tilde{\beta}_d^2 + (1-\sqrt{3})\tilde{\gamma}_d^2]. \end{aligned} \quad (128)$$

In the last approximate equalities, $\epsilon_2 = 2\epsilon_1$ in Eq. (26) is put. The mixing angle of the 1st- and 2nd-family as:

$$\tan 2\theta_{12}^d = \frac{2|\delta_{d2}|}{\frac{3}{2}(\tilde{\alpha}_d^2 + 2D\tilde{\beta}_d^2 + A\tilde{\gamma}_d^2)} \simeq \frac{4}{3\sqrt{2}} \frac{9-5\sqrt{3}}{A} |\epsilon_1^*| \simeq \frac{4}{3\sqrt{2}} (3+\sqrt{3}) |\epsilon_1^*| \simeq 4.46 |\epsilon_1^*|, \quad (129)$$

where the denominator comes from the (2, 2) element of Eq. (119). In the second approximate equality, $\tilde{\gamma}_d \gg \tilde{\alpha}_d, \tilde{\beta}_d$ is taken. Since the magnitudes of θ_{12}^u and θ_{12}^d in Eqs. (125) and (129) are almost same, the phase of ϵ_1 is important to reproduce the Cabibbo angle. If we take $|\epsilon_1| = 0.1$ (see $\tau = i + \epsilon$ and $\epsilon_1 = 2.05 i \epsilon$ in Eq. (26)), both $\theta_{12}^{u(d)}$ are approximately 0.22. Thus, the magnitude of Cabibbo angle is easily reproduced by taking the relevant phase of ϵ . Indeed, the observed CKM elements are reproduced at $\tau \simeq i + (0.05-0.09) e^{i\phi}$ with relevant ϕ as numerically discussed in section 7.

6.2.3 Quark mass matrix II at $\tau = i$

Let us discuss the quark mass matrix II in Eq. (115) at fixed points of τ by using modular forms in Table 1. At $\tau = i$, both up-type and down-type quark mass matrices are given in the base of S of Eq. (9) as:

$$\begin{aligned} M_q &= \begin{pmatrix} \tilde{\alpha}_q & 0 & 0 \\ 0 & \tilde{\beta}_q & 0 \\ 0 & 0 & \tilde{\gamma}_q \end{pmatrix} \times \\ &\begin{pmatrix} 2\sqrt{3}-3+g_q(7\sqrt{3}-12) & 12-7\sqrt{3}+g_q(9-5\sqrt{3}) & 5\sqrt{3}-9+g_q(3-2\sqrt{3}) \\ 1 & 1 & 1 \\ -2+\sqrt{3} & 1-\sqrt{3} & 1 \end{pmatrix}, \end{aligned} \quad (130)$$

where $\tilde{\alpha}_q = 3v_q Y_0^3 \alpha_q$, $\tilde{\beta}_q = (6-3\sqrt{3})v_q Y_0^2 \beta_q$ and $\tilde{\gamma}_q = v_q Y_0 \gamma_q$ ($q = u, d$).

Let us move them to the diagonal base of S . By using the unitary transformation of Eq. (17), V_{S3} , the matrix $M_q^\dagger M_q$ is transformed as $(M_q V_{S3})^\dagger M_q V_{S3}$. Then, we have

$$\begin{aligned} \mathcal{M}_q^{2(0)} &\equiv V_{S3} M_q^\dagger M_q V_{S3}^\dagger \\ &= \frac{3}{2} \begin{pmatrix} A\tilde{\gamma}_q^2 + 3(A + B_{1q} + |g_q|^2 C)\tilde{\alpha}_q^2 & -[D\tilde{\gamma}_q^2 + 3(B_{2q} + Ag_q + Cg_q^*)\tilde{\alpha}_q^2] & 0 \\ -[D\tilde{\gamma}_q^2 + 3(B_{2q} + Ag_q^* + Cg_q)\tilde{\alpha}_q^2] & \tilde{\gamma}_q^2 + 3(C + B_{1q} + |g_q|^2 A)\tilde{\alpha}_q^2 & 0 \\ 0 & 0 & 2\tilde{\beta}^2 \end{pmatrix}, \end{aligned} \quad (131)$$

with

$$\begin{aligned} A &= 7 - 4\sqrt{3}, \quad B = 26 - 15\sqrt{3}, \quad C = 97 - 56\sqrt{3}, \quad D = 2 - \sqrt{3}, \\ B_{1q} &= B(g_q + g_q^*) = 2B \operatorname{Re}[g_q], \quad B_{2q} = B(1 + |g_q|^2), \quad A^2 = C, \quad D^2 = A, \quad A + C = 4B, \end{aligned} \quad (132)$$

where A , B , C and D in Eq. (68) are again presented for convenience. The mass eigenvalues satisfy:

$$m_{q1}^2 m_{q2}^2 = 81C \tilde{\alpha}_q^2 \tilde{\gamma}_q^2, \quad m_{q1}^2 + m_{q2}^2 = 6D \tilde{\gamma}_q^2 + 9B(2 + 2\operatorname{Re}[g_q] + |g_q|^2)\tilde{\alpha}_q^2, \quad m_{q3}^2 = 3\tilde{\beta}_q^2. \quad (133)$$

The mixing angle between 1st- and 2nd-family, θ_{12}^q , is given as:

$$\tan 2\theta_{12}^q = -\frac{\sqrt{[D\tilde{\gamma}_q^2 + 3(B_2 + E_q)\tilde{\alpha}_q^2]^2 + 9F_q^2\tilde{\alpha}_q^4}}{(2\sqrt{3} - 3)\tilde{\gamma}_q^2 + 3(45 - 26\sqrt{3})(1 - |g_q|^2)\tilde{\alpha}_q^2}, \quad (134)$$

where

$$E_q = (A + C)\operatorname{Re}[g_q] = (104 - 60\sqrt{3})\operatorname{Re}[g_q], \quad F_q = (A - C)\operatorname{Im}[g_q] = (52\sqrt{3} - 90)\operatorname{Im}[g_q]. \quad (135)$$

Neglecting the imaginary part of g_q ($g_q = \operatorname{Re}[g_q]$), it is simply given as:

$$\tan 2\theta_{12}^q = -\frac{1}{\sqrt{3}} \frac{\tilde{\gamma}_q^2 + 3(7 - 4\sqrt{3})(1 + 4g_q + g_q^2)\tilde{\alpha}_q^2}{\tilde{\gamma}_q^2 - 3(7 - 4\sqrt{3})(1 - g_q^2)\tilde{\alpha}_q^2}. \quad (136)$$

where $|g_q|$ is supposed to be $\mathcal{O}(1)$. We take $\tilde{\alpha}_q^2, \tilde{\gamma}_q^2 \ll \tilde{\beta}_q^2$ due to the mass hierarchy of quark masses. There are two possible choices of $\tilde{\alpha}_q^2 \ll \tilde{\gamma}_q^2$ and $\tilde{\gamma}_q^2 \ll \tilde{\alpha}_q^2$.

In the case of $\tilde{\alpha}_q^2 \ll \tilde{\gamma}_q^2$,

$$\tan 2\theta_{12}^q \simeq -\frac{1}{\sqrt{3}} [1 + 6(7 - 4\sqrt{3})(1 + 2g_q)\frac{\tilde{\alpha}_q^2}{\tilde{\gamma}_q^2}] \simeq -\frac{1}{\sqrt{3}}, \quad (137)$$

which gives $\theta_{12}^q = -15^\circ$ at the limit of $\tilde{\alpha}_q^2/\tilde{\gamma}_q^2 = 0$. This is common for both up-quark and down-quark mass matrices because it is independent of g_q . Then, the flavor mixing (CKM) between 1st- and 2nd-family vanishes due to the cancellation between up-quarks and down-quarks.

On the other hand, in the case of $\tilde{\gamma}_q^2 \ll \tilde{\alpha}_q^2$, we obtain

$$\tan 2\theta_{12}^q \simeq \frac{1}{\sqrt{3}} \frac{1 + 4g_q + g_q^2}{1 - g_q^2}, \quad (138)$$

where the imaginary part of g_q and terms of $\tilde{\gamma}_q^2$ are neglected. The Cabibbo angle could be reproduced by choosing relevant values of g_d and g_u of order one. However, the CKM matrix elements V_{cb} and V_{ub} vanish at $\tau = i$. In order to obtain desirable CKM matrix, τ should be deviated from i a little bit.

6.2.4 Quark mass matrix II at nearby $\tau = i$

By using modular forms of weight 2, 4 and 6 in Appendix C.1, we obtain the deviation from $\mathcal{M}_q^{2(0)}$ in Eq. (131). Then, the additional contribution $\mathcal{M}_q^{2(1)}$ to $\mathcal{M}_q^{2(1)}$ of Eq. (131) of order ϵ is:

$$\mathcal{M}_q^{2(1)} \simeq \begin{pmatrix} \mathcal{O}(\tilde{\alpha}_q^2, \tilde{\gamma}_q^2, \epsilon_1, \epsilon_2) & \mathcal{O}(\tilde{\alpha}_q^2, \tilde{\gamma}_q^2, \epsilon_1, \epsilon_2) & \frac{\tilde{\beta}_q^2}{\sqrt{2}}[(\sqrt{3}-1)\epsilon_1^* + (2-\sqrt{3})\epsilon_2^*] \\ \mathcal{O}(\tilde{\alpha}_q^2, \tilde{\gamma}_q^2, \epsilon_1, \epsilon_2) & \mathcal{O}(\tilde{\alpha}_q^2, \tilde{\gamma}_q^2, \epsilon_1, \epsilon_2) & \frac{\tilde{\beta}_q^2}{\sqrt{6}}[(3+\sqrt{3})\epsilon_1^* + \sqrt{3}\epsilon_2^*] \\ \frac{\tilde{\beta}_q^2}{\sqrt{2}}[(\sqrt{3}-1)\epsilon_1 + (2-\sqrt{3})\epsilon_2] & \frac{\tilde{\beta}_q^2}{\sqrt{6}}[(3+\sqrt{3})\epsilon_1 + \sqrt{3}\epsilon_2] & \tilde{\beta}_q^2[4\text{Re}(\epsilon_1) + 2(2-\sqrt{3})\text{Re}(\epsilon_2)] \end{pmatrix}, \quad (139)$$

where $\mathcal{O}(\tilde{\alpha}_q^2, \tilde{\gamma}_q^2, \epsilon_1, \epsilon_2)$ terms are highly suppressed compared with elements (1,3), (3,1), (2,3), (3,2), (3,3) due to $\tilde{\beta}_q^2 \gg \tilde{\alpha}_q^2, \tilde{\gamma}_q^2$. Therefore, the 2nd- and 3rd-family mixing angle θ_{23}^q is given as:

$$\theta_{23}^q \simeq \frac{\frac{1}{\sqrt{6}}\tilde{\beta}_q^2|(3+\sqrt{3})\epsilon_1^* + \sqrt{3}\epsilon_2^*|}{3\tilde{\beta}_q^2} = \frac{3+\sqrt{3}}{\sqrt{6}}|\epsilon_1^*| \simeq 2.23|\epsilon^*|, \quad (140)$$

and the 1st- and 3rd-family mixing angle θ_{13}^q is:

$$\theta_{13}^q \simeq \frac{\frac{1}{\sqrt{2}}\tilde{\beta}_q^2|(\sqrt{3}-1)\epsilon_1^* + (2-\sqrt{3})\epsilon_2^*|}{3\tilde{\beta}_q^2} = \frac{3-\sqrt{3}}{3\sqrt{2}}|\epsilon_1^*| \simeq 0.613|\epsilon^*|, \quad (141)$$

where $3\tilde{\beta}_q^2$ in the denominators is the (3,3) element of Eq. (131), and $\epsilon_2 = 2\epsilon_1 = 4.10i\epsilon$ of Eq. (26) is used. The ratio $\theta_{13}^q/\theta_{23}^q \simeq 0.27$ is rather large compared with observed CKM ratio $|V_{ub}/V_{cb}| \simeq 0.08$. This rather large θ_{13}^q spoils to reproduce observed CKM elements V_{cb} and V_{ub} at the nearby fixed point $\tau = i$.

6.3 Quark mass matrix at the fixed point of $\tau = \omega$

6.3.1 Quark mass matrix I at $\tau = \omega$

In the quark mass matrix I of Eq. (114), the up-type and down-type mass matrices are given at $\tau = \omega$ by using modular forms in Table 1:

$$M_u = \begin{pmatrix} -g_u\tilde{\alpha}_q & 0 & 0 \\ 0 & -g_u\tilde{\beta}_q & 0 \\ 0 & 0 & -g_u\tilde{\gamma}_q \end{pmatrix} \begin{pmatrix} 1 & -2\omega^2 & -2\omega \\ -2\omega & 1 & -2\omega^2 \\ -2\omega^2 & -2\omega & 1 \end{pmatrix}, \quad (142)$$

$$M_d = \begin{pmatrix} \tilde{\alpha}_d & 0 & 0 \\ 0 & \tilde{\beta}_d & 0 \\ 0 & 0 & \tilde{\gamma}_d \end{pmatrix} \begin{pmatrix} 1 & -\frac{1}{2}\omega^2 & \omega \\ \omega & 1 & -\frac{1}{2}\omega^2 \\ -\frac{1}{2}\omega^2 & \omega & 1 \end{pmatrix},$$

where $\tilde{\alpha}_u = (9/8)v_u Y_0^3 \alpha_q$, $\tilde{\beta}_u = (9/8)v_u Y_0^3 \beta_q$ and $\tilde{\gamma}_u = (9/8)v_u Y_0^3 \gamma_q$ for up-type quarks, and $\tilde{\alpha}_d = v_d Y_0 \alpha_d$, $\tilde{\beta}_d = v_d Y_0 \beta_d$ and $\tilde{\gamma}_d = v_d Y_0 \gamma_d$ for down-type quarks, respectively. By using the unitary transformation of Eq. (22), V_{ST4} , the mass matrix $M_u^\dagger M_u$ is transformed as:

$$\mathcal{M}_u^{2(0)} \equiv V_{ST4} M_u^\dagger M_u V_{ST4}^\dagger = 9 \begin{pmatrix} |g_{u2}|^2 \tilde{\beta}_u^2 & 0 & 0 \\ 0 & |g_{u1}|^2 \tilde{\alpha}_u^2 & 0 \\ 0 & 0 & |g_{u3}|^2 \tilde{\gamma}_u^2 \end{pmatrix}. \quad (143)$$

The mass matrix $M_d^\dagger M_d$ is transformed as:

$$\mathcal{M}_d^{2(0)} \equiv V_{ST4} M_d^\dagger M_d V_{ST4}^\dagger = \frac{9}{4} \begin{pmatrix} \tilde{\alpha}_d^2 & 0 & 0 \\ 0 & \tilde{\gamma}_d^2 & 0 \\ 0 & 0 & \tilde{\beta}_d^2 \end{pmatrix}. \quad (144)$$

It is remarked that both are diagonal ones.

6.3.2 Quark mass matrix I at nearby $\tau = \omega$

Quark mass matrix I in Eq. (142) is corrected due to the deviation from the fixed point of $\tau = \omega$. By using modular forms of weight 2, 4 and 6 in Appendix C.2, we obtain the deviations from $\mathcal{M}_u^{2(0)}$ and $\mathcal{M}_d^{2(0)}$ in Eqs. (143) and (144). In the diagonal base of ST , the corrections are given by only a small variable ϵ as seen in Eq. (27). In the 1st order perturbation of ϵ_1 , the corrections $\mathcal{M}_u^{2(1)}$ and $\mathcal{M}_d^{2(1)}$ are given as:

$$\mathcal{M}_u^{2(1)} = \begin{pmatrix} \delta_{u1} & \delta_{u2} & \delta_{u3} \\ \delta_{u2}^* & \delta_{u4} & \delta_{u5} \\ \delta_{u3}^* & \delta_{u5}^* & \delta_{u6} \end{pmatrix}, \quad \mathcal{M}_d^{2(1)} = \begin{pmatrix} \delta_{d1} & \delta_{d2} & \delta_{d3} \\ \delta_{d2}^* & \delta_{d4} & \delta_{d5} \\ \delta_{d3}^* & \delta_{d5}^* & \delta_{d6} \end{pmatrix}, \quad (145)$$

where off diagonal elements δ_{q2} , δ_{q3} and δ_{q5} are:

$$\delta_{u2} = 2\tilde{\beta}_u^2 |g_{u2}|^2 (2\epsilon_1 - \epsilon_2) - 2\tilde{\alpha}_u^2 (2 + g_{u1}^*) g_{u1} (\epsilon_1^* + \epsilon_2^*) = -6(2 + g_{u1}^*) g_{u1} \epsilon_1^* \tilde{\alpha}_u^2, \quad (146)$$

$$\delta_{u3} = 2\tilde{\beta}_u^2 (2 + g_{u2}) g_{u2}^* (\epsilon_1 + \epsilon_2) + 2\tilde{\gamma}_u^2 |g_{u3}|^2 (-2\epsilon_1^* + \epsilon_2^*) = 6(2 + g_{u2}) g_{u2}^* \epsilon_1 \tilde{\beta}_u^2, \quad (147)$$

$$\delta_{u5} = 2\tilde{\gamma}_u^3 (2 + g_{u3}^*) g_{u3} (\epsilon_1^* + \epsilon_2^*) + 2\tilde{\alpha}_u^2 |g_{u1}|^2 (-2\epsilon_1 + \epsilon_2) = 6(2 + g_{u3}^*) g_{u3} \epsilon_1^* \tilde{\gamma}_u^2, \quad (148)$$

$$\delta_{d2} = i \tilde{\alpha}_d^2 (\epsilon_1 - \frac{1}{2}\epsilon_2) + \frac{1}{2} i \tilde{\gamma}_d^2 (\epsilon_1^* + \epsilon_2^*) = \frac{3}{2} i \epsilon_1^* \tilde{\gamma}_d^2, \quad (149)$$

$$\delta_{d3} = \frac{1}{2} i \tilde{\alpha}_d^2 (\epsilon_1 + \epsilon_2) + i \tilde{\beta}_d^2 (\epsilon_1^* - \frac{1}{2}\epsilon_2^*) = \frac{3}{2} i \epsilon_1 \tilde{\alpha}_d^2, \quad (150)$$

$$\delta_{d5} = -\frac{1}{2} i \tilde{\beta}_d^2 (\epsilon_1^* + \epsilon_2^*) - i \tilde{\gamma}_d^2 (\epsilon_1 - \frac{1}{2}\epsilon_2) = -\frac{3}{2} i \epsilon_1^* \tilde{\beta}_d^2. \quad (151)$$

In last equalities, $\epsilon_2 = 2\epsilon_1$ of Eq. (28) is used.

Taking account of $\tilde{\gamma}_u^2 \gg \tilde{\alpha}_u^2 \gg \tilde{\beta}_u^2$ and $\tilde{\beta}_d^2 \gg \tilde{\gamma}_d^2 \gg \tilde{\alpha}_d^2$ as seen in Eqs. (143) and (144), mixing angles θ_{12}^q and θ_{23}^q are given as:

$$\theta_{12}^u \simeq \frac{2}{3} |(2 + g_{u1}^*) g_{u1} \epsilon_1^*|, \quad \theta_{23}^u \simeq \frac{2}{3} |(2 + g_{u3}^*) g_{u3} \epsilon_1^*|, \quad \theta_{12}^d \simeq \theta_{23}^d \simeq \frac{2}{3} |\epsilon_1^*|, \quad (152)$$

respectively, while both θ_{13}^q ($q = u, d$) are highly suppressed.

Since up-type quark mixing angles depend on the magnitudes of g_{u1} and g_{u3} , the magnitudes of CKM matrix elements V_{us} and V_{cb} could be reproduced by choosing relevant g_{u1} and g_{u3} . For example, we can take $\theta_{12}^u \sim \lambda$ and $\theta_{23}^u \sim \theta_{12}^d \sim \theta_{23}^d \sim \lambda^2$, where $\lambda \simeq 0.2$ is put to reproduce observed $|V_{us}|$, $|V_{cb}|$ and $|V_{ub}|$. However, this scheme leads to $|V_{td}| \sim \lambda^4$, which is much smaller than the observed one. Indeed, the observed $|V_{td}|$ is not reproduced at nearby $\tau = \omega$ in section 7.

6.3.3 Quark mass matrix II at $\tau = \omega$

We discuss the quark mass matrix II at the fixed point $\tau = \omega$ by using modular forms in Table 1. In the base of S and T of Eq. (9), it is given at the fixed point $\tau = \omega$:

$$M_q = \begin{pmatrix} -g_q \tilde{\alpha}_q & 0 & 0 \\ 0 & \tilde{\beta}_q & 0 \\ 0 & 0 & \tilde{\gamma}_q \end{pmatrix} \begin{pmatrix} 1 & -2\omega^2 & -2\omega \\ -\frac{1}{2}\omega & 1 & \omega^2 \\ -\frac{1}{2}\omega^2 & \omega & 1 \end{pmatrix}, \quad (153)$$

where $\tilde{\alpha}_q = (9/8)v_q Y_0^3 \alpha_q$, $\tilde{\beta}_q = \frac{3}{2}v_q Y_0^2 \beta_q$ and $\tilde{\gamma}_q = v_q Y_0 \gamma_q$. By using the unitary transformation of Eq. (22), V_{ST5} , the mass matrix $M_q^\dagger M_q$ is transformed as:

$$\mathcal{M}_q^{2(0)} \equiv V_{ST5} M_q^\dagger M_q V_{ST5}^\dagger = \frac{9}{4} \begin{pmatrix} 0 & 0 & 0 \\ 0 & 0 & 0 \\ 0 & 0 & 4g_q^2 \tilde{\alpha}_q^2 + \tilde{\beta}_q^2 + \tilde{\gamma}_q^2 \end{pmatrix}, \quad (154)$$

which gives two massless quarks. Therefore, it seems very difficult to reproduce observed quark masses and CKM elements even if we shift τ from $\tau = \omega$ a little bit and choose relevant g_q .

6.3.4 Quark mass matrix II at nearby $\tau = \omega$

Quark mass matrix II in Eq. (153) is corrected due to the deviation from the fixed point of $\tau = \omega$. By using modular forms of weight 2, 4 and 6 in Appendix C.2, we obtain the deviation from $\mathcal{M}_q^{2(0)}$ in Eq. (154). In the diagonal base of ST , the correction is given by only a small variable ϵ as seen in Eq. (27). In the 1st order approximation of ϵ_i , the correction $\mathcal{M}_q^{2(1)}$ is given as:

$$\mathcal{M}_q^{2(1)} = \begin{pmatrix} 0 & 0 & \delta_{q3} \\ 0 & 0 & \delta_{q5} \\ \delta_{q3}^* & \delta_{q5}^* & \delta_{q6} \end{pmatrix}, \quad (155)$$

where δ_{qi} are given in terms of ϵ , g_q , $\tilde{\alpha}_q^2$, $\tilde{\beta}_q^2$ and $\tilde{\gamma}_q^2$. In order to estimate the flavor mixing angles, we present relevant δ_{qi} as:

$$\begin{aligned} \delta_{q3} &= -2\tilde{\alpha}_q^2 g_q (2 + g_q^*) (\epsilon_1^* + \epsilon_2^*) + \frac{1}{6} \tilde{\beta}_q^2 (\epsilon_1^* - 8\epsilon_2^*) + \frac{1}{2} i \tilde{\gamma}_q^2 (\epsilon_1^* + \epsilon_2^*) \\ &\simeq -6\tilde{\alpha}_q^2 g_q (2 + g_q^*) \epsilon_1^* - \frac{5}{2} \tilde{\beta}_q^2 \epsilon_1^* + \frac{3}{2} i \tilde{\gamma}_q^2 \epsilon_1^*, \\ \delta_{q5} &= \tilde{\alpha}_q^2 |g_q|^2 (-4\epsilon_1^* + 2\epsilon_2^*) + \tilde{\beta}_q^2 \left(\frac{1}{3} \epsilon_1^* - \frac{7}{6} \epsilon_2^* \right) + i \tilde{\gamma}_q^2 \left(\epsilon_1^* - \frac{1}{2} \epsilon_2^* \right) \simeq -2\tilde{\beta}_q^2 \epsilon_1^*, \end{aligned} \quad (156)$$

where $\epsilon_2 = 2\epsilon_1$ of Eq. (28) is used in last approximate equalities. By using Eqs. (154) and (155), we obtain $\text{Det}[\mathcal{M}_Q^{2(0)} + \mathcal{M}_Q^{2(1)}] = 0$. Therefore, it is impossible to reproduce observed quark masses at nearby $\tau = \omega$ in the 1st order perturbation of ϵ . Indeed, this model cannot reproduce the observed CKM elements at nearby $\tau = \omega$ in section 7.

6.4 Quark mass matrix at $\tau = i\infty$

6.4.1 Quark mass matrix I and II at $\tau = i\infty$

The mass matrices of I and II in Eqs. (115) and (114) are simply given by using modular forms in Table 1 at $\tau = i\infty$ since the modular forms of weight 2, 4 and 6 are same. Those are both diagonal ones as follows:

$$M_q = \begin{pmatrix} \tilde{\alpha}_q & 0 & 0 \\ 0 & \tilde{\beta}_q & 0 \\ 0 & 0 & \tilde{\gamma}_q \end{pmatrix}, \quad (157)$$

where $\tilde{\alpha}_u = v_u Y_0^3 \alpha_q$, $\tilde{\beta}_u = v_u Y_0^3 \beta_u$, $\tilde{\gamma}_u = v_u Y_0^3 \gamma_u$, $\tilde{\alpha}_d = v_d Y_0 \alpha_d$, $\tilde{\beta}_d = v_d Y_0 \beta_d$ and $\tilde{\gamma}_d = v_d Y_0 \gamma_d$ for quark mass matrix I, and $\tilde{\alpha}_q = v_q Y_0^3 \alpha_q$, $\tilde{\beta}_q = v_q Y_0^2 \beta_q$ and $\tilde{\gamma}_q = v_q Y_0 \gamma_q$ for quark mass matrix II.

In the diagonal base of T of Eq. (9), the mass matrix $M_q^\dagger M_q$ is given as:

$$\mathcal{M}_q^{2(0)} \equiv M_q^\dagger M_q = \begin{pmatrix} \tilde{\alpha}_q^2 & 0 & 0 \\ 0 & \tilde{\beta}_q^2 & 0 \\ 0 & 0 & \tilde{\gamma}_q^2 \end{pmatrix}. \quad (158)$$

Mixing angles appear through the finite effect of $\text{Im}[\tau]$.

6.4.2 Quark mass matrix I towards $\tau = i\infty$

Quark mass matrix I in Eq. (157) is corrected due to the finite effect of $\tau = i\infty$. By using modular forms of Eqs. (192), (193) and (194) in Appendix C.3, we obtain the deviation from $\mathcal{M}_q^{2(0)}$ in Eq. (158) for the quark mass matrix I. We present the first order corrections $\mathcal{M}_q^{2(1)}$ for up-type quarks and down-type quarks to $\mathcal{M}_q^{2(0)}$ of Eq. (158), respectively:

$$\mathcal{M}_u^{2(1)} \simeq \begin{pmatrix} 0 & (1 + 2g_{u2}^*) \tilde{\beta}_u^2 \delta^* & (1 + 2g_{u1}) \tilde{\alpha}_u^2 \delta \\ (1 + 2g_{u2}) \tilde{\beta}_u^2 \delta & 0 & (1 + 2g_{u3}^*) \tilde{\gamma}_u^2 \delta^* \\ (1 + 2g_{u1}^*) \tilde{\alpha}_u^2 \delta^* & (1 + 2g_{u3}) \tilde{\gamma}_u^2 \delta & 0 \end{pmatrix}, \quad (159)$$

$$\mathcal{M}_d^{2(1)} \simeq \begin{pmatrix} 0 & \tilde{\beta}_d^2 \delta^* & \tilde{\alpha}_d^2 \delta \\ \tilde{\beta}_d^2 \delta & 0 & \tilde{\gamma}_d^2 \delta^* \\ \tilde{\alpha}_d^2 \delta^* & \tilde{\gamma}_d^2 \delta & 0 \end{pmatrix},$$

where δ is given in Eq.(105). We obtain mixing angles as:

$$\theta_{12}^u \simeq |(1 + 2g_{u2}^*) \delta^*|, \quad \theta_{23}^u \simeq |(1 + 2g_{u3}^*) \delta^*|, \quad \theta_{12}^d \simeq \theta_{23}^d \simeq |\delta^*|, \quad (160)$$

respectively. The 1st- and 3rd-family mixing angle θ_{13}^q is suppressed due to the factor $\tilde{\alpha}_q^2/\tilde{\gamma}_q^2$ for both up- and down-type quarks. Since θ_{12}^u and θ_{23}^u depend on the magnitudes of g_{u2} and g_{u3} , the CKM matrix elements V_{us} and V_{cb} could be reproduced by choosing relevant g_{u2} and g_{u3} . For example, we can take $\theta_{12}^u \sim \lambda$ and $\theta_{23}^u \sim \theta_{12}^d \sim \theta_{23}^d \sim \lambda^2$, where $\lambda \simeq 0.2$ to reproduce observed $|V_{us}|$, $|V_{cb}|$ and $|V_{ub}|$. However, this scheme leads to $|V_{td}| \sim \lambda^4$, which is much smaller than the observed one. Indeed, the successful CKM matrix elements are not reproduced at large $\text{Im}\tau$ in the numerical results of section 7.

6.4.3 Quark mass matrix II towards $\tau = i\infty$

Quark mass matrix II in Eq. (157) is corrected due to the finite effect of $\tau = i\infty$. By using modular forms of Eqs. (192), (193) and (194) in Appendix C.3, we obtain the deviation from $\mathcal{M}_q^{2(0)}$ in Eq. (158) for the quark mass matrix II. The first order correction $\mathcal{M}_q^{2(1)}$ to $\mathcal{M}_q^{2(0)}$ of Eq. (158) is given as:

$$\mathcal{M}_q^{2(1)} \simeq \begin{pmatrix} 0 & -\delta^* \tilde{\beta}_q^2 & (1 + 2g_q) \delta^* \tilde{\alpha}_q^2 \\ -\delta \tilde{\beta}_q^2 & 0 & \delta^* \tilde{\gamma}_q^2 \\ (1 + 2g_q^*) \delta \tilde{\alpha}_q^2 & \delta \tilde{\gamma}_q^2 & 0 \end{pmatrix}, \quad (161)$$

where $\tilde{\alpha}_q^2 \ll \tilde{\beta}_q^2 \ll \tilde{\gamma}_q^2$. Therefore, the mixing angles θ_{12}^q and θ_{23}^q , are given as:

$$\theta_{12}^q \simeq \frac{|\delta^*| \tilde{\beta}_q^2}{\tilde{\beta}_q^2} \simeq |\delta^*|, \quad \theta_{23}^q \simeq \frac{|\delta^*| \tilde{\gamma}_q^2}{\tilde{\gamma}_q^2} = |\delta^*|, \quad (162)$$

respectively. On the other hand, 1st- and 3rd-family mixing angle θ_{13}^q is highly suppressed due to the factor $\tilde{\alpha}_q^2/\tilde{\gamma}_q^2$. Since θ_{12}^q and θ_{23}^q are the same magnitude for both up-type and down-type quarks, it is impossible to reproduce observed CKM mixing angles.

In conclusion of section 6, it is found that the only quark mass matrix I works well at nearby $\tau = i$.

7 Numerical results at nearby fixed points

We have presented analytical discussions of lepton and quark mass matrices at nearby fixed points of modulus. In this section, we show numerical results at the nearby fixed points of $\tau = i$, $\tau = \omega$ and $\tau = i\infty$ to confirm above discussions and give predictions.

7.1 Frameworks of numerical calculations

In order to calculate the left-handed flavor mixing of leptons numerically, we generate random number for model parameters. The modulus τ is scanned around fixed points $\tau = i$ and $\tau = \omega$. It is also scanned $\text{Im}\tau \geq 1.2$ towards $\tau = i\infty$. We keep the parameter sets, in which the neutrino experimental data and charged lepton masses are reproduced within 3σ interval of error-bars. We continue this procedure to obtain enough points for plotting allowed region.

As input of the neutrino data, we take three mixing angles of the PMNS matrix and the observed neutrino mass ratio $\Delta m_{\text{sol}}^2/\Delta m_{\text{atm}}^2$ with 3σ , which are given by NuFit 4.1 in Table 4 [99]. Since there are two possible spectrum of neutrinos masses m_i , which are the normal hierarchy (NH), $m_3 > m_2 > m_1$, and the inverted hierarchy (IH), $m_2 > m_1 > m_3$, we investigate both cases. We also take account of the sum of three neutrino masses $\sum m_i$ since it is constrained by the recent cosmological data [100–102]. We impose the constraint of the upper-bound $\sum m_i \leq 120$ meV.

Since the modulus τ obtains the expectation value by the breaking of the modular invariance at the high mass scale, the observed masses and lepton mixing angles should be taken at the GUT scale by the renormalization group equations (RGEs). However, we have not included the RGE effects in the lepton mixing angles and neutrino mass ratio $\Delta m_{\text{sol}}^2/\Delta m_{\text{atm}}^2$ in our numerical calculations. We suppose that those corrections are very small between the electroweak and GUT scales. This assumption is confirmed well in the case of $\tan\beta \leq 5$ unless neutrino masses are almost degenerate [27]. Since we impose the sum of neutrino masses to be smaller than 120meV, this criterion is satisfied in our analyses.

On the other hand, we also take the charged lepton masses at the GUT scale 2×10^{16} GeV with $\tan \beta = 5$ in the framework of the minimal SUSY breaking scenarios [103, 104]:

$$y_e = (1.97 \pm 0.024) \times 10^{-6}, \quad y_\mu = (4.16 \pm 0.050) \times 10^{-4}, \quad y_\tau = (7.07 \pm 0.073) \times 10^{-3}, \quad (163)$$

where lepton masses are given by $m_\ell = y_\ell v_H$ with $v_H = 174$ GeV.

observable	3σ range for NH	3σ range for IH
Δm_{atm}^2	$(2.436\text{--}2.618) \times 10^{-3} \text{ eV}^2$	$-(2.419\text{--}2.601) \times 10^{-3} \text{ eV}^2$
Δm_{sol}^2	$(6.79\text{--}8.01) \times 10^{-5} \text{ eV}^2$	$(6.79\text{--}8.01) \times 10^{-5} \text{ eV}^2$
$\sin^2 \theta_{23}$	0.433–0.609	0.436–0.610
$\sin^2 \theta_{12}$	0.275–0.350	0.275–0.350
$\sin^2 \theta_{13}$	0.02044–0.02435	0.02064–0.02457

Table 4: The 3σ ranges of neutrino parameters from NuFIT 4.1 for NH and IH [99].

For the quark sector, we also adopt numerical values of Yukawa couplings of quarks at the GUT scale 2×10^{16} GeV with $\tan \beta = 5$ in the framework of the minimal SUSY breaking scenarios [103, 104]:

$$\begin{aligned} y_d &= (4.81 \pm 1.06) \times 10^{-6}, & y_s &= (9.52 \pm 1.03) \times 10^{-5}, & y_b &= (6.95 \pm 0.175) \times 10^{-3}, \\ y_u &= (2.92 \pm 1.81) \times 10^{-6}, & y_c &= (1.43 \pm 0.100) \times 10^{-3}, & y_t &= 0.534 \pm 0.0341, \end{aligned} \quad (164)$$

which give quark masses as $m_q = y_q v_H$ with $v_H = 174$ GeV.

We also use the following CKM mixing angles at the GUT scale 2×10^{16} GeV with $\tan \beta = 5$ [103, 104]:

$$\theta_{12}^{\text{CKM}} = 13.027^\circ \pm 0.0814^\circ, \quad \theta_{23}^{\text{CKM}} = 2.054^\circ \pm 0.384^\circ, \quad \theta_{13}^{\text{CKM}} = 0.1802^\circ \pm 0.0281^\circ. \quad (165)$$

Here θ_{ij}^{CKM} is given in the PDG notation of the CKM matrix V_{CKM} [102]. In addition, we impose the recent data of LHCb [102]:

$$\left| \frac{V_{ub}}{V_{cb}} \right| = 0.079 \pm 0.006, \quad (166)$$

where V_{ij} 's are CKM matrix elements. This ratio is stable against radiative corrections. The observed CP violating phase is given at the GUT scale as:

$$\delta_{\text{CP}}^{\text{CKM}} = 69.21^\circ \pm 6.19^\circ, \quad (167)$$

which is also in the PDG notation. The error intervals in Eqs. (164), (165), (166) and (167) represent 1σ interval.

7.2 Allowed regions of τ at nearby fixed points

We have examined eighteen cases of leptons and quarks in above framework numerically as shown in Table 5. In this Table, the successful cases for the mass matrix I and II at nearby fixed points are

Modulus	nearby $\tau = i$			nearby $\tau = \omega$			towards $\tau = i\infty$		
Lepton/Quark	Lepton		Quark	Lepton		Quark	Lepton		Quark
Neutrino mass hierarchy	NH	IH		NH	IH		NH	IH	
mass matrix I for M_E and M_q	○	○	○	⊗	×	×	○	×	×
mass matrix II for M_E and M_q	○	⊗	×	○	○	×	○	⊗	×

Table 5: The successful cases for the mass matrix I and II at nearby fixed points are denoted by ○. On the other hand, × denotes a failure to reproduce observed mixing angles, and ⊗ denotes the case in which observed mixing angles are reproduced, but $\sum m_i \geq 120$ meV.

denoted by ○. On the other hand, × denotes a failure to reproduce observed mixing angles, and ⊗ denotes the case in which observed PMNS mixing angles are reproduced, but $\sum m_i \geq 120$ meV.

Among eighteen cases, seven cases of leptons and one case of quarks are consistent with recent observed data. It is emphasized that the all cases of the mass matrix I work well at nearby $\tau = i$. These results confirm our previous discussions.

We show allowed regions of τ at nearby $\tau = i$, $\tau = \omega$ and towards $\tau = i\infty$ for eleven cases in Figs. 1, 2 and 3, respectively. In these figures, green points denote allowed ones by inputting masses and mixing angles with the constraint $\sum m_i \leq 120$ meV for leptons, but blue points denote the regions in which the sum of neutrino masses $\sum m_i$ is larger than 120 meV. It is noted that blue points are hidden under green points in the case of the charged lepton II (NH) of Fig. 2 and charged lepton I (NH) of Fig. 3. Green points for quarks denote allowed region of τ by inputting masses, mixing angles and CP violating phase $\delta_{\text{CP}}^{\text{CKM}}$.

As seen in Fig. 1, the constraint $\sum m_i \leq 120$ meV excludes the charged lepton II with IH of neutrinos. The allowed regions of τ (green points) deviate from the fixed point $\tau = i$ in magnitude of 5–10%, which confirm the discussions in section 5. It is reasonable that the allowed points appear frequently at nearby $\tau = i$ since one flavor mixing angle is generated even at the fixed point $\tau = i$ as discussed in section 5.2. In the quark sector, the mass matrix I works well, but the matrix II does not because the mixing angles are canceled out each other in the same type mass matrices of up-type and down-type quarks. It is emphasized that there is the common region of τ between charged lepton I (NH) and quark I. Indeed, the region around $\tau = \pm 0.04 + 1.05i$ is common in quarks and leptons. This common region has already discussed in context with the quark-lepton unification in Ref. [52].

As seen in Fig. 2, at nearby $\tau = \omega$, the charged lepton mass matrix I with NH is excluded by the constraint of $\sum m_i \leq 120$ meV. In the charged lepton mass matrix I with IH, the PMNS mixing angles are not reproduced. On the other hand, the allowed regions are marginal in the charged lepton II. Indeed, the green points are 0.1 for NH and 0.15 for IH away from $\tau = \omega$, respectively. The perturbative discussion of this IH case is possibly broken. Moreover, we cannot find allowed region of quarks at nearby $\tau = \omega$. That is expected in the discussion in section 6.3.

As seen in Fig. 3, towards $\tau = i\infty$, both charged lepton mass matrix I and II reproduce the observed PMNS mixing angles for NH of neutrinos. In the charged lepton mass matrix I with IH, the PMNS mixing angles are not reproduced. Although the charged lepton mass matrix II with IH reproduces three PMNS mixing angles, it is excluded by the constraint of $\sum m_i \leq 120$ meV. We cannot find allowed region for quarks. These results are also consistent with discussions of section 5.4 and 6.4.

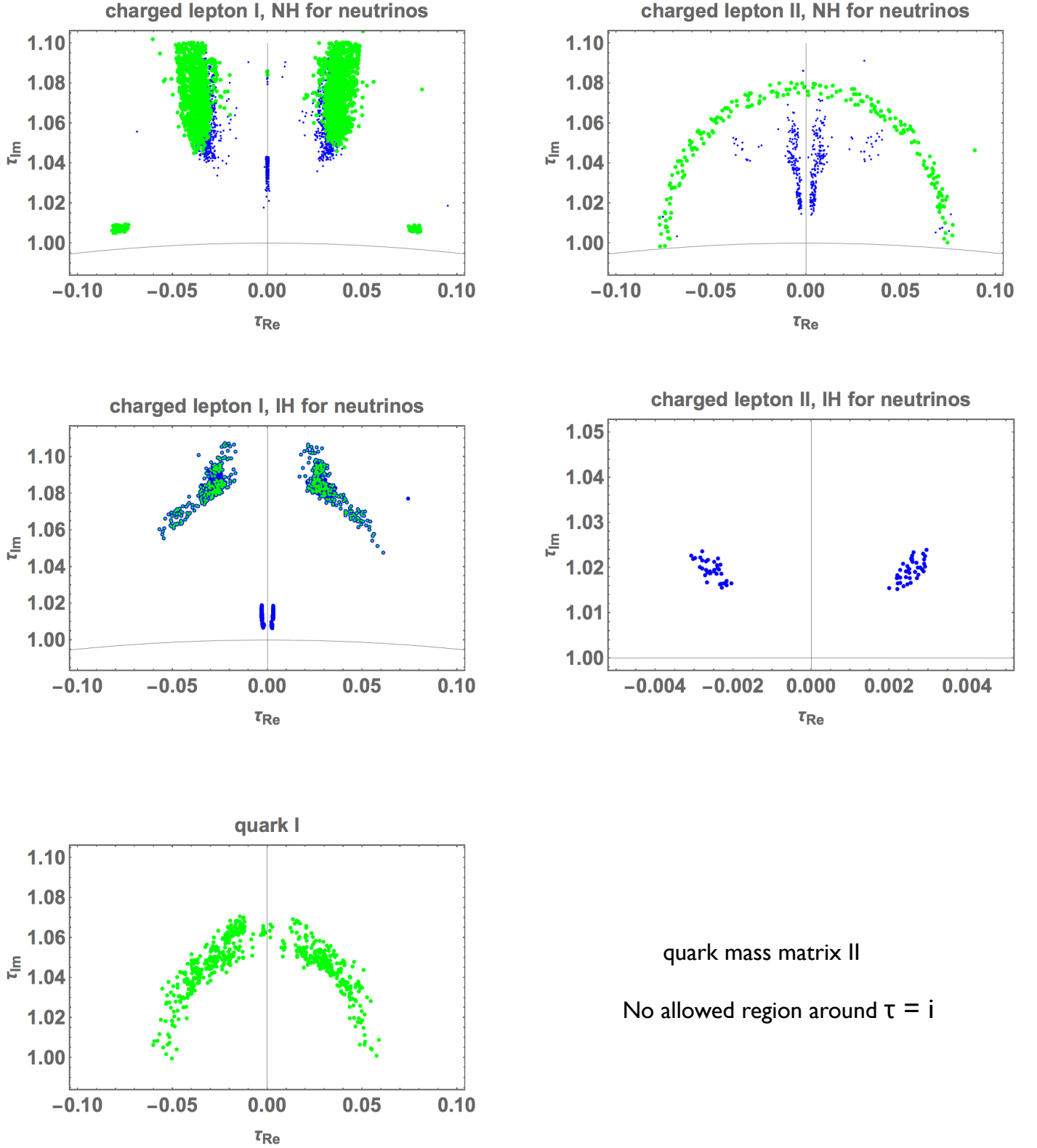
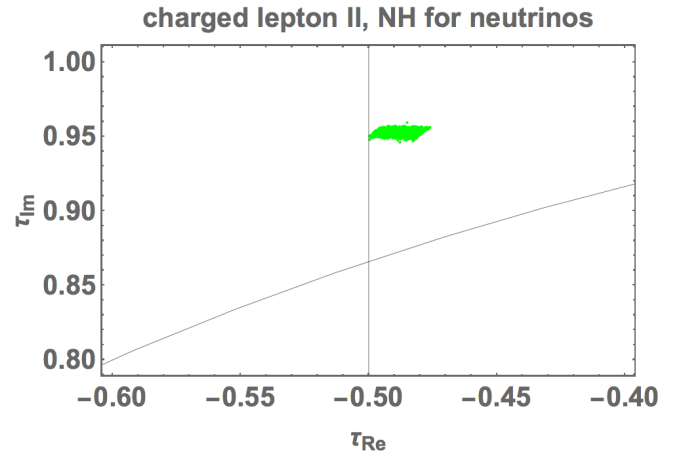
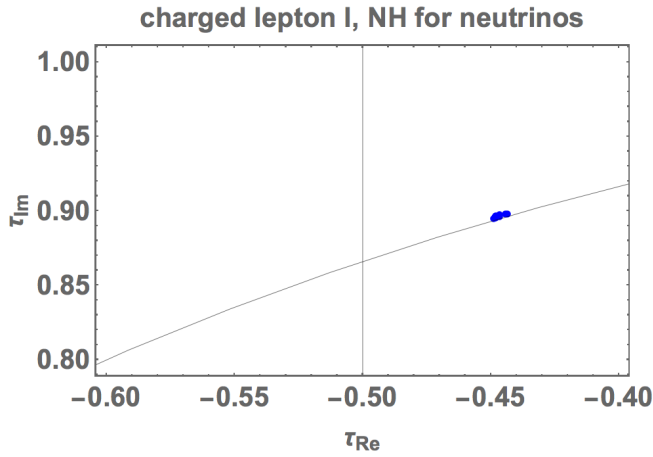
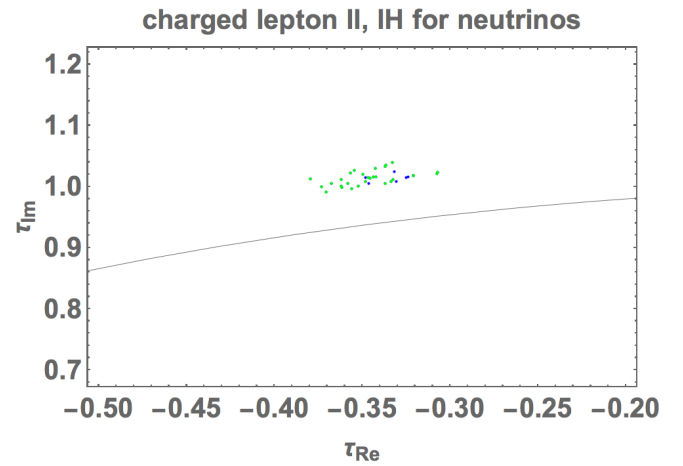


Figure 1: Allowed regions of τ at nearby $\tau = i$ are shown by green points for charged lepton mass matrices I and II with NH and IH of neutrinos, and quark mass matrices I, respectively. Blue points denote regions in which the sum of neutrino masses $\sum m_i$ is larger than 120 meV.



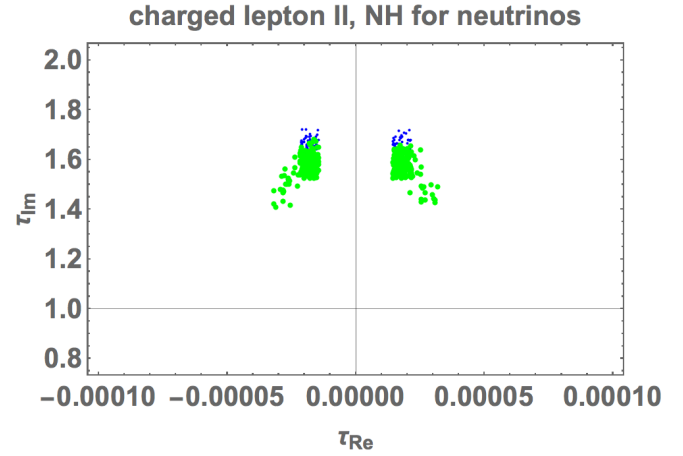
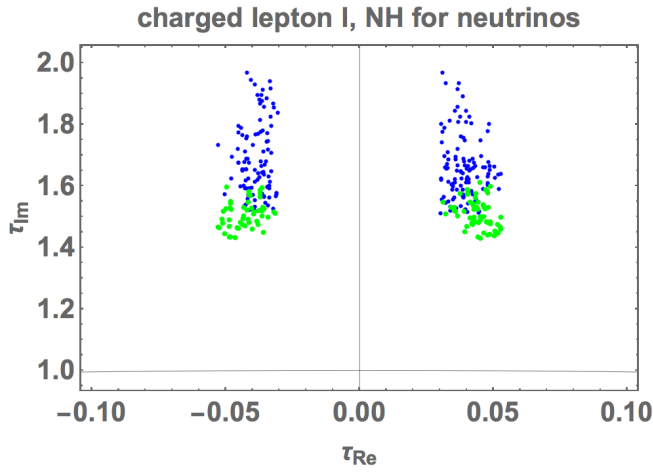
charged lepton mass matrix I
IH for neutrino masses
No allowed region around $\tau = \omega$



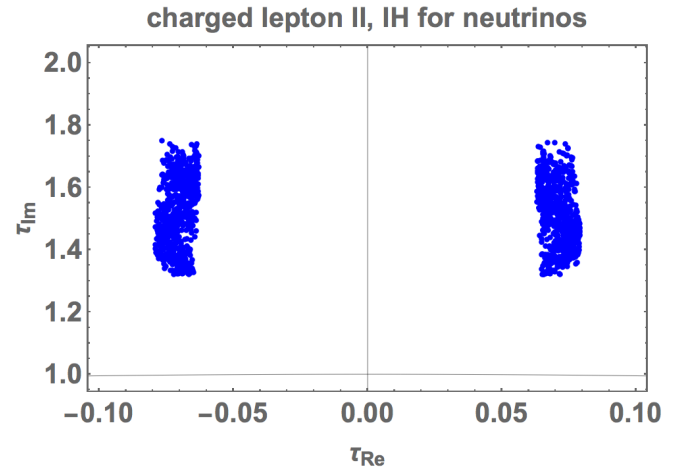
quark mass matrix I
No allowed region around $\tau = \omega$

quark mass matrix II
No allowed region around $\tau = \omega$

Figure 2: Allowed regions of τ at nearby $\tau = \omega$ are shown by green points for the charged lepton mass matrix I and II with NH and IH of neutrinos, respectively. Blue points denote regions in which the sum of neutrino masses $\sum m_i$ is larger than 120 meV.



charged lepton mass matrix I
 IH for neutrino masses
 No allowed region around $\tau = i\infty$



quark mass matrix I
 No allowed region towards $\tau = i\infty$

quark mass matrix II
 No allowed region towards $\tau = i\infty$

Figure 3: Allowed regions of τ towards $\tau = i\infty$ are shown by green points for charged lepton mass matrices I and II with NH and IH of neutrinos, respectively. Blue points denote regions in which the sum of neutrino masses $\sum m_i$ is larger than 120 meV.

7.3 Predictions of CP violation and masses of neutrinos

We predict the leptonic CP violating phase δ_{CP}^ℓ , the sum of neutrino masses $\sum m_i$ and the effective mass for the $0\nu\beta\beta$ decay $|\langle m_{ee} \rangle|$ for each case of leptons since we input four observed quantities of neutrinos (three mixing angles of leptons and observed neutrino mass ratio $\Delta m_{\text{sol}}^2/\Delta m_{\text{atm}}^2$) and three charged lepton masses. For quark sector, there is no prediction because ten observed quantities (quark masses and CKM elements) are put to obtain the region of the modulus τ .

In Table 6, the predicted ranges of the effective mass for the $0\nu\beta\beta$ decay, $\langle m_{ee} \rangle$ are presented for each case. We also summarize magnitudes of parameters $g_{\nu 1}$, $g_{\nu 2}$, g_e for leptons and g_{u1} , g_{u2} , g_{u3} for quarks. Their phases are broad. We add hierarchies of $\tilde{\alpha}_e^2$, $\tilde{\beta}_e^2$, $\tilde{\gamma}_e^2$ and $\tilde{\alpha}_q^2$, $\tilde{\beta}_q^2$, $\tilde{\gamma}_q^2$.

	$\langle m_{ee} \rangle$ [meV]	$ g_{\nu 1} $	$ g_{\nu 2} $	$ g_e $	$\tilde{\alpha}_e^2, \tilde{\beta}_e^2, \tilde{\gamma}_e^2$
NH, charged lepton I, $\tau \simeq i$	15–31	0.02–18	0.63–19	—	$\tilde{\gamma}_e^2 \gg \tilde{\alpha}_e^2 \gg \tilde{\beta}_e^2$
IH, charged lepton I, $\tau \simeq i$	17–31	0.56–3.9	1.6–4.9	—	$\tilde{\gamma}_e^2 \gg \tilde{\alpha}_e^2 \gg \tilde{\beta}_e^2$
NH, charged lepton II, $\tau \simeq i$	1.4–27	0.53–7.0	0.56–6.9	0.63–8.9	$\tilde{\alpha}_e^2 \gg \tilde{\gamma}_e^2 \gg \tilde{\beta}_e^2$
NH, charged lepton II, $\tau \simeq \omega$	2.4–3.0	0.03–0.05	0.53–0.65	0.22–0.28	$\tilde{\alpha}_e^2 \gg \tilde{\beta}_e^2 \gg \tilde{\gamma}_e^2$
IH, charged lepton II, $\tau \simeq \omega$	16–25	1.2–1.8	1.1–1.5	5.5–9.8	$\tilde{\alpha}_e^2 \gg \tilde{\beta}_e^2 \gg \tilde{\gamma}_e^2$
NH, charged lepton I, $\tau \simeq i\infty$	16–18	0.25–0.53	1.0–1.2	—	$\tilde{\gamma}_e^2 \gg \tilde{\beta}_e^2 \gg \tilde{\alpha}_e^2$
NH, charged lepton II, $\tau \simeq i\infty$	8.8–14	0.13–0.33	0.76–0.87	3.1–5.6	$\tilde{\alpha}_e^2 \gg \tilde{\gamma}_e^2 \gg \tilde{\beta}_e^2$
		$ g_{u1} $	$ g_{u2} $	$ g_{u3} $	$\tilde{\alpha}_q^2, \tilde{\beta}_q^2, \tilde{\gamma}_q^2$
quark mass matrices I, $\tau \simeq i$	—	0.01–0.86	0.14–1.29	0.02–0.07	$\tilde{\gamma}_u^2 \gg \tilde{\beta}_u^2 \gg \tilde{\alpha}_u^2$ $\tilde{\gamma}_d^2 \gg \tilde{\alpha}_d^2 \gg \tilde{\beta}_d^2$

Table 6: Magnitudes of parameters $g_{\nu 1}$, $g_{\nu 2}$, g_e for leptons and g_{u1} , g_{u2} , g_{u3} for quarks are shown. Predicted ranges of the effective mass for the $0\nu\beta\beta$ decay, $\langle m_{ee} \rangle$ [meV] are also given. In addition, hierarchies of $\tilde{\alpha}_e^2$, $\tilde{\beta}_e^2$, $\tilde{\gamma}_e^2$ and $\tilde{\alpha}_q^2$, $\tilde{\beta}_q^2$, $\tilde{\gamma}_q^2$ are presented.

We present numerical predictions on $\sum m_i - \delta_{\text{CP}}^\ell$ and $\delta_{\text{CP}}^\ell - \sin^2 \theta_{23}$ planes for successful seven cases in Figs. 4–10. In Fig. 4, we show them at nearby $\tau = i$ for the charged lepton mass matrix I with NH of neutrinos. The predicted range of the sum of neutrino masses is $\sum m_i = 86$ –120 meV. The predicted δ_{CP}^ℓ depends on $\sum m_i$. A crucial test will be presented in the near future by cosmological observations. The correlation between $\sin^2 \theta_{23}$ and δ_{CP}^ℓ is also helpful to test this case.

In Fig. 5, we show them at nearby $\tau = i$ for the charged lepton mass matrix I with IH of neutrinos. The predicted range of the sum of neutrino masses is $\sum m_i = 90$ –120 meV. The prediction of δ_{CP}^ℓ is clearly given versus $\sum m_i$. On the other hand, $\sin^2 \theta_{23}$ is predicted to be smaller than 0.52. Crucial test will be available by cosmological observations and neutrino oscillation experiments in the near future.

In Fig. 6, we show them at nearby $\tau = i$ for the charged lepton mass matrix II with NH of neutrinos. The predicted range of the sum of neutrino masses is $\sum m_i = 58$ –83 meV while δ_{CP}^ℓ is allowed in $[-\pi, \pi]$. There is no correlation between $\sin^2 \theta_{23}$ and δ_{CP}^ℓ . The rather small value of the sum of neutrino masses is a characteristic prediction in this case.

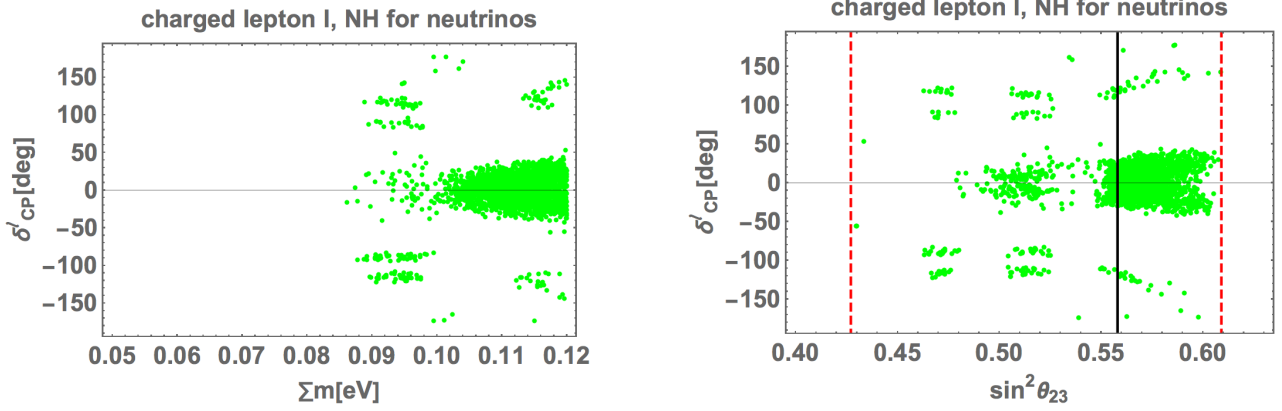


Figure 4: Allowed regions on $\sum m_i - \delta_{CP}^\ell$ and $\delta_{CP}^\ell - \sin^2 \theta_{23}$ planes at nearby $\tau = i$ for the charged lepton mass matrix I with NH of neutrinos. The solid black line denotes observed best-fit value of $\sin^2 \theta_{23}$, and red dashed-lines denote its upper(lower)-bound of 3σ interval.

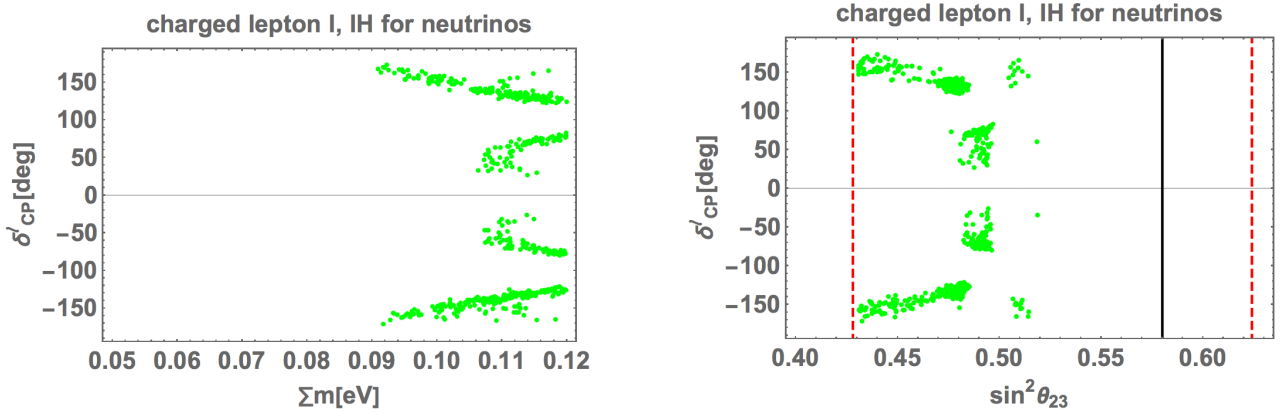


Figure 5: Allowed regions on $\sum m_i - \delta_{CP}^\ell$ and $\delta_{CP}^\ell - \sin^2 \theta_{23}$ planes at nearby $\tau = i$ for the charged lepton mass matrix I with IH of neutrinos.

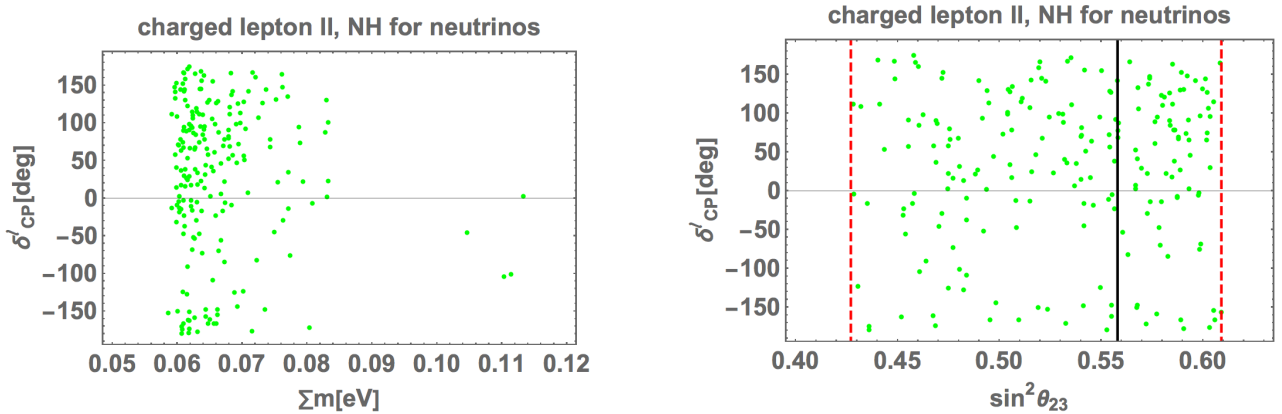


Figure 6: Allowed regions on $\sum m_i - \delta_{CP}^\ell$ and $\delta_{CP}^\ell - \sin^2 \theta_{23}$ planes at nearby $\tau = i$ for the charged lepton mass matrix II with NH of neutrinos.

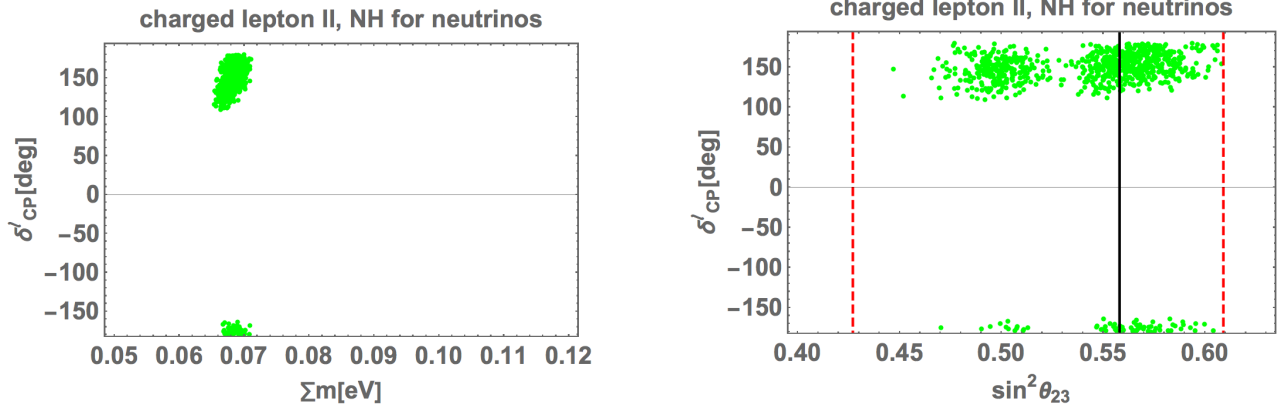


Figure 7: Allowed regions on $\sum m_i - \delta_{CP}^\ell$ and $\delta_{CP}^\ell - \sin^2 \theta_{23}$ planes at nearby $\tau = \omega$ for the charged lepton mass matrix II with NH of neutrinos.

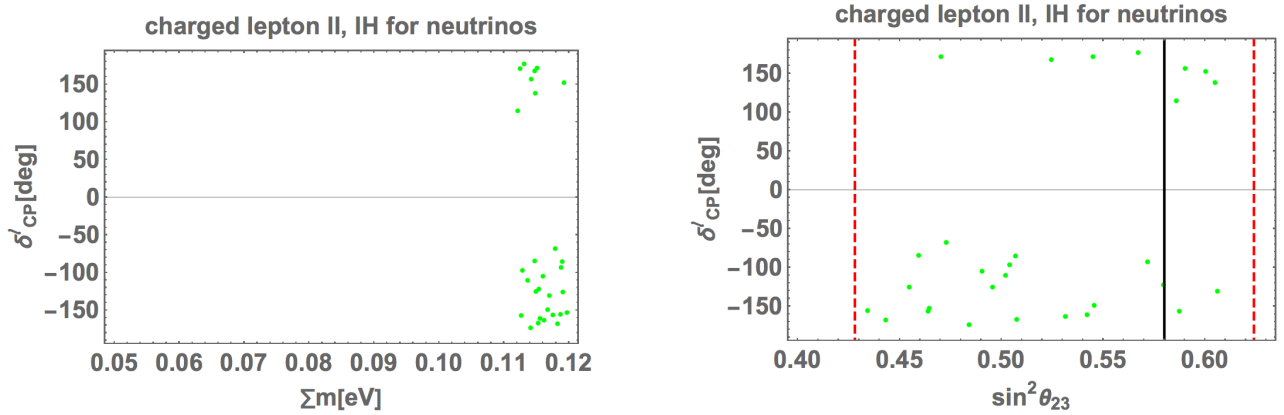


Figure 8: Allowed regions on $\sum m_i - \delta_{CP}^\ell$ and $\delta_{CP}^\ell - \sin^2 \theta_{23}$ planes at nearby $\tau = \omega$ for the charged lepton mass matrix II with IH of neutrinos.

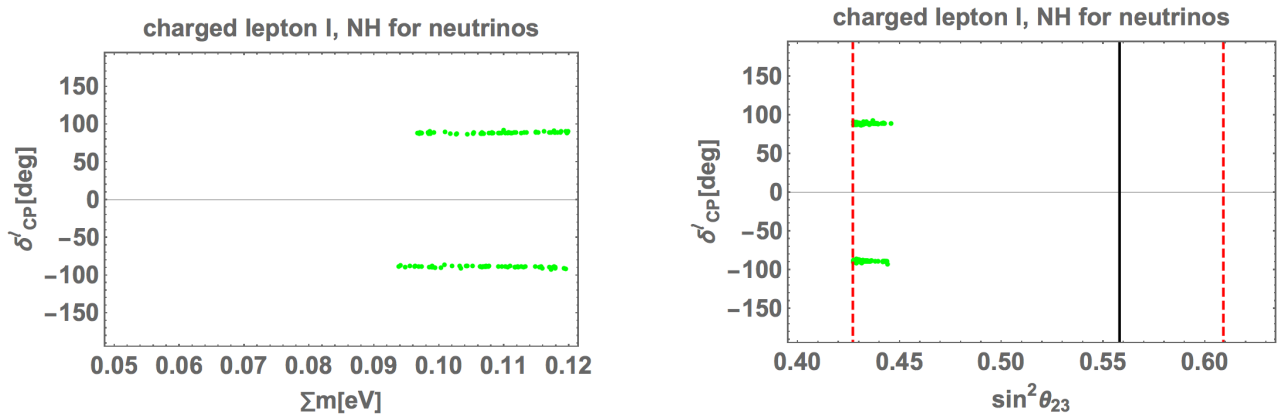


Figure 9: Allowed regions on $\sum m_i - \delta_{CP}^\ell$ and $\delta_{CP}^\ell - \sin^2 \theta_{23}$ planes towards $\tau = i\infty$ for the charged lepton mass matrix I with NH of neutrinos.

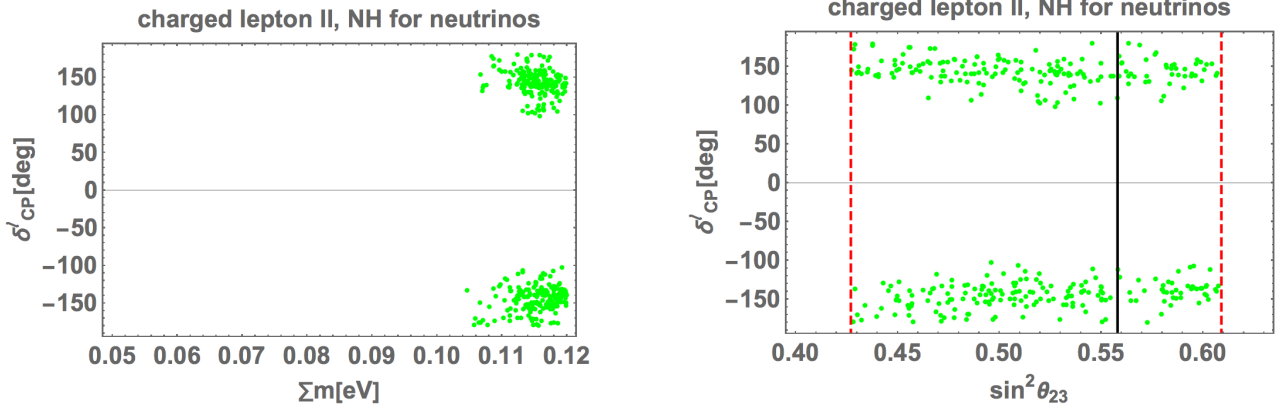


Figure 10: Allowed regions on $\sum m_i - \delta_{\text{CP}}^\ell$ and $\delta_{\text{CP}}^\ell - \sin^2 \theta_{23}$ planes towards $\tau = i\infty$ for the charged lepton mass matrix II with NH of neutrinos.

Let us give our predictions on $\sum m_i - \delta_{\text{CP}}^\ell$ and $\delta_{\text{CP}}^\ell - \sin^2 \theta_{23}$ planes at nearby $\tau = \omega$. In Fig. 7, we show them for the charged lepton mass matrix II with NH of neutrinos. The predicted range of the sum of neutrino masses is $\sum m_i = 65\text{--}71$ meV. The ranges of δ_{CP}^ℓ is clearly given in $[110^\circ, 180^\circ]$ and $[-180^\circ, -160^\circ]$. On the other hand, $\sin^2 \theta_{23}$ is predicted in both 1st- and 2nd-octant.

In Fig. 8, we show them for the charged lepton mass matrix II with IH of neutrinos at nearby $\tau = \omega$. The predicted range of the sum of neutrino masses is $\sum m_i = 112\text{--}120$ meV, which may be excluded in the near future due to the cosmological observations. The predicted CP violating phase is $\delta_{\text{CP}}^\ell = [-180^\circ, -60^\circ]$ and $[110^\circ, 180^\circ]$. There is no clear correlation between $\sin^2 \theta_{23}$ and δ_{CP}^ℓ .

It is noticed that the predicted CP violating phase δ_{CP}^ℓ is asymmetric for plus and minus signs in both Figs. 7 and 8. That is due to excluding the τ region at nearby $\tau = \omega$ outside the fundamental domain of $\text{PSL}(2, \mathbb{Z})$. Indeed, the excluded region corresponds to the other region inside at nearby the fixed point $\tau = -\omega^2$, where we obtain δ_{CP}^ℓ with the reversed sign of Figs. 7 and 8.

Finally, we show predictions on $\sum m_i - \delta_{\text{CP}}^\ell$ and $\delta_{\text{CP}}^\ell - \sin^2 \theta_{23}$ planes towards $\tau = i\infty$. In Fig. 9, we show them for the charged lepton mass matrix I with NH of neutrinos. The predicted range of the sum of neutrino masses is in the narrow range of $\sum m_i = 94\text{--}120$ meV. The predicted δ_{CP}^ℓ is close to $\pm\pi/2$. On the other hand, $\sin^2 \theta_{23}$ is predicted to be smaller than 0.45. The predicted CP violation is favored by the T2K experiment [85], however the predicted $\sin^2 \theta_{23}$ may be excluded in the near future since it is far from the best fit value.

In Fig. 10, we show them for the charged lepton mass matrix II with NH of neutrinos. The predicted range of the sum of neutrino masses is in $\sum m_i = 105\text{--}120$ meV. The predicted δ_{CP}^ℓ is clearly given in $\pm(100^\circ\text{--}180^\circ)$. On the other hand, $\sin^2 \theta_{23}$ is allowed in full range of 3σ error-bar. Crucial test will be available by cosmological observations and CP violation experiments of neutrinos in the future.

Thus, lepton mass matrices at nearby fixed points provide characteristic predictions for $\sum m_i$ and δ_{CP}^ℓ . On the other hand, there is no prediction for the quark sector.

8 Summary

In the modular invariant flavor model of A_4 , we have studied the hierarchical structure of lepton/quark flavors at the nearby fixed points of the modulus. There are only two inequivalent fixed points in the fundamental domain of $\text{PSL}(2, \mathbb{Z})$, $\tau = i$ and $\tau = \omega$. These fixed points correspond to the residual

symmetries $\mathbb{Z}_2^S = \{I, S\}$ and $\mathbb{Z}_3^{ST} = \{I, ST, (ST)^2\}$ of A_4 , respectively. There is also infinite point $\tau = i\infty$, in which the subgroup $\mathbb{Z}_3^T = \{I, T, T^2\}$ of A_4 is preserved. We have examined typical two-type mass matrices for charged leptons and quarks by using modular forms of weights 2, 4 and 6 while the neutrino mass matrix with the modular forms of weight 4 through the Weinberg operator. By performing Taylor expansion of modular forms around fixed points, we have obtained linear modular forms in good approximations. By using those explicit modular forms, we have found the hierarchical structure of these mass matrices in the diagonal base of S , T and ST , in which the flavor mixing angles are easily estimated. The observed PMNS mixing angles are reproduced at the nearby fixed point in ten cases of lepton mass matrices. Among them, seven cases satisfy the cosmological bound $\sum m_i \leq 120 \text{ meV}$. On the other hand, only one case of quark mass matrices is consistent with the observed CKM matrix. Our results have been confirmed by scanning model parameters numerically as seen in τ regions of Figs. 1, 2 and 3.

We have also presented predictions for $\sum m_i$ and δ_{CP}^ℓ for seven cases. Some cases will be tested in the near future. Although there is no prediction for the quark sector, the obtained τ provides an interesting subject, the possibility of the common τ between quarks and leptons. Indeed, there exists the common region around $\tau = \pm 0.04 + 1.05i$ for the charged lepton mass matrix I with NH of neutrinos as seen Fig. 1.

We have worked by using two-type specific mass matrices for charged leptons and quarks while one Majorana neutrino mass matrix in order to clarify the behavior at nearby fixed points. More studies including other mass matrices are necessary to understand the phenomenology of fixed points completely. The modular symmetry provides a good outlook for the flavor structure of leptons and quarks at nearby fixed points. We also should pay attention to the recent theoretical work: the spontaneous CP violation in Type IIB string theory is possibly realized at nearby fixed points, where the moduli stabilization is performed in a controlled way [80, 81]. Thus, the modular symmetry at nearby fixed points gives us an attractive approach to flavors.

Acknowledgments

This research was supported by an appointment to the JRG Program at the APCTP through the Science and Technology Promotion Fund and Lottery Fund of the Korean Government. This was also supported by the Korean Local Governments - Gyeongsangbuk-do Province and Pohang City (H.O.). H. O. is sincerely grateful for the KIAS member.

Appendix

A Tensor product of A_4 group

We take the generators of A_4 group for the triplet as follows:

$$S = \frac{1}{3} \begin{pmatrix} -1 & 2 & 2 \\ 2 & -1 & 2 \\ 2 & 2 & -1 \end{pmatrix}, \quad T = \begin{pmatrix} 1 & 0 & 0 \\ 0 & \omega & 0 \\ 0 & 0 & \omega^2 \end{pmatrix}, \quad (168)$$

where $\omega = e^{i\frac{2}{3}\pi}$ for a triplet. In this base, the multiplication rule is

$$\begin{aligned} \begin{pmatrix} a_1 \\ a_2 \\ a_3 \end{pmatrix}_{\mathbf{3}} \otimes \begin{pmatrix} b_1 \\ b_2 \\ b_3 \end{pmatrix}_{\mathbf{3}} &= (a_1b_1 + a_2b_3 + a_3b_2)_{\mathbf{1}} \oplus (a_3b_3 + a_1b_2 + a_2b_1)_{\mathbf{1}'} \\ &\oplus (a_2b_2 + a_1b_3 + a_3b_1)_{\mathbf{1}''} \\ &\oplus \frac{1}{3} \begin{pmatrix} 2a_1b_1 - a_2b_3 - a_3b_2 \\ 2a_3b_3 - a_1b_2 - a_2b_1 \\ 2a_2b_2 - a_1b_3 - a_3b_1 \end{pmatrix}_{\mathbf{3}} \oplus \frac{1}{2} \begin{pmatrix} a_2b_3 - a_3b_2 \\ a_1b_2 - a_2b_1 \\ a_3b_1 - a_1b_3 \end{pmatrix}_{\mathbf{3}} , \\ \mathbf{1} \otimes \mathbf{1} &= \mathbf{1} , \quad \mathbf{1}' \otimes \mathbf{1}' = \mathbf{1}'' , \quad \mathbf{1}'' \otimes \mathbf{1}'' = \mathbf{1}' , \quad \mathbf{1}' \otimes \mathbf{1}'' = \mathbf{1} , \end{aligned} \quad (169)$$

where

$$T(\mathbf{1}') = \omega , \quad T(\mathbf{1}'') = \omega^2. \quad (170)$$

More details are shown in the review [6, 7].

B Mass matrix in arbitrary base of S and T

Define the new basis of generators, \hat{S} and \hat{T} by a unitary transformation as:

$$\hat{S} = USU^\dagger, \quad \hat{T} = UTU^\dagger , \quad (171)$$

where \hat{S} , S , \hat{T} , T and U are 3×3 matrices. Since the A_4 triplet transforms under the S (T) transformation as:

$$\begin{pmatrix} a_1 \\ a_2 \\ a_3 \end{pmatrix}_{\mathbf{3}} \rightarrow S \ (T) \begin{pmatrix} a_1 \\ a_2 \\ a_3 \end{pmatrix}_{\mathbf{3}} = U^\dagger \hat{S} \ (\hat{T}) U \begin{pmatrix} a_1 \\ a_2 \\ a_3 \end{pmatrix}_{\mathbf{3}} . \quad (172)$$

Thus, in the new base, the A_4 triplet transforms as:

$$\begin{pmatrix} \hat{a}_1 \\ \hat{a}_2 \\ \hat{a}_3 \end{pmatrix}_{\mathbf{3}} \rightarrow \hat{S} \ (\hat{T}) \begin{pmatrix} \hat{a}_1 \\ \hat{a}_2 \\ \hat{a}_3 \end{pmatrix}_{\mathbf{3}} , \quad (173)$$

where

$$\begin{pmatrix} \hat{a}_1 \\ \hat{a}_2 \\ \hat{a}_3 \end{pmatrix}_{\mathbf{3}} = U \begin{pmatrix} a_1 \\ a_2 \\ a_3 \end{pmatrix}_{\mathbf{3}} . \quad (174)$$

Let us rewrite the Dirac mass matrix M_{RL} in the new base (\hat{S} , \hat{T}) of the triplet left-handed fields. Denoting L and \hat{L} to be triplets of the left-handed fields in the base of S and \hat{S} , respectively, and R to be right-handed singlets, the Dirac mass matrix is written as:

$$\bar{R}M_{RL}L = \bar{R}M_{RL}U^\dagger\hat{L} \quad (175)$$

where

$$\hat{L} = UL. \quad (176)$$

Then, the Dirac mass matrix \hat{M}_{RL} in the new base is given as:

$$\hat{M}_{RL} = M_{RL}U^\dagger. \quad (177)$$

On the other hand, the Majorana mass matrix M_{LL} in the new base (\hat{S}, \hat{T}) is written as

$$L^c M_{LL} L = \hat{L}^c U M_{LL} U^\dagger L. \quad (178)$$

Therefore, the Majorana mass matrix \hat{M}_{LL} is given as:

$$\hat{M}_{LL} = U M_{LL} U^\dagger. \quad (179)$$

C Modular forms at nearby fixed points

C.1 Modular forms at nearby $\tau = i$

Let us present the behavior of modular forms at nearby $\tau = i$. We obtain approximate linear forms of $Y_1(\tau)$, $Y_2(\tau)$ and $Y_3(\tau)$ by performing Taylor expansion of modular forms around $\tau = i$. We parametrize τ as:

$$\tau = i + \epsilon, \quad \text{with} \quad \epsilon = \epsilon_R + i \epsilon_I, \quad (180)$$

where $|\epsilon|$ is supposed to be enough small $|\epsilon| \ll 1$. For the case of the pure imaginary number of ϵ , that is $\epsilon = i \epsilon_I$ (ϵ_I is real), we obtain the linear fit of ϵ by

$$\frac{Y_2(\tau)}{Y_1(\tau)} \simeq (1 - 2.05 \epsilon_I) (1 - \sqrt{3}), \quad \frac{Y_3(\tau)}{Y_1(\tau)} \simeq (1 - 4.1 \epsilon_I) (-2 + \sqrt{3}), \quad (181)$$

where coefficients are obtained by numerical fittings. These ratios decrease linearly for $\epsilon_I \geq 0$.

On the other hand, for the case of the real number of ϵ , that is $\epsilon = \epsilon_R$, (ϵ_R is real), we obtain as:

$$\begin{aligned} \text{Re} \frac{Y_2(\tau)}{Y_1(\tau)} &\simeq (1 - 1.9 \epsilon_R^2) (1 - \sqrt{3}), & \text{Re} \frac{Y_3(\tau)}{Y_1(\tau)} &\simeq (1 - 8 \epsilon_R^2) (-2 + \sqrt{3}), \\ \text{Im} \frac{Y_2(\tau)}{Y_1(\tau)} &\simeq 2.05 \epsilon_R (1 - \sqrt{3}), & \text{Im} \frac{Y_3(\tau)}{Y_1(\tau)} &\simeq 4.1 \epsilon_R (-2 + \sqrt{3}), \end{aligned} \quad (182)$$

where the liner terms of ϵ disappear in the real parts. Finally, after neglecting $\mathcal{O}(\epsilon_R^2)$, we obtain approximately

$$\frac{Y_2(\tau)}{Y_1(\tau)} \simeq (1 + \epsilon_1) (1 - \sqrt{3}), \quad \frac{Y_3(\tau)}{Y_1(\tau)} \simeq (1 + \epsilon_2) (-2 + \sqrt{3}), \quad \epsilon_1 = \frac{1}{2} \epsilon_2 = 2.05 i \epsilon. \quad (183)$$

These approximate forms are agreement with exact numerical values within 0.1 % for $|\epsilon| \leq 0.05$.

We have also higher weight modular forms $Y_i^{(k)}$ in Eqs. (13) and (14) in terms of ϵ_1 and ϵ_2 . For weight 4, they are

$$\begin{aligned}\frac{Y_1^{(4)}(\tau)}{Y_1^2(\tau)} &\simeq 6 - 3\sqrt{3} + (5 - 3\sqrt{3})(\epsilon_1 + \epsilon_2), & \frac{Y_2^{(4)}(\tau)}{Y_1^2(\tau)} &\simeq 6 - 3\sqrt{3} + (\sqrt{3} - 1)\epsilon_1 + (14 - 8\sqrt{3})\epsilon_2, \\ \frac{Y_3^{(4)}(\tau)}{Y_1^2(\tau)} &\simeq 6 - 3\sqrt{3} + (8 - 4\sqrt{3})\epsilon_1 + (2 - \sqrt{3})\epsilon_2, & & \\ \frac{Y_1^{(4)}(\tau)}{Y_1^2(\tau)} &\simeq -9 + 6\sqrt{3} + (6\sqrt{3} - 10)(\epsilon_1 + \epsilon_2), & \frac{Y_{1'}^{(4)}(\tau)}{Y_1^2(\tau)} &\simeq 9 - 6\sqrt{3} + (2 - 2\sqrt{3})\epsilon_1 + (14 - 8\sqrt{3})\epsilon_2.\end{aligned}\tag{184}$$

For weight 6, they are

$$\begin{aligned}\frac{Y_1^{(6)}(\tau)}{3Y_1^3(\tau)} &\simeq 2\sqrt{3} - 3 + \left(2\sqrt{3} - \frac{10}{3}\right)(\epsilon_1 + \epsilon_2), \\ \frac{Y_2^{(6)}(\tau)}{3Y_1^3(\tau)} &\simeq 5\sqrt{3} - 9 + \left(\frac{31}{\sqrt{3}} - \frac{55}{3}\right)\epsilon_1 + \left(\frac{16}{\sqrt{3}} - \frac{28}{3}\right)\epsilon_2, \\ \frac{Y_3^{(6)}(\tau)}{3Y_1^3(\tau)} &\simeq 12 - 7\sqrt{3} + \left(\frac{38}{3} - \frac{22}{\sqrt{3}}\right)\epsilon_1 + \left(\frac{74}{3} - \frac{43}{\sqrt{3}}\right)\epsilon_2, \\ \frac{Y_{1'}^{(6)}(\tau)}{3Y_1^3(\tau)} &\simeq 7\sqrt{3} - 12 + \left(2\sqrt{3} - \frac{10}{3}\right)\epsilon_1 + \left(17\sqrt{3} - \frac{88}{3}\right)\epsilon_2, \\ \frac{Y_2'^{(6)}(\tau)}{3Y_1^3(\tau)} &\simeq 3 - 2\sqrt{3} + \left(\frac{2}{3} - \frac{2}{\sqrt{3}}\right)\epsilon_1 + \left(\frac{14}{3} - \frac{8}{\sqrt{3}}\right)\epsilon_2, \\ \frac{Y_3'^{(6)}(\tau)}{3Y_1^3(\tau)} &\simeq 9 - 5\sqrt{3} + \left(\frac{35}{3} - \frac{19}{\sqrt{3}}\right)\epsilon_1 + \left(\frac{38}{3} - \frac{22}{\sqrt{3}}\right)\epsilon_2, \\ \frac{Y_1^{(6)}(\tau)}{3Y_1^3(\tau)} &\simeq (15 - 9\sqrt{3})\epsilon_1 + (12\sqrt{3} - 21)\epsilon_2.\end{aligned}\tag{185}$$

C.2 Modular forms at nearby $\tau = \omega$

Let us present the behavior of modular forms at nearby $\tau = \omega$. We perform linear approximation of the modular forms $Y_1(\tau)$, $Y_2(\tau)$ and $Y_3(\tau)$ by performing Taylor expansion around $\tau = \omega$. We parametrize τ as:

$$\tau = \omega + \epsilon, \quad \text{with} \quad \epsilon = \epsilon_R + i\epsilon_I, \tag{186}$$

where we suppose $|\epsilon| \ll 1$. For the case of $\epsilon = i\epsilon_I$, which is a pure imaginary number, we obtain the linear fit of ϵ as:

$$\frac{Y_2(\tau)}{Y_1(\tau)} \simeq \omega(1 - 2.1\epsilon_I), \quad \frac{Y_3(\tau)}{Y_1(\tau)} \simeq -\frac{1}{2}\omega^2(1 - 4.2\epsilon_I), \tag{187}$$

where coefficients are obtained by numerical fittings. These ratios decrease linearly for $\epsilon_I \geq 0$. On the other hand, for the case of $\epsilon = \epsilon_R$, which is a real number, we obtain as:

$$\begin{aligned} \operatorname{Re} \frac{Y_2(\tau)}{Y_1(\tau)} &\simeq \omega (1 - 3 \epsilon_R^2), & \operatorname{Re} \frac{Y_3(\tau)}{Y_1(\tau)} &\simeq -\frac{1}{2} \omega^2 (1 - 11 \epsilon_R^2). \\ \operatorname{Im} \frac{Y_2(\tau)}{Y_1(\tau)} &\simeq \omega (2.1 \epsilon_R), & \operatorname{Im} \frac{Y_3(\tau)}{Y_1(\tau)} &\simeq -\frac{1}{2} \omega^2 (4.2 \epsilon_R), \end{aligned} \quad (188)$$

where the linear terms of ϵ disappear in the real parts. After neglecting $\mathcal{O}(\epsilon_R^2)$, we obtain approximately

$$\frac{Y_2(\tau)}{Y_1(\tau)} \simeq \omega (1 + \epsilon_1), \quad \frac{Y_3(\tau)}{Y_1(\tau)} \simeq -\frac{1}{2} \omega^2 (1 + \epsilon_2), \quad \epsilon_1 = \frac{1}{2} \epsilon_2 = 2.1 i \epsilon, \quad (189)$$

where $|\epsilon| \ll 1$. These approximate forms are agreement with exact numerical values within 1% for $|\epsilon| \leq 0.05$.

We have also higher weight modular forms $Y_i^{(k)}$ in Eqs. (13) and (14) in terms of ϵ_1 and ϵ_2 . For weight 4, they are

$$\begin{aligned} \frac{Y_1^{(4)}(\tau)}{Y_1^2(\tau)} &\simeq \frac{3}{2} (1 + \epsilon_1 + \epsilon_2), & \frac{Y_2^{(4)}(\tau)}{Y_1^2(\tau)} &\simeq -\frac{3}{2} \omega \left(\frac{1}{2} + \frac{2}{3} \epsilon_1 + \frac{1}{6} \epsilon_2 \right), & \frac{Y_3^{(4)}(\tau)}{Y_1^2(\tau)} &\simeq \frac{3}{2} \omega^2 \left(1 - \frac{4}{3} \epsilon_1 - \frac{2}{3} \epsilon_2 \right), \\ \frac{Y_{1'}^{(4)}(\tau)}{Y_1^2(\tau)} &\simeq -(\epsilon_1 + \epsilon_2), & \frac{Y_{1''}^{(4)}(\tau)}{Y_1^2(\tau)} &\simeq \frac{9}{4} \omega \left(1 + \frac{8}{9} \epsilon_1 + \frac{2}{9} \epsilon_2 \right). \end{aligned} \quad (190)$$

For weight 6, they are

$$\begin{aligned} \frac{Y_1^{(6)}(\tau)}{Y_1^3(\tau)} &\simeq -(\epsilon_1 + \epsilon_2), \\ \frac{Y_2^{(6)}(\tau)}{Y_1^3(\tau)} &\simeq -\omega (\epsilon_1 + \epsilon_2), \\ \frac{Y_3^{(6)}(\tau)}{Y_1^3(\tau)} &\simeq \frac{1}{2} \omega^2 (\epsilon_1 + \epsilon_2), \\ \frac{Y_{1'}^{(6)}(\tau)}{Y_1^3(\tau)} &\simeq -\frac{9}{8} \left(1 + \frac{8}{9} \epsilon_1 + \frac{11}{9} \epsilon_2 \right), \\ \frac{Y_{2'}^{(6)}(\tau)}{Y_1^3(\tau)} &\simeq \frac{9}{4} \omega \left(1 + \frac{8}{9} \epsilon_1 + \frac{2}{9} \epsilon_2 \right), \\ \frac{Y_{3'}^{(6)}(\tau)}{Y_1^3(\tau)} &\simeq \frac{9}{4} \omega^2 \left(1 + \frac{17}{9} \epsilon_1 + \frac{2}{9} \epsilon_2 \right), \\ \frac{Y_{1''}^{(6)}(\tau)}{Y_1^3(\tau)} &\simeq \frac{27}{8} \left(1 + \frac{4}{3} \epsilon_1 + \frac{1}{3} \epsilon_2 \right). \end{aligned} \quad (191)$$

C.3 Modular forms towards $\tau = i\infty$

We show the behavior of modular forms at large $\operatorname{Im} \tau$, where $q = \exp(2\pi i \tau)$ is suppressed. Taking leading terms of Eq. (11), we can express modular forms approximately as:

$$Y_1(\tau) \simeq 1 + 12p\epsilon, \quad Y_2(\tau) \simeq -6p^{\frac{1}{3}} \epsilon^{\frac{1}{3}}, \quad Y_3(\tau) \simeq -18p^{\frac{2}{3}} \epsilon^{\frac{2}{3}}, \quad p = e^{2\pi i \operatorname{Re} \tau}, \quad \epsilon = e^{-2\pi \operatorname{Im} \tau}. \quad (192)$$

Higher weight modular forms $Y_i^{(k)}$ in Eqs. (13) and (14) are obtained in terms of p and ϵ approximately. For weight 4, they are

$$\begin{aligned} Y_1^{(4)}(\tau) &\simeq 1 - 84p\epsilon, & Y_2^{(4)}(\tau) &\simeq 6p^{\frac{1}{3}}\epsilon^{\frac{1}{3}}, & Y_3^{(4)}(\tau) &\simeq 54p^{\frac{2}{3}}\epsilon^{\frac{2}{3}}, \\ Y_1^{\prime(4)}(\tau) &\simeq 1 + 240p\epsilon, & Y_1^{\prime(4)}(\tau) &\simeq -12p^{\frac{1}{3}}\epsilon^{\frac{1}{3}}. \end{aligned} \quad (193)$$

Weight 6 modular forms are given:

$$\begin{aligned} Y_1^{(6)}(\tau) &\simeq 1 + 252p\epsilon, & Y_2^{(6)}(\tau) &\simeq -6p^{\frac{1}{3}}\epsilon^{\frac{1}{3}}, & Y_3^{(6)}(\tau) &\simeq -18p^{\frac{2}{3}}\epsilon^{\frac{2}{3}}, \\ Y_1^{\prime(6)}(\tau) &\simeq 216p\epsilon, & Y_2^{\prime(6)}(\tau) &\simeq -12p^{\frac{1}{3}}\epsilon^{\frac{1}{3}}, & Y_3^{\prime(6)}(\tau) &\simeq 72p^{\frac{2}{3}}\epsilon^{\frac{2}{3}}, \\ Y_1^{(6)}(\tau) &\simeq 1 - 504p\epsilon. \end{aligned} \quad (194)$$

D Majorana and Dirac phases and $\langle m_{ee} \rangle$ in $0\nu\beta\beta$ decay

Supposing neutrinos to be Majorana particles, the PMNS matrix U_{PMNS} [83, 84] is parametrized in terms of the three mixing angles θ_{ij} ($i, j = 1, 2, 3; i < j$), one CP violating Dirac phase δ_{CP}^ℓ and two Majorana phases α_{21}, α_{31} as follows:

$$U_{\text{PMNS}} = \begin{pmatrix} c_{12}c_{13} & s_{12}c_{13} & s_{13}e^{-i\delta_{\text{CP}}^\ell} \\ -s_{12}c_{23} - c_{12}s_{23}s_{13}e^{i\delta_{\text{CP}}^\ell} & c_{12}c_{23} - s_{12}s_{23}s_{13}e^{i\delta_{\text{CP}}^\ell} & s_{23}c_{13} \\ s_{12}s_{23} - c_{12}c_{23}s_{13}e^{i\delta_{\text{CP}}^\ell} & -c_{12}s_{23} - s_{12}c_{23}s_{13}e^{i\delta_{\text{CP}}^\ell} & c_{23}c_{13} \end{pmatrix} \begin{pmatrix} 1 & 0 & 0 \\ 0 & e^{i\frac{\alpha_{21}}{2}} & 0 \\ 0 & 0 & e^{i\frac{\alpha_{31}}{2}} \end{pmatrix}, \quad (195)$$

where c_{ij} and s_{ij} denote $\cos\theta_{ij}$ and $\sin\theta_{ij}$, respectively.

The rephasing invariant CP violating measure of leptons [105, 106] is defined by the PMNS matrix elements $U_{\alpha i}$. It is written in terms of the mixing angles and the CP violating phase as:

$$J_{\text{CP}} = \text{Im} [U_{e1}U_{\mu 2}U_{e2}^*U_{\mu 1}^*] = s_{23}c_{23}s_{12}c_{12}s_{13}c_{13}^2 \sin\delta_{\text{CP}}^\ell, \quad (196)$$

where $U_{\alpha i}$ denotes the each component of the PMNS matrix.

There are also other invariants I_1 and I_2 associated with Majorana phases

$$I_1 = \text{Im} [U_{e1}^*U_{e2}] = c_{12}s_{12}c_{13}^2 \sin\left(\frac{\alpha_{21}}{2}\right), \quad I_2 = \text{Im} [U_{e1}^*U_{e3}] = c_{12}s_{13}c_{13} \sin\left(\frac{\alpha_{31}}{2} - \delta_{\text{CP}}^\ell\right). \quad (197)$$

We can calculate $\delta_{\text{CP}}^\ell, \alpha_{21}$ and α_{31} with these relations by taking account of

$$\begin{aligned} \cos\delta_{\text{CP}}^\ell &= \frac{|U_{\tau 1}|^2 - s_{12}^2s_{23}^2 - c_{12}^2c_{23}^2s_{13}^2}{2c_{12}s_{12}c_{23}s_{23}s_{13}}, \\ \text{Re} [U_{e1}^*U_{e2}] &= c_{12}s_{12}c_{13}^2 \cos\left(\frac{\alpha_{21}}{2}\right), & \text{Re} [U_{e1}^*U_{e3}] &= c_{12}s_{13}c_{13} \cos\left(\frac{\alpha_{31}}{2} - \delta_{\text{CP}}^\ell\right). \end{aligned} \quad (198)$$

In terms of these parameters, the effective mass for the $0\nu\beta\beta$ decay is given as follows:

$$\langle m_{ee} \rangle = \left| m_1c_{12}^2c_{13}^2 + m_2s_{12}^2c_{13}^2e^{i\alpha_{21}} + m_3s_{13}^2e^{i(\alpha_{31}-2\delta_{\text{CP}}^\ell)} \right|. \quad (199)$$

References

- [1] F. Wilczek and A. Zee, Phys. Lett. **70B** (1977) 418 Erratum: [Phys. Lett. **72B** (1978) 504].
- [2] S. Pakvasa and H. Sugawara, Phys. Lett. **73B** (1978) 61.
- [3] M. Fukugita, M. Tanimoto and T. Yanagida, Phys. Rev. D **57** (1998) 4429 [hep-ph/9709388].
- [4] Y. Fukuda *et al.* [Super-Kamiokande Collaboration], Phys. Rev. Lett. **81** (1998) 1562 [hep-ex/9807003].
- [5] G. Altarelli and F. Feruglio, Rev. Mod. Phys. **82** (2010) 2701 [arXiv:1002.0211 [hep-ph]].
- [6] H. Ishimori, T. Kobayashi, H. Ohki, Y. Shimizu, H. Okada and M. Tanimoto, Prog. Theor. Phys. Suppl. **183** (2010) 1 [arXiv:1003.3552 [hep-th]].
- [7] H. Ishimori, T. Kobayashi, H. Ohki, H. Okada, Y. Shimizu and M. Tanimoto, Lect. Notes Phys. **858** (2012) 1, Springer.
- [8] D. Hernandez and A. Y. Smirnov, Phys. Rev. D **86** (2012) 053014 [arXiv:1204.0445 [hep-ph]].
- [9] S. F. King and C. Luhn, Rept. Prog. Phys. **76** (2013) 056201 [arXiv:1301.1340 [hep-ph]].
- [10] S. F. King, A. Merle, S. Morisi, Y. Shimizu and M. Tanimoto, New J. Phys. **16**, 045018 (2014) [arXiv:1402.4271 [hep-ph]].
- [11] M. Tanimoto, AIP Conf. Proc. **1666** (2015) 120002.
- [12] S. F. King, Prog. Part. Nucl. Phys. **94** (2017) 217 [arXiv:1701.04413 [hep-ph]].
- [13] S. T. Petcov, Eur. Phys. J. C **78** (2018) no.9, 709 [arXiv:1711.10806 [hep-ph]].
- [14] F. Feruglio and A. Romanino, arXiv:1912.06028 [hep-ph].
- [15] E. Ma and G. Rajasekaran, Phys. Rev. D **64**, 113012 (2001) [arXiv:hep-ph/0106291].
- [16] K. S. Babu, E. Ma and J. W. F. Valle, Phys. Lett. B **552**, 207 (2003) [arXiv:hep-ph/0206292].
- [17] G. Altarelli and F. Feruglio, Nucl. Phys. B **720** (2005) 64 [hep-ph/0504165].
- [18] G. Altarelli and F. Feruglio, Nucl. Phys. B **741** (2006) 215 [hep-ph/0512103].
- [19] Y. Shimizu, M. Tanimoto and A. Watanabe, Prog. Theor. Phys. **126** (2011) 81 [arXiv:1105.2929 [hep-ph]].
- [20] S. T. Petcov and A. V. Titov, Phys. Rev. D **97** (2018) no.11, 115045 [arXiv:1804.00182 [hep-ph]].
- [21] S. K. Kang, Y. Shimizu, K. Takagi, S. Takahashi and M. Tanimoto, PTEP **2018**, no. 8, 083B01 (2018) [arXiv:1804.10468 [hep-ph]].
- [22] F. Feruglio, doi:10.1142/9789813238053-0012 arXiv:1706.08749 [hep-ph].

- [23] R. de Adelhart Toorop, F. Feruglio and C. Hagedorn, Nucl. Phys. B **858**, 437 (2012) [arXiv:1112.1340 [hep-ph]].
- [24] T. Kobayashi, K. Tanaka and T. H. Tatsuishi, Phys. Rev. D **98** (2018) no.1, 016004 [arXiv:1803.10391 [hep-ph]].
- [25] J. T. Penedo and S. T. Petcov, Nucl. Phys. B **939** (2019) 292 [arXiv:1806.11040 [hep-ph]].
- [26] P. P. Novichkov, J. T. Penedo, S. T. Petcov and A. V. Titov, JHEP **1904** (2019) 174 [arXiv:1812.02158 [hep-ph]].
- [27] J. C. Criado and F. Feruglio, SciPost Phys. **5** (2018) no.5, 042 [arXiv:1807.01125 [hep-ph]].
- [28] T. Kobayashi, N. Omoto, Y. Shimizu, K. Takagi, M. Tanimoto and T. H. Tatsuishi, JHEP **1811** (2018) 196 [arXiv:1808.03012 [hep-ph]].
- [29] G. J. Ding, S. F. King and X. G. Liu, JHEP **1909** (2019) 074 [arXiv:1907.11714 [hep-ph]].
- [30] P. P. Novichkov, J. T. Penedo, S. T. Petcov and A. V. Titov, JHEP **1904** (2019) 005 [arXiv:1811.04933 [hep-ph]].
- [31] T. Kobayashi, Y. Shimizu, K. Takagi, M. Tanimoto and T. H. Tatsuishi, JHEP **02** (2020), 097 [arXiv:1907.09141 [hep-ph]].
- [32] X. Wang and S. Zhou, JHEP **05** (2020), 017 [arXiv:1910.09473 [hep-ph]].
- [33] G. J. Ding, S. F. King and X. G. Liu, Phys. Rev. D **100** (2019) no.11, 115005 [arXiv:1903.12588 [hep-ph]].
- [34] X. G. Liu and G. J. Ding, JHEP **1908** (2019) 134 [arXiv:1907.01488 [hep-ph]].
- [35] P. Chen, G. J. Ding, J. N. Lu and J. W. F. Valle, arXiv:2003.02734 [hep-ph].
- [36] P. P. Novichkov, J. T. Penedo and S. T. Petcov, [arXiv:2006.03058 [hep-ph]].
- [37] X. G. Liu, C. Y. Yao and G. J. Ding, [arXiv:2006.10722 [hep-ph]].
- [38] T. Asaka, Y. Heo, T. H. Tatsuishi and T. Yoshida, JHEP **2001** (2020) 144 [arXiv:1909.06520 [hep-ph]].
- [39] M. K. Behera, S. Mishra, S. Singirala and R. Mohanta, [arXiv:2007.00545 [hep-ph]].
- [40] S. Mishra, [arXiv:2008.02095 [hep-ph]].
- [41] F. J. de Anda, S. F. King and E. Perdomo, Phys. Rev. D **101** (2020) no.1, 015028 [arXiv:1812.05620 [hep-ph]].
- [42] T. Kobayashi, Y. Shimizu, K. Takagi, M. Tanimoto and T. H. Tatsuishi, arXiv:1906.10341 [hep-ph].
- [43] P. P. Novichkov, S. T. Petcov and M. Tanimoto, Phys. Lett. B **793** (2019) 247 [arXiv:1812.11289 [hep-ph]].

- [44] T. Kobayashi and S. Tamba, Phys. Rev. D **99** (2019) no.4, 046001 [arXiv:1811.11384 [hep-th]].
- [45] A. Baur, H. P. Nilles, A. Trautner and P. K. S. Vaudrevange, Phys. Lett. B **795** (2019) 7 [arXiv:1901.03251 [hep-th]].
- [46] G. J. Ding, S. F. King, C. C. Li and Y. L. Zhou, JHEP **08** (2020), 164 [arXiv:2004.12662 [hep-ph]].
- [47] I. de Medeiros Varzielas, S. F. King and Y. L. Zhou, Phys. Rev. D **101** (2020) no.5, 055033 [arXiv:1906.02208 [hep-ph]].
- [48] P. P. Novichkov, J. T. Penedo, S. T. Petcov and A. V. Titov, JHEP **1907** (2019) 165 [arXiv:1905.11970 [hep-ph]].
- [49] T. Kobayashi, Y. Shimizu, K. Takagi, M. Tanimoto, T. H. Tatsuishi and H. Uchida, Phys. Rev. D **101** (2020) no.5, 055046 [arXiv:1910.11553 [hep-ph]].
- [50] T. Kobayashi, Y. Shimizu, K. Takagi, M. Tanimoto, T. H. Tatsuishi and H. Uchida, Phys. Lett. B **794** (2019) 114 [arXiv:1812.11072 [hep-ph]].
- [51] H. Okada and M. Tanimoto, Phys. Lett. B **791** (2019) 54 [arXiv:1812.09677 [hep-ph]].
- [52] H. Okada and M. Tanimoto, arXiv:1905.13421 [hep-ph].
- [53] T. Nomura and H. Okada, Phys. Lett. B **797** (2019) 134799 [arXiv:1904.03937 [hep-ph]].
- [54] H. Okada and Y. Orikasa, Phys. Rev. D **100** (2019) no.11, 115037 [arXiv:1907.04716 [hep-ph]].
- [55] Y. Kariyazono, T. Kobayashi, S. Takada, S. Tamba and H. Uchida, Phys. Rev. D **100** (2019) no.4, 045014 [arXiv:1904.07546 [hep-th]].
- [56] T. Nomura and H. Okada, arXiv:1906.03927 [hep-ph].
- [57] H. Okada and Y. Orikasa, arXiv:1908.08409 [hep-ph].
- [58] T. Nomura, H. Okada and O. Popov, Phys. Lett. B **803** (2020) 135294 [arXiv:1908.07457 [hep-ph]].
- [59] J. C. Criado, F. Feruglio and S. J. D. King, JHEP **2002** (2020) 001 [arXiv:1908.11867 [hep-ph]].
- [60] G. J. Ding, S. F. King, X. G. Liu and J. N. Lu, JHEP **1912** (2019) 030 [arXiv:1910.03460 [hep-ph]].
- [61] I. de Medeiros Varzielas, M. Levy and Y. L. Zhou, [arXiv:2008.05329 [hep-ph]].
- [62] D. Zhang, Nucl. Phys. B **952** (2020) 114935 [arXiv:1910.07869 [hep-ph]].
- [63] T. Nomura, H. Okada and S. Patra, arXiv:1912.00379 [hep-ph].
- [64] T. Kobayashi, T. Nomura and T. Shimomura, Phys. Rev. D **102** (2020) no.3, 035019 [arXiv:1912.00637 [hep-ph]].
- [65] J. N. Lu, X. G. Liu and G. J. Ding, Phys. Rev. D **101** (2020) no.11, 115020 [arXiv:1912.07573 [hep-ph]].
- [66] X. Wang, Nucl. Phys. B **957** (2020), 115105 [arXiv:1912.13284 [hep-ph]].

- [67] S. J. D. King and S. F. King, JHEP **09** (2020), 043 [arXiv:2002.00969 [hep-ph]].
- [68] M. Abbas, arXiv:2002.01929 [hep-ph].
- [69] H. Okada and Y. Shoji, arXiv:2003.11396 [hep-ph].
- [70] H. Okada and Y. Shoji, arXiv:2003.13219 [hep-ph].
- [71] G. J. Ding and F. Feruglio, JHEP **06** (2020), 134 [arXiv:2003.13448 [hep-ph]].
- [72] T. Nomura and H. Okada, [arXiv:2007.04801 [hep-ph]].
- [73] T. Nomura and H. Okada, arXiv:2007.15459 [hep-ph].
- [74] T. Asaka, Y. Heo and T. Yoshida, [arXiv:2009.12120 [hep-ph]].
- [75] T. Kobayashi, Y. Shimizu, K. Takagi, M. Tanimoto and T. H. Tatsuishi, Phys. Rev. D **100** (2019) no.11, 115045 Erratum: [Phys. Rev. D **101** (2020) no.3, 039904] [arXiv:1909.05139 [hep-ph]].
- [76] H. P. Nilles, S. Ramos-Sánchez and P. K. S. Vaudrevange, JHEP **02** (2020), 045 [arXiv:2001.01736 [hep-ph]].
- [77] H. P. Nilles, S. Ramos-Sánchez and P. K. S. Vaudrevange, Nucl. Phys. B **957** (2020), 115098 [arXiv:2004.05200 [hep-ph]].
- [78] S. Kikuchi, T. Kobayashi, H. Otsuka, S. Takada and H. Uchida, [arXiv:2007.06188 [hep-th]].
- [79] S. Kikuchi, T. Kobayashi, S. Takada, T. H. Tatsuishi and H. Uchida, [arXiv:2005.12642 [hep-th]].
- [80] H. Abe, T. Kobayashi, S. Uemura and J. Yamamoto, Phys. Rev. D **102** (2020) no.4, 045005 [arXiv:2003.03512 [hep-th]].
- [81] T. Kobayashi and H. Otsuka, Phys. Rev. D **102** (2020) no.2, 026004 [arXiv:2004.04518 [hep-th]].
- [82] H. Okada and M. Tanimoto, [arXiv:2005.00775 [hep-ph]].
- [83] Z. Maki, M. Nakagawa and S. Sakata, Prog. Theor. Phys. **28** (1962) 870.
- [84] B. Pontecorvo, Sov. Phys. JETP **26** (1968) 984 [Zh. Eksp. Teor. Fiz. **53** (1967) 1717].
- [85] K. Abe *et al.* [T2K Collaboration], Nature **580** (2020) 339.
- [86] P. Adamson *et al.* [NOvA Collaboration], Phys. Rev. Lett. **118** (2017) no.23, 231801 [arXiv:1703.03328 [hep-ex]].
- [87] J. Lauer, J. Mas and H. P. Nilles, Phys. Lett. B **226**, 251 (1989); Nucl. Phys. B **351**, 353 (1991).
- [88] W. Lerche, D. Lust and N. P. Warner, Phys. Lett. B **231**, 417 (1989).
- [89] S. Ferrara, D. Lust and S. Theisen, Phys. Lett. B **233**, 147 (1989).
- [90] D. Cremades, L. E. Ibanez and F. Marchesano, JHEP **0405**, 079 (2004) [hep-th/0404229].

- [91] T. Kobayashi and S. Nagamoto, Phys. Rev. D **96**, no. 9, 096011 (2017) [arXiv:1709.09784 [hep-th]].
- [92] T. Kobayashi, S. Nagamoto, S. Takada, S. Tamba and T. H. Tatsuishi, Phys. Rev. D **97**, no. 11, 116002 (2018) [arXiv:1804.06644 [hep-th]].
- [93] S. Ferrara, D. Lust, A. D. Shapere and S. Theisen, Phys. Lett. B **225**, 363 (1989).
- [94] M. Chen, S. Ramos-Sánchez and M. Ratz, Phys. Lett. B **801** (2020), 135153 [arXiv:1909.06910 [hep-ph]].
- [95] R. C. Gunning, *Lectures on Modular Forms* (Princeton University Press, Princeton, NJ, 1962).
- [96] B. Schoeneberg, *Elliptic Modular Functions* (Springer-Verlag, 1974).
- [97] N. Koblitz, *Introduction to Elliptic Curves and Modular Forms* (Springer-Verlag, 1984).
- [98] S. F. King and Y. L. Zhou, Phys. Rev. D **101** (2020) no.1, 015001 [arXiv:1908.02770 [hep-ph]].
- [99] I. Esteban, M. C. Gonzalez-Garcia, A. Hernandez-Cabezudo, M. Maltoni and T. Schwetz, JHEP **1901**, 106 (2019) [arXiv:1811.05487 [hep-ph]].
- [100] S. Vagnozzi, E. Giusarma, O. Mena, K. Freese, M. Gerbino, S. Ho and M. Lattanzi, Phys. Rev. D **96** (2017) no.12, 123503 [arXiv:1701.08172 [astro-ph.CO]].
- [101] N. Aghanim *et al.* [Planck], Astron. Astrophys. **641** (2020), A6 [arXiv:1807.06209 [astro-ph.CO]].
- [102] M. Tanabashi *et al.* [Particle Data Group], Phys. Rev. D **98** (2018) no.3, 030001.
- [103] S. Antusch and V. Maurer, JHEP **1311** (2013) 115 [arXiv:1306.6879 [hep-ph]].
- [104] F. Björkeröth, F. J. de Anda, I. de Medeiros Varzielas and S. F. King, JHEP **1506** (2015) 141 [arXiv:1503.03306 [hep-ph]].
- [105] C. Jarlskog, Phys. Rev. Lett. **55** (1985) 1039.
- [106] P. I. Krastev and S. T. Petcov, Phys. Lett. B **205** (1988) 84.